Palaeoenvironmental reconstruction in South Africa's year-round rainfall zone using multi-proxy geochemical analyses on lake sediments from Swartvlei

Master's Thesis

By: Matjie Lillian Maboya

Supervisors: Prof. Michael Meadows and Prof. Torsten Haberzettl

Department of Environmental and Geographical Sciences

University of Cape Town

January 2019

Plagiarism declaration

1. Plagiarism is to use another's work and to pretend that it is one's own. I know that plagiarism is wrong.

2. I have used the Harvard convention for citation and referencing. Each significant contribution to and quotation in this report from the work or works of the other people has been attributed and has been cited and referenced.

3. This thesis is my own work.

4. I have not allowed and will not allow anyone to copy my work with the intention of passing it off as his or her own work.

Signature: Signed by candidate Date: 7 January 2019

Student Name: Matjie Lillian Maboya

Acknowledgements

This study would not have been possible without funding from the following organisations:

- German Federal Ministry of Education and Research (BMBF) under the collaborative project "Regional Archives for Integrated Investigations" (RAIN)
- German Academic Exchange Service (DAAD)
- National Research Foundation (NRF)
- Palaeontological Scientific Trust (PAST)
- University of Cape Town (UCT) Postgraduate funding

Gratitude

I am grateful for support from my supervisors, Prof. Mike Meadows and Prof. Torsten Haberzettl who provided guidance and support at every step of this project, and to Kelly Kirsten for her invaluable help throughout. I would also like to thank laboratory assistance from Nico Blaubach, Carmen Kirchner, Thomas Kasper, Paul Strobel, Bastian Reinwarth, Christian Gregori and Tobi. I am thankful for consistent support from my family and friends during this project. It truly takes a village! Go Moraswi le Kgaladi, ke leboga go menagane! Thekgo ya lena go tloga mathomong e nkgontšhitše mošomo wo.

Abstract

Coastal lakes in the south coast of South Africa contain sediments with good records of palaeoenvironmental changes. Swartvlei is the largest of the lakes in the Wilderness Embayment and is connected to the Indian Ocean via an estuary. The lake is believed to have been formed during sea-level regressions in the quaternary, and separated from Groenvlei lake between 4000 and 2000 cal BP. There are questions about dominant precipitation regimes as well as the onset, cessation and altitude of marine transgressions in the area. In this study, Holocene sediments from Swartvlei Lake were extracted and investigated using multiple methods. These include organic and inorganic geochemical proxies and multi-dating approach through radiocarbon and OSL dating. A composite profile was made using marker layers with lithostratigraphic distinctions combining three cores into one continuous, 7 m long core spanning 8600 cal BP. The core was subdivided into two distinct zones namely, Unit A (8600 to 3500 cal BP) and Unit B (3500 cal BP to present), identified using cluster analysis on particle size data. The results reveal low sea-levels with limited precipitation and aquatic productivity during the early Holocene, followed by a marine incursion from 4500 to 3500 cal BP and moister conditions thereafter. This marine incursion, marked by increased Ca and TIC concentrations, occurred when the physical barriers were breached, and the estuarine channel widened due to a landward strandline migration. Pronounced riverine input due to increased precipitation was observed after 3500 cal BP, with strong minerogenic input and lowered sea-level. An influx of silt and clay material that dominate the top half of the core marks Swartvlei's evolution into more lacustrine conditions and its separation from Groenvlei during the same period. A more humid climate is further inferred from organic proxies that indicate a greater in-wash of vascular vegetation during this period, as well as higher productivity from 3500 to 1400 cal BP. In addition, high biogenic silica concentrations indicate increased bio-productivity during the Little Ice Age (LIA) while increased sedimentation rates suggest that anthropogenic activity impacted the lake from 150 cal BP. This study adds insight to the geomorphic evolution of Swartvlei and highlights the usefulness of geochemical analyses in the elucidation of regional quaternary environmental and climatic changes.

Table of Contents

List of Figures

Chapter 1: Introduction

Palaeoenvironmental reconstructions are an essential tool to understand long-term environmental and climatic changes and are critical in southern Africa where existing records are scarce and future climate change rates are predicted to be high (Niang et al., 2014). Extrapolation of regional history of climate change becomes considerably more challenging when using only sparsely distributed or temporally incomplete palaeoclimate evidence. Lake sediments and the geochemical signatures that they preserve over time have proved to be incredibly useful in reconstructions of climate and environmental changes globally (Last and Smol, 2001), however, in South Africa's year-round rainfall zone (YRZ), such situations are less common (Haberzettl et al., 2014). Coastal lakes in the southern Cape, including Eilandvlei and Groenvlei, have nonetheless provided detailed Holocene environmental histories that span the last 8900 years, and have demonstrated their use in unravelling past climate dynamics in the region. Geochemical signatures in these sediments are important tools for identifying details about environmental changes and their implications (Dellwig et al., 1999). Palaeoecological proxies have, however, seemingly dominated such reconstructions, in particular those using pollen (e.g., Martin, 1968; Quick et al., 2015; Quick et al., 2018) and diatoms (e.g., Kirsten et al., 2018); proxies based on geochemistry have emerged only more recently with the general trend towards multi-proxy studies (e.g. Regional Archives Investigations (RAiN) project, Haberzettl et al., 2014; Wündsch et al., 2016; Wündsch et al., 2018). These studies have so far revealed drier conditions and greater marine influence from 8900-3000 cal BP and moister conditions thereafter when the coastal embayment evolved into freshwater lakes. The timing of marine transgressions and magnitude of associated regional sea-level rise require finer resolution; furthermore, major changes in the nature and amount of past riverine input remain largely unknown.

Swartvlei is the largest lake in the Wilderness embayment, although understanding of the processes that led to the development of the lake and the environmental changes that occurred in the Holocene remains very limited. Holocene environmental changes at Swartvlei Lake were pioneered initially by Watling (1977). This was followed by research on shallow cores (< 1m) by Birch et al. (1978) and Franz (2012). These investigations were on surface or near- surface samples in an attempt to define the source of several elemental contributions to the modern sediments and, as such, are temporally constrained. Whitfield et al. (2017) attempted a reconstruction of mid-Holocene developments at Swartvlei estuary with a focus on the interactions between the Swartvlei estuary and Groenvlei, which were shown to have been connected in the mid-Holocene. However, apart from being collected primarily at Groenvlei, the evidence on which

this reconstruction was based was of low resolution and the assumed timing of the enclosure of the Swartvlei estuary following the mid-Holocene regression was imprecise.

The present study analyses a 7 m long core from Swartvlei Lake using high-resolution multi-proxy geochemical analyses underpinned by a high resolution chronology from radiocarbon and OSL dating. Results are used to develop a more finely resolved picture of the evolution of the Swartvlei during the Holocene, and to compare the record with other sites to better understand changes in the broader southern Cape region. The study explores the influence of climate drivers on the YRZ as a whole, including Antarctic sea-ice extent, which is known to influence moisture in the southwestern Cape winter rainfall zone (WRZ), and also migrations of the Intertropical Convergence Zone (ITCZ) that affect moisture in the summer-rainfall zone (SRZ) to the east. The unique positioning of Swartvlei which is situated at the confluence of large-scale atmospheric circulations such as the tropical easterly flow and the southern westerlies make it an ideal site for such investigations due to its sensitivity to changes in their strength and position, and to upwelling on the eastern Agulhas Bank (Cohen and Tyson, 1995; Chase and Meadows; 2007). The multi-proxy record from a longer sediment core at Swartvlei can help to shed light in this regard and to distinguish between local and regional palaeoenvironmental variations.

1.1. Aim

The primary aim of this study is to reconstruct Holocene palaeoenvironments of Swartvlei in the year-round-rainfall zone of South Africa, through sedimentological and geochemical analyses.

1.2. Objectives

- To establish the nature of environmental changes that have occurred in the Swartvlei, Wilderness Lakes region, during the Holocene and how these changes have been revealed through existing palaeoecological records.
- To reconstruct climatic and landscape changes that have occurred through a detailed analysis of the grain size and geochemical dynamics recorded within Swartvlei sediments.
- To compare information revealed by the analysis of the Swartvlei cores to other palaeoecological records in the Wilderness, and their relationship to major regional, Southern Hemisphere and global events over the same period.

1.3. Thesis outline

Chapter 2 contains a rationale of the study and suitability of the different proxies used. Chapter 3 sets the environmental context (climate, geology, biology, contemporary lake morphology) and a review of sources that have been used to establish the history of palaeoclimatic and palaeoenvironmental changes in the southern Cape during the Holocene. Details of the methods employed in the study are provided in Chapter 4. This is followed by the results chapter starting with the chronology, inclusive of an illustration of the relationships between the geochemical proxies. Chapter 6 provides interpretations of the results and a discussion on the palaeoenvironmental history using evidence from this study. It gives an overview of the palaeoclimatic changes inferred from the geochemical proxies, particle size data and organic matter accumulation in the lake, as well as the landscape modifications that were largely influenced by changes in sea-level and local dune morphology. Finally, Chapter 7 concludes the thesis with a palaeoenvironmental summary and an assessment of how well the objectives of the study have been met.

Chapter 2: Palaeoenvironmental indicators in lake sediments

2.1. Significance of palaeoenvironmental reconstructions in the Wilderness Lakes region

Swartvlei is located in the south coast of South Africa within Wilderness National Park which is now incorporated into the broader Garden Route National Park (GRNP) (Figure 1). One of the objectives of the park is to facilitate research on freshwater and estuarine systems in the region to support park management policy and practice (South African National Parks [SANParks], 2016). The GRNP is home to the country's largest indigenous forest and SANParks manages 67% of them on the southern coastline (SANParks, 2016). A large proportion of the species-rich fynbos biome is found on the southern Cape Coast and is regarded as a major component that makes up the Cape Floristic Region which represents an astonishing 3% percent of the world's plant species (Mucina and Rutherford, 2006). The fynbos is regarded as one of the most ecologically diverse and unique ecotones in the world and the establishment of various national parks have helped to protect the species. Critical loss of biodiversity has been reported due to various reasons such as human interference and climate change. Endemic invertebrates are also found in the area, for example, Swartvlei is also home to endangered Knysna Sea-Horse *Hippocampus capensis* which is listed as a threatened species on the International Union for Conservation of Nature (IUCN). Various other species living in the area have drawn tourists, both locally and globally, to engage in recreational activities on the lake such as boating and fishing, with accommodation facilities available to guests. Questions around recreational carrying capacity of estuaries in the GRNP such as Knysna Estuary have been put forward in an effort to create responsible resource management (SANParks, 2016).

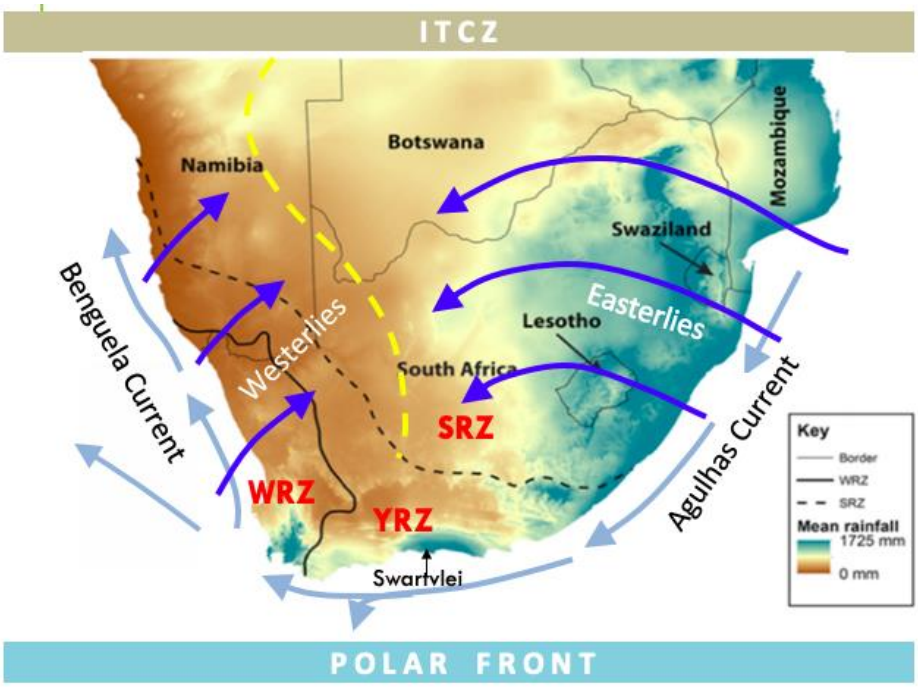

Figure 1: Regional map showing the location of Swartvlei within the year-sound rainfall zone (YRZ) along with SRZ = summer rainfall zone, WRZ = winter rainfall zone (after Mills et al., 2012)

Extreme climate events of flooding in 1981, 2006 and 2007 had profound changes in Swartvlei's ecology due to higher temperatures and salinity changes resulting from the breached sand-bar that allowed greater entry of sea-water into the lake as the lake was open for longer than normal (Whitfield et al., 2010; Russell, 2015). The resulting high salinity led to a reduction in lake biota including a 99% reduction in submerged vegetation and a further reduction in the waterbird species that rely on them (Russell, 2015). Swartvlei's ecological health is dependent on both freshwater and marine inputs. Yet, rising population growth in the area exerts further stress on freshwater resources, implying reduced freshwater due to lower fluvial inputs at Swartvlei resulting from increased water abstraction in the catchment (Russell, 1999). Drought projections and increased sea-water intrusions will lead to Swartvlei becoming progressively saline in the future (SANParks, 2016). Palaeoenvironmental studies could also provide information about changes to biomass and lake productivity during periods of higher salinity as they have occurred in the past during marine transgressions, and this can help SANParks to anticipate and manage future ecological responses. Lake salinity changes can also occur through intrusion of sea-water into the lake facilitated by strengthening wind regime, as well as lower precipitation and higher evaporation.

Western Cape Province has been deemed vulnerable to climate change owing to challenges in socio-economic development, local governance and capacity of the ecosystems to adapt to rapid change

(Pascuini et al., 2013; Ziervogel et al., 2014). In addition to forecasting the nature of climatic changes that are anticipated, there is a need to understand how climate variability affects ecosystems and how ecosystems respond to the change. A wealth of information has been generated through studies on the ecology of lakes in the Wilderness area (e.g. Robarts, 1976; Coetzee, 1982; Kok and Whitfield, 1986; Whitfield, 1988). Particularly at Swartvlei Lake, most studies have focused on describing the ecology and investigating the ecosystem changes during flood events since the 1980's and impacts on the fish communities and emergent vegetation arising from artificial opening and closing of the sand bar. Other studies sought to describe physio-chemical differences between Swartvlei Lake and Swartvlei estuary (e.g. Russell, 2015) and how these are manifested during extreme weather events. These studies have helped, and continue to inform, management strategies for conservation in the GRNP. However, none of them have extended their temporal scale to cover the Holocene and, as such, very little is known about the palaeohydrology of Swartvlei. Climate is a long-term phenomenon, it is important to study these changes on a longer-term scale in order to provide a benchmark against which the nature of current and possible future environmental dynamics can be more fully appreciated. This study seeks to deepen knowledge about the freshwater, estuarine and marine influences at Swartvlei as they have occurred in the past. This information helps to explain and distinguish certain changes in the lake that have occurred as a result of natural variations compared with those caused, or exacerbated, by anthropogenic activity. Assessing the scale of the natural contribution of these changes and the extent of human influence is fundamental to successful management strategies that will prioritise conversation and access to these water resources.

2.2. Lake sediments as archives for environmental change

Over time, signals of environmental changes, both natural and anthropogenic, may become preserved in lacustrine sediments. Although human impact has, to an extent, accelerated the cycling of some geochemical elements (Wolin and Duthie, 1999; Ma et al., 2016), such as through the introduction of chemicals for agriculture and release of others through mining, natural processes are still often involved in the transportation of geochemical elements from sources and processes to where they are captured in lakes (Braun et al., 2013). Closed lakes have been used extensively for palaeoenvironmental reconstruction of the Quaternary due to their ability to capture and preserve multi-proxy data from freshwater, marine and aeolian signals (Sayer et al., 2010). In South Africa, sediments preserved within the southern cape help with understanding palaeoenvironments that prevailed at archaeological sites that were previously occupied by our ancestors and how they related to climate change, water availability and changing landscapes (Cawthra et al., 2014). In addition, the Wilderness lakes have good preservation of

fluctuations in marine influence (Martin, 1968), and these can be used to reconstruct rhythms of marine transgressions and regressions, as well as the response of the terrestrial environment to these. Furthermore, the examination of sources and sinks of organic matter distribution in coastal lake sediments is key to understanding regional and global biogeochemistry cycles.

Lake sediments may capture evidence of intra-basin variation and environmental changes on their surrounding catchments over long periods of time (Foster and Walling, 1994), allowing them to serve as rich archives for palaeoenvironmental reconstruction. Various proxies preserved in lake sediments can provide analogues for understanding past, present and future environmental change. Multiproxy studies focus on different aspects of the sediments such as biological (e.g. diatoms, pollen, ostracoda), chemical (e.g. elemental, isotopic), physical (e.g. density, magnetic susceptibility, particle size) and offer greater prospects for discerning regional climatic and environmental signals. Multiple proxies employed to reconstruct climatic and landscape changes that have occurred at Swartvlei in the Wilderness region and these are discussed below.

2.3. Overview of multiproxy studies on lake sediments

2.3.1. Physical proxies

Granulometric analysis can provide information about sediment origin, transportation and deposition and reveal the environmental processes that may have morphed the sediments over a given period of time. Particle size is an important proxy to understand sediment provenance and to interpret changes in the dominant transport mechanism that delivered sediments into the lake (Clift et al., 2014; Schillereff et al., 2014). Specifically, the depositional environment, weathering and transportation mechanism can be reconstructed using grain size because aeolian and fluvial systems are known to transport grains within in a particular size range (Lewin, 1978). Furthermore, small grained particles would be expected during calm climate conditions while coarse sediments are indicative of turbulent depositional conditions such as floods, snow-melt and storm surges (Schillereff et al., 2014). It is important to know the underlying geology of a site in order to locate origins of the sediments found in the record as some of the particles may have been derived from direct weathering of the surrounding bedrock and still others from further afield in the catchment. Laser diffraction is the preferred method for granulometric analysis because it

offers rapid, affordable and reliable analysis of small samples (<50 mg) (Beuselinck et al., 1998; Pye & Blott, 2004).

Sediment water content and bulk density are useful proxies to classify sediments in terms of their environment of deposition. Sediment density and compaction are highly dependent on primary textural properties such as particle size and shape (Last and Smol, 2001). The relationship between water content, organic matter and sediment density is explored by Avnimelech et al. (2001) who explain that fine organic-rich sediments tend to possess low density (1.25 $g.cm^{-3}$; Boyd, 2012) and high water content. The latter occurs in part due to its role in facilitating bioproductivity such as the gaseous exchanges for photosynthesis and respiration, where water acts as a medium for the exchanges. A 1% addition of hydrated organic matter can increase the sediment volume and thus lower the density (Avnimelech et al., 2001). Coarse sediments on the other hand are often compacted and feature high density values as they are deposited in high energy environments that are unfavourable to bioproductivity. According to Klute and Dinauer (1986), density values for inorganic sediments typically lie between 2.6 and 2.7. $g.cm^{-3}$

The concentration of magnetizable minerals found in lake sediments are produced and transported by different environmental processes that operate in response to changes in climate and limnology (Last and Smol, 2001). Magnetic susceptibility (MS) is a measurement of magnetizability of sediment components in response to an external magnetic field applied to the sediment core (Thompson et al., 1975). MS is measured by inducing a magnetic signal onto the sediment surface using a probe and measuring the returned signal. Sections of a core with highly magnetizable material will produce a strong signal, and typically contain ferrimagnetic minerals that are easily magnetised, while organic matter with high water content has a diamagnetic effect (Dearing, 1999). Interpretation of MS data assumes that detrital magnetic assemblages have not been altered or undergone authigenesis post-deposition (Snowball and Sandgren, 2001). MS measurements have been used in many palaeolimnology studies and have helped to locate periods of increased minerogenic input and long periods of organic matter deposition.

2.3.2. Inorganic geochemical proxies

Element assemblages in sedimentary records are key indicators of palaeoenvironmental conditions because their presence, reduction/oxidation statuses and quantitative ratios are indicative of specific environmental conditions that prevailed at the time of their deposition or thereafter (Ma et al., 2016). Climate is one of the factors that influences weathering and erosional processes, thus, the origin of

elements and the nature of weathering they undergo can be indicative of certain climate conditions such as increased moisture, aridity or windier conditions. Inorganic geochemical palaeolimnology uses analytical tools such to quantify elemental compositions and use those to infer variation in the environment (Dellwig et al., 1999). These quantities are commonly ascertained through X-ray fluorescence (XRF) and inductively coupled plasma atomic emission spectroscopy (ICP-OES) on sediment cores, and the illustrated relationships between the elements are used to reconstruct environmental change. XRF measures the downcore intensities of each element while ICP-OES gives absolute quantities of the elements in the core. It is useful to compare the geochemical variations with a conservative element such as Al which is less susceptible to diagenic effects (Löwemark et al., 2011), thus leading to the use of elemental ratios. For example, depending on the catchment rock composition, Ti/Al and Fe/Al ratios are often associated with silicates, thus temporal changes in their abundance can serve as proxy for minerogenic input into the lake (Kylander et al., 2011).

2.3.3. Organic proxies

Organic matter preserved in lake sediments contains indicators of intra and extra basin palaeoproductivity and can be a helpful proxy for climate reconstruction (Meyers, 1997). Temporal changes in the deposition and extent of terrestrial organic matter can give information about hydrological pathways. In addition, determinations of the amounts and origins of sediment organic matter (elemental and isotopic) are an important tool to understand ecosystem changes as a result of natural and anthropogenic changes to the landscape. Organic matter measurements such as total organic carbon (TOC) are an important tool used to measure the amount of organic matter in sediments (Meyers et al., 1999). Other elemental proxies linked with organic matter include elements that are essential for productivity such as Phosphorus (P) and Nitrogen (N), and those released by organic matter upon decomposition such as Sulphur (S) (Stevenson et al., 1999). Ratios between TOC and these elements can provide information about other aspects of environmental changes around the lake e.g. TOC/TN ratios can help to distinguish between aquatic production and terrestrial vascular plant addition to the lake sediments (Meyers, 2003), from which we can infer palaeohydrological changes in the catchment area. TOC can also be linked with other physical proxies such as particle size, as illustrated by Thompson and Eglinton (1978) who found an abundance of organic matter in core sections with small grain sizes. Biogenic silica content is another common proxy for lake productivity as it indicated the dominance of siliceous microfossils such as diatoms (Batterbee et al.,

2002), sponges (Conley and Schelske al., 2002; Conley and Schelske, 1993) and phytoliths (McCarty and Schwandes, 1998)

Chapter 3: Literature Review

3.1. Study site description

3.1.1. Modern regional climate

According to the Köppen climate classification system, the Wilderness is defined as Cfb – wet year-round with long and cool summers (Schulze et al., 1947). The rainfall is influenced by polar westerlies and subtropical easterlies (Tyson and Preston-Whyte, 2000) and averages 800 to 1 000 mm yr^{-1} throughout the year (Russell et al., 2012). Another source of moisture and humidity for the area is the Agulhas current which occurs at the convergence of the Indian and Atlantic Ocean and brings maritime moisture over the area which influences the temperature regime (Scott and Lee-Thorp, 2004; Cohen and Tyson, 1995). Figure 3 shows a photograph of Swartvlei Lake in relation to the Indian Ocean and estuary. The Outeniqua mountains (1 500 m above mean sea-level) introduce orographic rain to the area (Parsons, 2014), as well as fog and humidity (Martin, 1968). Furthermore, the Cape Fold Belt prevents advection of moisture towards the north (Martin, 1968). The wind regime is dominated by south-westerly winds which blow throughout the year. Slight seasonal changes in wind occur, whereby south to southeasterly winds blow inland, and north to northwesterly winds off-shore (Deacon and Lancaster, 1988). Temperature varies seasonally, with an average minimum of 15 ^{o}C and a maximum of 25 ^{o}C in summer and between 7-19 ^{o}C in winter (Whitfield et al., 1983).

3.1.2. Contemporary Swartvlei

Swartvlei is the largest coastal lake located on the eastern part of the Wilderness Embayment, 32 km from the town of George (Figure 1). The lake has a surface area of 8.8 km^2 and is connected to the sea via a 7.2 km long shallow estuary channel, which has an average depth of 4 m (Whitfield et al., 1983). Lake depth varies: the outer edges are about 2 m deep, while a littoral shelf in the centre reaches depths of about 12 m (Whitfield et al., 1983). More recently, Clausnitzer (2011) found the maximum depth of Swartvlei to be 15.5 m using evidence from seismic investigations. Freshwater inputs are sourced from three rivers namely; Wolwe, Hoekraal and Karatara. Additional sources of freshwater are direct rainfall and groundwater (Martin, 1962). The lake also experiences salinity fluctuations due to periodic sea-water inflow (Kok and Whitfield, 1986). Swartvlei is a meromictic lake i.e., experiences a vertical stratification

with layers of varying densities, where salinity values of the surface waters can be between 1-12 ‰, while the bottom waters could contain 20 ‰ (Whitfield et al., 1983). The propagation of sea-water into the lake is influenced by onshore winds, while south-westerly winds assist with the movement of littoral sand, often leading to the formation of a sandbar that closes off the river mouth (Martin, 1962; James and Harrison, 2008). Littoral sand movement occasionally blocks the estuary mouth, which opens and closes naturally, but artificial breaching has been undertaken to prevent flooding to the low-lying urban areas (Russell, 2015). The Wolwe River is responsible for much of the fine sediment deposited into the lake that forms soft mud on the lake basin at a depth of 12 m (Whitfield et al., 1983), surrounded by quartzitic sand deposits on the lake margins (Birch et al., 1978). The high levels of leached organic matter and humic acids from the Karatara River brings forth distinctively black coloured waters (Figure 3), after which the lake is named. The inflow from the Karatara introduces acidic waters with pH ranging between 4 and 5 (Whitfield et al., 1983).

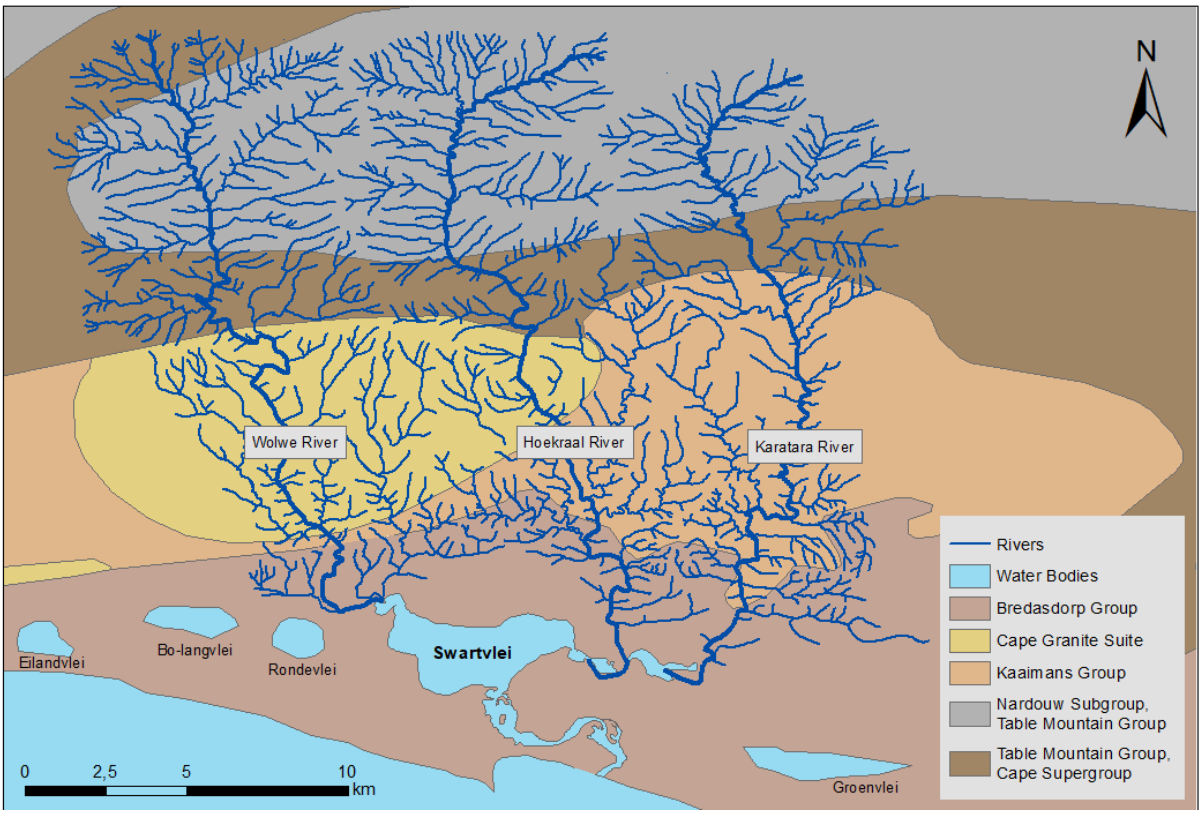

Figure 2: Map showing Table Mountain Sandstones and Granite as rocks underlying the Swartvlei river catchments (Map: Alexander Sokolovs)

These slightly acidic and saline water conditions give rise to the diverse species that thrive in and around the Swartvlei system. Howard-Williams and Allanson (1979) described the primary producers within

Swartvlei to consist mainly of planktonic algae that occupy the pelagic zone, while the littoral shelf is largely covered in *Potamogeton*, and *Cladophora* and *Cocconeis* algae to a lesser extent. Terrestrial vegetation composed of typical sand dune vegetation occupies the lake periphery: perennial *Ehrharta* grasses, *Rhus* shrubs, and pockets of indigenous fynbos (Whitfield et al., 1983). There are also large *Pinus* plantations on the outskirts of Swartvlei that have invaded a majority of the indigenous vegetation. The lake also hosts a diverse community of invertebrates due to the combination of freshwater from the rivers feeding the lake and the estuarine water that enters the lake from the estuary mouth. Davies (1982) identified up to 33 fish species dominated by *Monodaotylus faloiformis* and *Rhabdosagus holubi* as well as bivalves, Ostracoda and crabs.

Figure 3: Photograph showing modern day Swartvlei lake, the estuary and vegetated sand dunes parallel to the ocean (Photo: Dominique de la Croix)

3.1.3. Geology

The Wilderness Embayment is of Tertiary age, cut into late Pre-Cambrian granite rocks that can be found on the north-western edge of Swartvlei, underlying the Wolwe River Catchment (Illenberger, 1996) (Figure

2). The Hoekraal and Karatara catchments lie on the exposed sandstones of the Kaaiman's group adjacent to the Wolwe River catchment (Figure 2). The Kaaiman's group is underlain by the Table Mountain Supergroup, composed of highly resilient sandstones which form the Cape Fold Belt, positioned further inland. These high-relief mountains have Ordovician orogeny and underwent intense folding about 180 Ma during the break-up of Gondwana land (de Wit and Ransome, 1992; Compton, 2004). The three major river channels feeding Swartvlei originate at the base of the folded mountains on the southern margin of the Outeniqua Mountain Range. Closer to the coast, the Wilderness embayment is covered in quaternary sands with prominent sand ridges (aeolianites) that lie parallel to the beach (Martin, 1962; Marker & Holmes, 2005; Holmes et al., 2007). Illenberger (1996) described three major dune cordons in the Wilderness Embayment namely; sea-ward, middle and landward cordons. Swartvlei is situated between the sea-ward and the middle cordon, with the seaward cordon stretching between 75 - 180 m above sea level on the south west region of Swartvlei (Bateman et al., 2004; Cawthra et al., 2014). Eastward longshore drift along the south coast is as a major source of sediment supply for the Wilderness Embayment, sustaining the dunes (Birch, 1980). The dunes are at least 128 000 years old and were constructed during multiple sea-level high-stands, covered in unconsolidated Holocene deposits at the surface (Bateman et al., 2004).

3.1.4. Existing knowledge about lake genesis

Swartvlei lies within a deeply incised valley formed during sea-level regressions during Marine Isotope Stage (MIS) 6 and MIS 4 (Cawthra et al., 2014), subsequently filled in by windblown sands from the exposed continental shelf bearing large dune fields as well as those from wave-cutting of the surrounding dunes (Martin, 1962; Birch and du Plessis, 1977). South-flowing rivers, currently feeding Swartvlei, cut through the valley and flowed directly into the sea some 100 km further from the current shoreline during the Last Glacial Maximum due to significantly lower sea level (~120m below mean sea level) (Bateman et al., 2011; Cawthra et al., 2014). During the current interglacial, the proto-Swartvlei valley was drowned by the rising sea water (Birch and du Plessis, 1977). Sea-level is estimated to have been 2.5 m above present level at 6000 BP and regressed at around 4000 BP (Martin, 1962). During the marine transgression at 6000 BP, the estuary mouth would have been 2 km wide, creating an open inlet *sans* sand bar (Whitfield et al., 1983). Furthermore, a palaeochannel is believed to have once connected Swartvlei and Groenvlei but was separated in the mid- to late Holocene when sand movement filled in the channel (Martin, 1962; Kirsten, 2008). Low topographic gradient of the embayment and the prominent aeolianite dune deposits

led to the damming of water evident in the modern-day series of lakes in the Wilderness including Swartvlei (Bateman et al., 2011).

3.2. Holocene environmental changes

There has been significant effort to investigate palaeoenvironments of the southern Cape during the Holocene using evidence from different localities. The sites vary from caves such as the Cango Caves (Talma and Vogel, 1992), Boomplaas (Thackeray and Avery, 1990), Seweweekspoort (Chase et al., 2013) and Nelson Bay Cave (Cohen, 1993; Cohen and Tyson, 1995), to coastal lakes Groenvlei (Martin, 1968; Wündsch et al., 2016) and Eilandvlei (Kirsten et al., 2018; Quick et al., 2018; Wündsch et al., 2018) as well as peat deposits from Norga (Scholtz, 1986). Palaeoclimatic reconstructions of the early Holocene in the southern Cape are sourced from a variety of sources including pollen, diatoms, rock hyrax middens, marine molluscs and stalagmite records. While the studies reach consensus about the regional driving forces of moisture and temperature, there are several inconsistencies, mostly relating to temporal control in the earlier studies and in the timing of marine transgressions. Although the studies are based in the YRZ references are made to studies in the winter-rainfall zone (WRZ) and summer rainfall zone (SRZ) relating to differences in the moisture sources.

3.2.1. Palaeoclimate reconstructions: patterns of moisture availability and temperature fluctuations

3.2.1.1. Early Holocene

The Holocene epoch covers the last 11 500 cal BP and has undergone significant climate fluctuations globally (Mayewski et al., 2004). Generally, this period represented a transition from cool conditions in the late Pleistocene to warm Holocene conditions (Scott et al., 1995). The transition from cooler to warmer temperatures was not gradual - it contained some oscillations, but most records covering this period are poorly dated and are not detailed enough to depict short-term changes and oscillations. Nonetheless, micro-mammallian fossils at Boomplaas Cave showed accelerated temperature increases recorded around 11500 BP by Avery (1982). Afterwards, between 10100 and 8900 BP, microfaunal, pollen and charcoal evidence from Boomplaas Cave revealed that a cooler episode prevailed before the Holocene, possibly associated with the Younger Dryas (Partridge et al., 1990). During early Holocene, the influence of westerlies weakened while the tropical systems strengthened their influence of SRZ moisture

(Chase et al., 2017), and possibly led to more humid conditions on the eastern part of the YRZ. Humphries et al. (2017) agreed with an observation that early Holocene warming and humidity was driven by strengthening of the tropical easterly flow.

Quick et al. (2018) concluded that the early Holocene was cool and arid, based on examination of pollen data that revealed the dominance of drought-resistant fynbos taxa in the Eilandvlei sediment record. This is supported by earlier findings, whereby Quick et al. (2015) noted significant changes in measured geochemical, palynological (pollen), and microscopic charcoal proxies from a sediment record at Still Bay in the period after 9 000 cal BP (between 9000-6000 cal BP) which are interpreted as a period of slight aridity at Still Bay. The same study however showed high productivity and moisture in the Rietvlei wetland based on organic geochemical proxies (TOC) (Quick et al., 2015). These contradicting interpretations in moisture denote the early Holocene as either a transitional period in the southern Cape, or a period when the environment responded to different moisture bearing systems with distinct spatial differences.

3.2.2.2. Mid-Holocene

The transition from early Holocene to late Holocene is interpreted differently in relation to temperature and moisture conditions depending on site locality. For example, Quick et al. (2018) find decreased humidity at Eilandvlei between 8900 and 5700 cal BP, while Chase et al. (2013) found increasing humidity at Seweeweskpoort around the same time. The period between 7000 and 5000 cal BP was found to be associated with relatively arid conditions based on the isotope geochemistry of hyrax middens at Seweweekpoort (Chase et al., 2013), driven by a reduction in the influence of westerlies on moisture provision for the area. There is agreement between records from Seweweekspoort and Cango Cave palaeotemperature reconstructions suggesting that warmer periods occurred in the southern Cape between 7800 to 7300 cal BP and 6800 to 5500 cal BP. Martin (1968) suggested warmer conditions in the palynological recorded at Groenvlei around 7800 cal BP, although this interpretation may be obscured by increased dune activity in the area and marine influence from a higher sea-level. Faunal assemblages at Boomplaas also exhibited concordance with these higher temperatures as it reveals the mid-Holocene altithermal between 7000 and 4500 BP to have been warmer than the prior period (Thackeray and Avery, 1990). Studies by Meadows et al. (1996) and Parkington (2000) suggested that the Holocene altithermal (4000–8000 BP) was very dry in the WRZ as indicated by increases in xeric taxa and Elands Bay, and this is supported by increased aeolian activity due to strong wind stress recorded in coversands studied by Chase and Thomas (2007) on the west coast.

During this time, the SRZ also experienced warmer and more humid conditions from 6500 to 5200 BP based on ^{18}O and ^{13}C isotopes from Cold Air Cave, driven by reduced Antarctic circumpolar circulation (Lee-Thorp et al., 2001). Talma and Vogel (1992) gave a more complete record of mid-Holocene temperature reconstruction which identified two periods that were cooler than present i.e. 4700 to 4200 BP and 3200 to 2500 BP, intercepted by a slightly warm phase. Quick et al. (2015) found the mid-Holocene to be drier and warmer based on significantly low productivity (inferred from reduced organic matter preservation) in the period between 7 000 and 5000 cal BP.

A humid phase is observed in the period 7800 – 4700 cal BP when Eilandvlei captured steep increases in afrotemperate forest taxa (Quick et al., 2018). Between 6000 and 4000 cal BP evidence from Mfabeni swamp on the east coast (Humphries et al., 2017) suggests greater aridity. Although there is spatial variation in the sea-surface temperature (SST) along southern Cape, low amplitude variations in the annual SST observed by Loftus et al. (2017) suggested increased upwelling occurred in the mid-Holocene linked with higher precipitation in the SRZ. Humid conditions prevailed at Seweweeksport between 5000 and 3000 cal BP (Chase et al., 2013), furthermore, rainfall in the YRZ evolved to a more aseasonal system during the same period (Chase and Meadows, 2007).

During the period between 4500 and 3000 BP, temperature was in a band of variation between +1 °C and -2 °C compared to modern temperatures (Talma and Vogel, 1992). Talma and Vogel (1992) found that the southern Cape had rainfall seasonality that shifted more towards the WRZ pattern instead of the modern-day all-season rainfall, an interpretation based on carbon isotope values that captured predominant vegetation cover in the landscape surrounding the cave. While older phases of increased dune activity coincided were associated with humid conditions driven by glacial phases in the Vostok ice record, the aridity could not be explained using the available data. Moreover, geomorphological activity in the region supported an arid climate in the WRZ observed in reworked aeolian deposits between 4 400 and 5 800 cal BP (Chase and Thomas, 2007).

Cohen and Tyson (1995) evaluated oxygen isotope composition in marine mollusc shells from Nelson Bay Cave to reconstruct Holocene sea surface temperatures and found higher temperatures than in the period between 6800 and 5400 cal BP. This finding countered the suggestion of low SST's on the Agulhas Bank from 6650 to 5500 cal yr B.P in an earlier study from the same site (Cohen, 1993). The model presented by Cohen and Tyson (1995) suggested that periods with low SST on the Agulhas Bank were coupled with

wet conditions in the interior. Similarly, on the east coast, Loftus et al. (2017) concluded that increased upwelling during the mid-Holocene occurred alongside increased precipitation in the SRZ. Support for this finding comes from plant macrofossils examined by Gabriel et al. (2017) from coastal peatlands in Kwa-Zulu Natal at the heart of South Africa's SRZ showed increase in humidity at about 6 260 cal BP

3.2.3.3. Late Holocene

The transition to the late Holocene seems in general to have featured warmer climatic conditions in the YRZ with slightly more humidity. Between 4000 and 2500 BP, organic sediments preserved at Norga reveal forest spreading that occurred due to greater moisture availability facilitated by higher summer rainfall in the YRZ (Scholtz, 1986). δ15N and δ13C records from Seweweekspoort also indicate a trend to significantly moister and warmer conditions in the late Holocene compared to the early Holocene, starting from 3500 cal BP (Chase et al., 2013). A study of Groenvlei sediments by Wündsch et al. (2016a) found that the period from 4200 to 2700 cal BP was characterised by conditions that were drier than the whole late Holocene period. Phases around 3500 and 2500 cal BP featured maximum summer SSTs that were perhaps 1°C lower than today (Cohen and Tyson, 1995). Reduction in summer rainfall led to a drier environment that was not conducive to the preservation of *Podorcarpus* forest elements between 2600 and 1300 BP (Scholtz 1986). Deacon and Lancaster (1988) also found dry conditions at Norga peat, specifically from 2800 to 1600 BP. Following this, a peak in abundance of C4 grasses was observed at Cango Cave stalagmite record, indicative of warm tropical conditions at 2100 cal BP (Talma and Vogel, 1992).

The last 2000 cal BP was characterised by generally wet and warm conditions with two notable phases that globally have been recorded as being associated with strong climate contrasts, *viz*. the Medieval Climate Anomaly (MCA) and the Little Ice Age (LIA). According to Lüning et al. (2018), the MCA occurred between 950 cal BP and 750 cal BP and, during this period, southern Africa became wetter, with the exception of the WRZ. SRZ experienced wetter conditions due to intensification of the easterlies, while drier conditions in the WRZ occurred due to a reduction in the Atlantic westerlies (Hahn et al., 2016; Hahn et al., 2017). Climate variability in the late Holocene from 2000 cal BP is associated with the ENSO which brings warm and drier conditions to the SRZ (Zhang et al., 2015; Humphries et al., 2017), however the impact of the ENSO is mostly experienced on the northeastern parts of the country and does not affect YRZ moisture significantly (Mulenga et al., 2003). It appears that the WRZ precipitation benefited from the intensified easterlies as studies indicate wetter conditions during the MCA. Warmer climate conditions reappeared at Norga Peat between 1300 and 850 cal BP as seen in the increase in pollen evidence of more

mesic vegetation (Scholtz, 1986) and in the stalagmite record at Cango Cave (Talma and Vogel, 1992). Cohen and Tyson (1995) and Holmgren (1999) also showed evidence for warmer and wetter conditions during the MCA in southern Africa. Furthermore, it was more humid than present at Groenvlei from 1200 cal BP until today (Martin 1968; Wündsch et al., 2016). Quick et al. (2018) lends support to this, citing that at Eilandvlei, current coastal thicket and afrotemperate forest system evolved in the last 900 cal BP (Quick et al., 2018). Further support for a warmer climate occurs offshore, where Hahn et al. (2017) indicated low SST's during the MCA from core GeoB 18308 on the Agulhas Bank which occurred due to the southerly shift of the South Indian Ocean anticyclone (SIA) which resulted in increased upwelling and warm onshore conditions.

The recent Groenvlei record also indicated that the LIA was cooler than present (610 to 140 cal BP) (Wündsch et al., 2018). Evidence of this lies in the mean annual temperatures that were 1-2 °C lower than today during the LIA as shown through the 18O record from Cango Caves (Talma and Vogel, 1992). In the WRZ, at Voelvlei and Buffeljacht, Carr et al. (2006) noted lunette formation at 700 and 450 cal BP, suggesting drier conditions during the LIA.: drier palaeoclimate conditions during the LIA were influenced by the reduction in precipitation from tropical moisture bearing systems as well as a reduction in the landward moving rainfall systems that source moisture from the Agulhas (Carr et al., 2006).

3.3. Sea-level variation and landscape modifications

3.3.1. Marine influence, freshwater inflows, changes in lake morphology

Palaeoenvironmental reconstruction of onshore environments remains difficult to establish due to the lack of well preserved fluvial and lake records that got removed through frequent strandline migration prior to the Holocene (Compton, 2001). Quaternary sea-level changes in southern Africa have been composed through studies using dated beach rocks, lagoonal sediments and wave-cut platforms (Miller et al, 1995; Ramsay, 1995; Compton, 2006). Recent studies have demonstrated the use of ecological proxies such as marine diatoms (Kirsten et al., 2018) and intertidal foraminifera (Strachan et al., 2014) to reconstruct sea-level changes in coastal lakes. Two regional sea-level curves are available: one on the east coast by Ramsay (1995) (Figure 4 a) supplemented by Strachan et al. (2014) (Figure 4 b) and another by Compton (2006) for the west coast. The south coast is yet to have a comprehensive sea-level reconstruction curve.

The Agulhas Bank is an extensive continental shelf on the southernmost margin of the African continent. A significant portion of the Agulhas Bank was submerged by the increasing sea-level at the onset of the current interglacial, and during periods of marine transgression during the Holocene (Compton, 2001). Tectonic activity is thought to have played a minor role in sea-level variation due to the low amplitude of tectonic uplift/subsidence in southern Africa during the quaternary (Compton and Wiltshire, 2009) and negligible vertical crustal motion (Fisher et al., 2010). Instead, the inland barrier dunes would have influenced local sea-level (Cawthra et al., 2014). Prior to the Holocene, global sea-level had been the lowest during the last glacial maximum at 18 000 cal BP (Fairbanks, 1989; Ramsay and Cooper, 2002). Evidence from offshore palaeodunes on the Agulhas Bank suggested that sea-level was -100 m below present sea level during this period (Bateman et al., 2011; Cawthra et al., 2016). Post LGM climate amelioration led to warmer global temperatures and a rapid process of deglaciation that led to sea-level rise. According to Ramsay (1995), sea-level rise in South Africa between 9000 and 8000 BP was in the range of 8 mm yr^{-1}. Cawthra et al. (2014) conducted a detailed seismic survey at Swartvlei and discovered a submerged Pleistocene aeolianite, and eroded substrates of the aeolianite found at the centre of modern-day Swartvlei that were probably reworked and deposited during the accelerated sea-level rise. Following this, a deceleration in sea-level occurred, and was the primary driver behind the formation of many coastal lakes and lagoons around South Africa. Low topographic gradient of the Wilderness Embayment and the prominent aeolianite dune deposits led to damming of water evident in the modern-day series of lakes in the Wilderness including Swartvlei (Bateman et al., 2011).

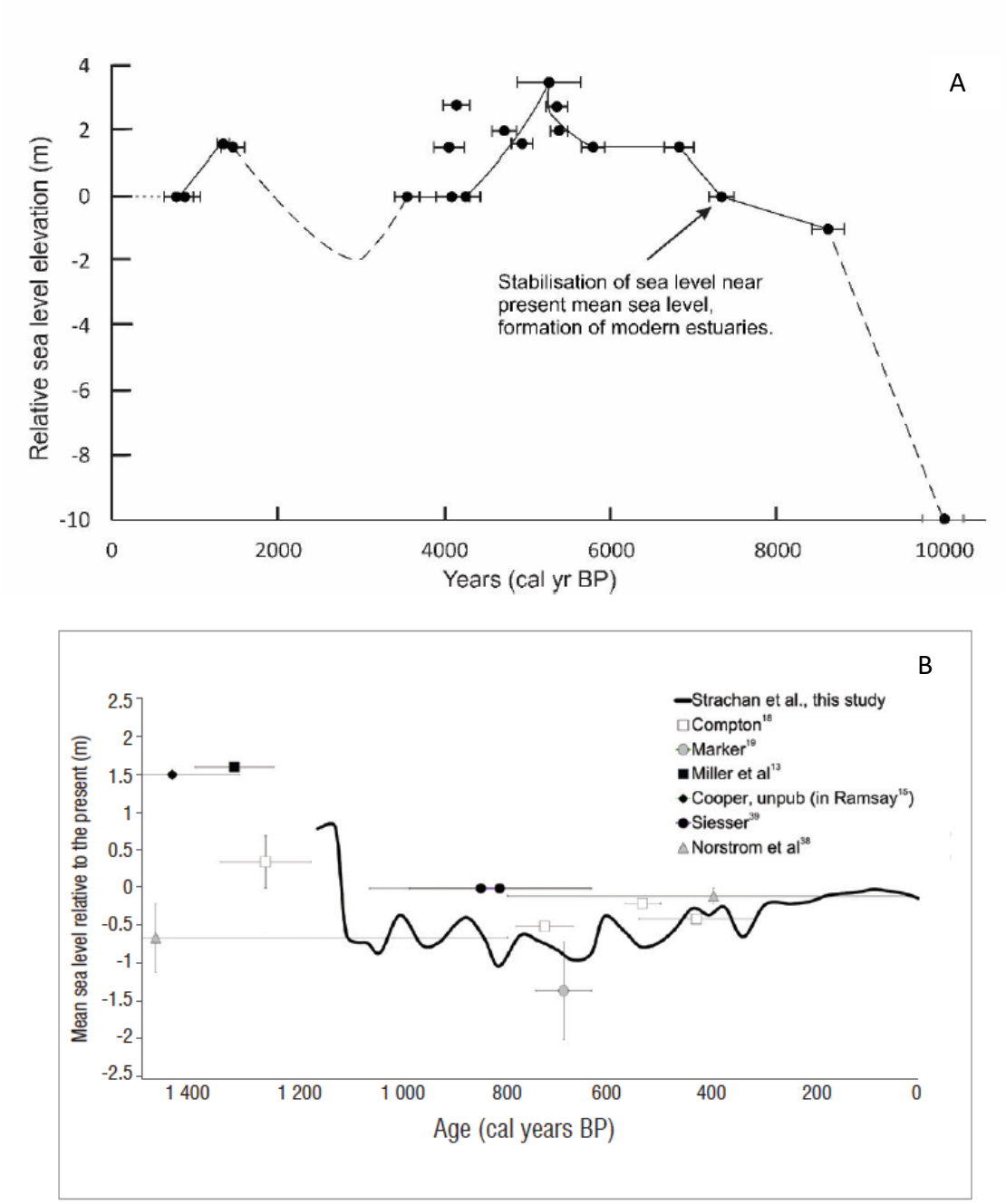

Figure 4: a) Holocene sea-level Fluctuations in sea level on the east coast of South Africa (Ramsay, 1995). Age calibration used Southern Hemisphere atmospheric curve SHCal13 (Adapted from Higgs (2017)) b) Late Holocene east coast sea-level curve from Strachan et al. (2014)

Following formation of the estuaries, sea-level continued to vary during the Holocene. Many studies have recorded a marine transgression during the Holocene, although, uncertainties remain in respect of the timing, elevation and extent thereof. For the west coast, Baxter and Meadows (1999) have suggested that the mid-Holocene Highstand at 6000 BP was 1.5 m to 3m higher than present day mean sea-level. Baxter

and Meadows (1999) also noted a brief marine regression period around 7000 cal BP where sea level regressed by 3-4 m. Scott and Lee-Thorp (2004) found the mid-Holocene highstand to have exceeded 2 m above present sea-level, terminating at 5600 BP. The Eilandvlei system was markedly impacted by the strong marine influence between 8900 and 4700 cal BP (Wündsch et al., 2018; Kirsten et al., 2018). Sea-levels then receded after the mid-Holocene (Carr et al., 2015). When the sea regressed after the mid-Holocene, a low energy environment prevailed, facilitated by sediment accretion on the dunes surrounding Swartvlei which constricted the estuary mouth (Cawthra et al., 2014). A sea-level lowstand then occurred in the southern Cape between 3700 and 2300 cal BP as inferred from the dominance of saltmarsh vegetation at Eilandvlei (Quick et al., 2018). Following this, Ramsay (1995) proposed that sea-level returned to present day levels and subsequently rose by 1.5 m at around 1600 cal BP. Furthermore, according to evidence from a beach rock studied by Marker (1997), relative sea-level nearby Knysna Estuary was as high as 0.7 to 2 m above present sea-level at 1250 cal BP. Baxter and Meadows (1999) noted the brief increase in sea-level earlier, at around 1400 cal BP on the West coast. It appears however, that any rise in sea-level after 3000 cal BP was not recorded in the Wilderness Lakes Eilandvlei and Groenvlei, probably due to the elevated sand dunes that developed and separated the lakes from the ocean after 3500 cal BP due to increased aeolian activity (Bateman et al., 2011; Whitfield et al., 2017). Abundance of freshwater diatoms at Eilandvlei between 1800 and 1400 cal BP indicated that the system developed into a coastal lake with progressively less sea-water entry, making it less likely for a later marine incursion to reach the lake (Kirsten et al., 2018).

Chapter 4: Methods

The chapter begins by describing the fieldwork methods that were employed in coring the lake to collect sediments. This is followed by a description of the post-coring laboratory procedures beginning with the dating methods followed. Finally, statistical tools used to analyse the sediment profile based on XRF and grain size results are presented.

4.1. Fieldwork methods

Site Selection and Coring Procedure

Hydro-acoustic investigations were conducted on the Wilderness lakes in 2010 using a parametric echo sounder (Innomar SES 96 light, frequency: 96 and 105kHz) (Clausnitzer, 2011)) in order to find, in particular, regions of high sediment accumulation. These investigations identified long, continuous and undisturbed sediment sequences and indicated preferred coring locations in Swartvlei (Figure 5). Subsequently, in 2013, a field campaign was undertaken on multiple lakes in the Wilderness region including Swartvlei. The campaign yielded several cores from the preferred locations (SV 13) and a high rate of sediment retrieval was achieved. A UWITEC piston coring device (www.uwitec.at/html/pistoncorer) was used to collect three parallel sediment cores:

SV13-1V, SV13-6 and SV13-7 were extracted at a water depth of 9 m located in the mid-eastern section of the lake, covering 700 cm depth. Locations of the cores are found in Figure 5 below. The three sediment cores were combined into one continuous composite profile through the correlation of distinct macroscopic layers. With the exception of a 40 cm core loss at the base of SV 13-6 (4-6), all of the sediments remained in the PVC tubing once retrieved; following shipment to Germany, the cores have been stored in the dark at 4 °C in the cold storage room at the Physical Geography department of the Friedrich-Schiller-University Jena.

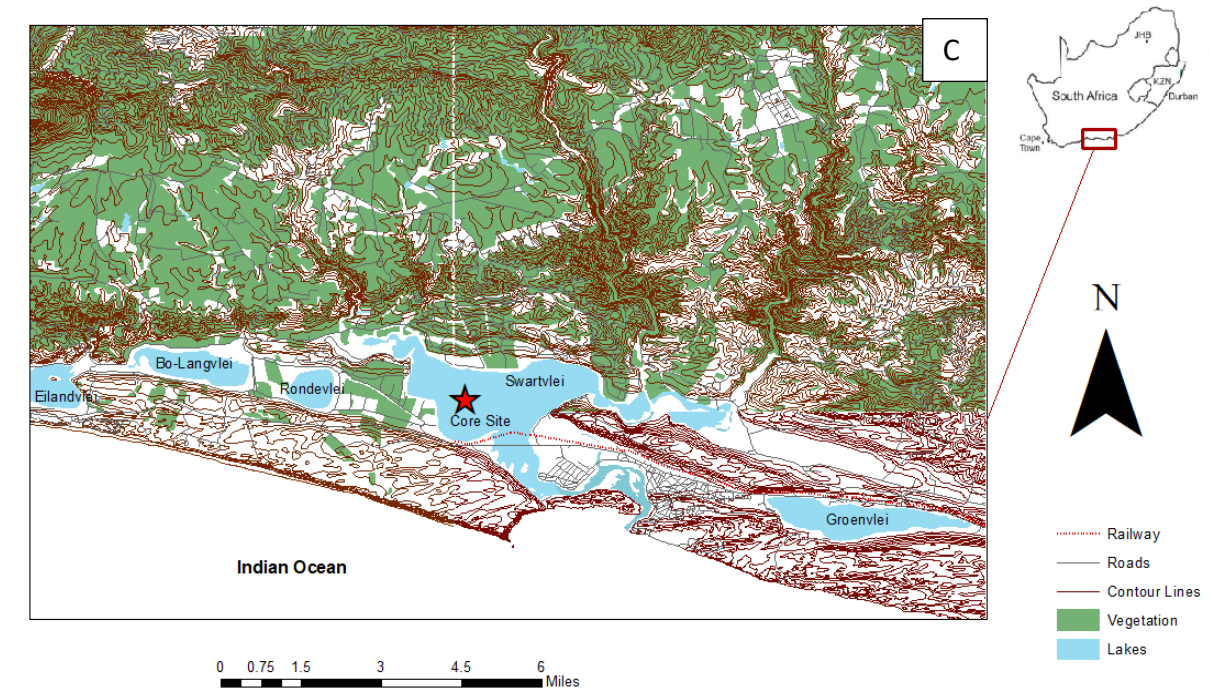

Figure 5: c) Map of the wilderness lakes with SV core site marked by red star d) Satellite image showing the Swartvlei coring sites (Source: Google Earth, 2018)

The core labelling system used for Swartlvei is explained using an example as follows “SV 13-6 (2-4) B”: “SV” = Swartvlei. “13” = year in which the core was extracted (in this case, 2013). “(2-4)” = the sediment

depth covered by that specific core, in this case between 2 m and 4 m. “B” = denotes whether this core section was at the top of bottom section of the 2 m core that was split into two sections to ease core handling. Letter B refers to the top section, while letter A refers to the bottom section.

Table 1: Location and depth retrieval of each core

Core ID	Latitude (S)	Longitude (E)	Coring device	Section depth (m)
SV 13-1 V	33°59.767'	22°45.071'	Gravity with Hammer	0 - 1.3
SV 13-5	33°59.763'	22°45.078'	Piston	0 - 4
SV13-6	33°59.759'	22°45.079'	Piston	2 - 7.2
SV 13-7	33°59.761'	22°45.079'	Piston	1.5 - 3.5

Piston coring was deemed appropriate for this lake due the system’s ability to collect undisturbed samples from the sediment-water interface. Piston coring works by creating a vacuum in the coring chamber that helps to prevent sediment compression as the sediments are drawn from the lake bed into the PVC tube (Blomqvist 1991; Wright, 1993). Piston coring process is illustrated in Figure 6. Poor collection of sandy material is a limitation of the system and occurs because the weak cohesion forces of the sand grains allow them to escape the coring tube when the core is pulled to the surface. To account for this, a core catcher is used at the bottom of the piston corer and has proved to minimise sediment loss significantly. Notwithstanding this limitation and the high cost of the piston coring system, it was chosen as the coring mechanism for this lake because of the ability to reach deep sediments (Glew et al., 2001).

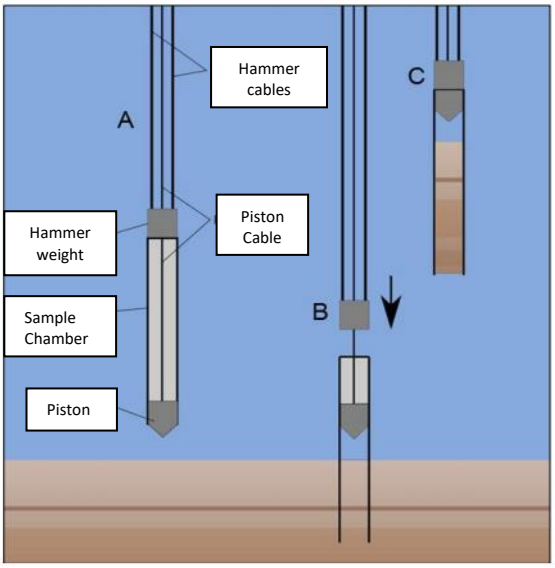

Figure 6: Three step illustration of piston coring system with a hammer weight (A) shows the submerged piston before it reaches the sediment surface. B) coring device penetrates the sediment with the wire holding the piston in place C) piston corer is pulled to the surface with the retrieved sediment held by the vacuum between the sediment and the piston (Adapted from Frew and Craig (2014))

4.2. Laboratory Methods

After coring, various laboratory techniques described below were used to establish the chronology and to examine the physical and chemical properties of the sediments. The methods used in this study (illustrated with a flowchart in Figure 7) were carefully selected based on their wide use in palaeoenvironmental studies and ability to produce reliable results.

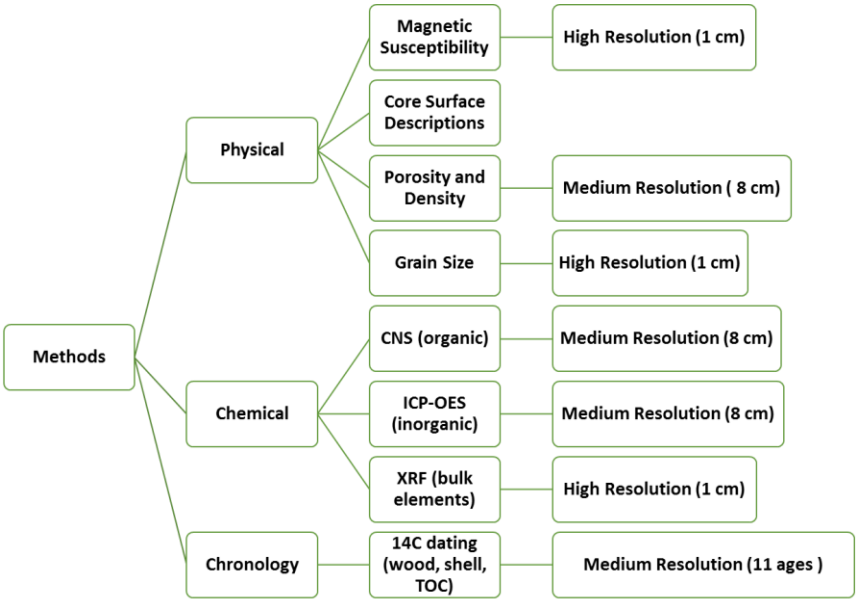

Figure 7: Flowchart showing methods followed in this study and the resolution level based on sampling details

4.2.1. Age-Model development / chronology establishment

Seven samples of wood, marine shells and bulk organic matter were taken through Accelerator Mass Spectrometry (AMS) at Poznań Radiocarbon Laboratory in Poland to measure residual radioactivity of the organic content found in the sediment cores. Two OSL ages were obtained and kindly provided by Prof. Dr. Reunhard Laupe, University of Greifswald.

Radiocarbon data were processed with BACON age modelling program underpinned by statistical analysis software, R (version 2.3.4) (Blaauw and Christen, 2011). BACON incorporates Bayesian Statistical Modelling that takes into account different rates of accumulation of sediments and uses prior information of ages gathered for that area. Four ages that were not in stratigraphic order, as well as the OSL ages due to large errors, were excluded from the Bacon age development model. SH13 calibration was applied for terrestrial sediments that were likely deposited during lacustrine conditions (Hogg et al., 2013.), while Marine13 calibration curve was used to calibrate the marine samples (Reimer et al., 2013). Marine reservoir correction (Δ R) was applied further applied to the marine sample to account for the difference in radiocarbon (^{14}C) between the atmosphere and the marine surface ocean (Maboya et al., 2017).

4.2.2. Core splitting, photography and description

Cores were split lengthwise and then photographed in 15 cm sections using a mounted Nikon D40 camera within one hour of core opening. 2D photographs taken immediately after core splitting help to preserve the colour on core surface which can change due to oxidation and water loss. Prior to photography, the open cores were prepared by scraping a sharp knife carefully across the exposed surface, the knife was cleaned after each scrape to avoid contamination. Lighting was kept constant throughout photography as it took place in a dimly lit room with the core inside a dark box illuminated by a controlled lamp of known colour temperature. The photographs were adjusted for brightness and contrast and reconstituted using Adobe Photoshop CS6 (Version 7.0) to produce continuous photographs for each core. The cores were then described lithologically with notes made on discernible sediment facies, texture, colour and visible macrofossils. Sediment surface structures such as laminations, gas bubbles and burrows, where observed, were noted in the core description sheets. A composite profile was made using layers with similar macroscopic features.

4.2.3. Particle Size

Samples of approximately 1 cm^3 were taken in 1 cm intervals for the upper 2.5 m from sediment cores SV13-1V, SV 13-7B and SV13-7A sub-sampled using Nakagagwa's double-L channel sampling method (Nakagagwa, 2007). The sampled sections were cleaned using a scalpel and cut in a horizontal direction to the axis of the core to avoid contamination from material above or below. These samples were measured using a laser diffraction particle analyser (Beckmann Coulter LS 13320). The Beckmann Coulter laser diffraction instrument employs Fraunhofer theory which assumes that the particles are spherical, and that only diffraction takes place on the surface of the particles. This theory does not account for transmission of light through the particles unlike its competitor, the Mie theory which includes an absorption coefficient (Uncles & Mitchell, 2017). While the Fraunhofer theory is widely applied, it does not provide accurate measurement for samples <10µm in diameter; hence it can overestimate the clay fraction of the sediment, when compared to gravimetric techniques (Pye & Blott, 2004). In order to overcome this, seven runs of measurements are made per sample, and continued until a reproducible signal is evident. In the pre-treatment phase, the samples were treated with a mixture of acids to destroy carbonates and organic matter (10% H_2O_2 and 10% HCl) and a second round of the same acids with a 30% concentration. 5 ml $NaHPO_4$ was added to aid with dispersal for separation of the particles. Only particles with sizes between 0.1 and 2000 µm entered the diffraction analyser for size measurements and mean

grain size measurements were conducted using Blott and Pye's geometric methods of moment (Blott & Pye, 2001). Statistical analysis of the particle size distribution was conducted on the first reproducible run using Gradistat 4.2 software package (Blott and Pye, 2001), showing mean, mode, sorting, kurtosis and skewness. The formulae and categories of the statistical parameters are shown in Figure 8 and Figure 9. Constrained Incremental Sum of Squares (CONISS) was used for cluster analysis to form zones with similar sediment characteristics (Grimm, 1987). CONISS is a multivariate analysis that clusters adjacent stratigraphic zones and is typically used in the interpretation of pollen data. CONISS was used in this study in order to investigate the gradient of change in grain size within the identified stratigraphic zones.

Grain Size phi	Grain Size mm	Descriptive term	
-10	1024	Very Large	Boulder
-9	512	Large	
-8	256	Medium	
-7	128	Small	
-6	64	Very small	
-5	32	Very coarse	Gravel
-4	16	Coarse	
-3	8	Medium	
-2	4	Fine	
-1	2	Very fine	
0	1	Very coarse	Sand
	microns		
1	500	Coarse	
2	250	Medium	
3	125	Fine	
4	63	Very fine	
5	31	Very coarse	Silt
6	16	Coarse	
7	8	Medium	
8	4	Fine	
9	2	Very fine	
		Clay	

Figure 8: Size classification used for particle size data used in GRADISTAT, modified from Udden (1914) and Wentworth (1922)

Mean	Standard Deviation	Skewness	Kurtosis
$\bar{x}_g = \exp \frac{\Sigma f \ln m_m}{100}$	$\sigma_g = \exp \sqrt{\frac{\Sigma f (\ln m_m - \ln \bar{x}_g)^2}{100}}$	$Sk_g = \frac{\Sigma f (\ln m_m - \ln \bar{x}_g)^3}{100 \ln \sigma_g^3}$	$K_g = \frac{\Sigma f (\ln m_m - \ln \bar{x}_g)^4}{100 \ln \sigma_g^4}$

Sorting (σ_g)		Skewness (Sk_g)		Kurtosis (K_g)	
Very well sorted	< 1.27	Very fine skewed	$< {}^{-}1.30$	Very platykurtic	< 1.70
Well sorted	1.27 – 1.41	Fine skewed	${}^{-}1.30 - {}^{-}0.43$	Platykurtic	1.70 – 2.55
Moderately well sorted	1.41 – 1.62	Symmetrical	${}^{-}0.43 - {}^{+}0.43$	Mesokurtic	2.55 – 3.70
Moderately sorted	1.62 – 2.00	Coarse skewed	${}^{+}0.43 - {}^{+}1.30$	Leptokurtic	3.70 – 7.40
Poorly sorted	2.00 – 4.00	Very coarse skewed	$> {}^{+}1.30$	Very leptokurtic	> 7.40
Very poorly sorted	4.00 – 16.00				
Extremely poorly sorted	> 16.00				

Figure 9: Formulae used for the calculation of sorting, skewness and kurtosis using the Geometric Methods of Moments in GRADISTAT

4.2.4. Magnetic susceptibility

Magnetic susceptibility was measured using a Bartington MS2E sensor (Dearing 1999) in 1 cm measurements for all cores. The sensor was lifted every 5 cm to capture air measurements to reduce measuring bias that may be caused by a potential temperature drift of the sensor. Five MS measurements were taken at each depth and an average was calculated per cm.

4.2.5. Sediment density and water content

Accordingly, mass and volume measurements of samples at 8 cm intervals throughout the core were taken prior to and after freeze-drying for 48 hours. Samples were collected with plastic syringes in varying volumes between 4-6 cm^3 depending on how dense and cohesive the sediment were to be successfully retrieved by the syringes and were cleaned after each use to avoid contamination. The wet and dry masses were measured using a laboratory scale, contained in glass jars. The data was used to calculate wet and dry bulk density of the sediments, as well as water content by measuring the amount of water lost after oven drying. Dry Bulk Density and water content were calculated using the following formulae:

Dry Bulk Density (g cm^{-3}) = mass (g) / volume (cm^3) (1)

Water content = (mass of wet sediment (g) - mass of dry sediment (g)) * 100 (2)

4.2.6. XRF scanning

XRF Core Scanner data were collected every 1 cm down-core over a 1.2 cm^2 area with down-core slit size of 10 mm using generator settings of 30 kV, current of 1 mA, and a sampling time of 15 seconds directly at the split core surface with XRF Core Scanner II (AVAATECH Serial No. 2) at the MARUM - University of Bremen. A second run was done with a generator setting of 10kV, current of 0.2mA and a sampling time of 15 seconds. The split core surface was covered with a 4 µm thin SPEXCerti Prep Ultralene1 foil to avoid contamination of the XRF measurement unit and desiccation of the sediment. The data reported here have been acquired by a Canberra X-PIPS Silicon Drift Detector (SDD; Model SXD 15C-150-500) with 150eV X-ray resolution, the Canberra Digital Spectrum Analyzer DAS 1000, and an Oxford Instrument 50W XTF5011 X-Ray tube with rhodium (Rh) target material. Raw data spectra were processed by the analysis of X-ray spectra by Iterative Least square software (WIN AXIL) package from Canberra Eurisys.

4.2.7. ICP-OES analysis

Samples from every 8th cm were extracted for analysis to determine absolute quantities of 21 elements. In total, 77 samples were collected to represent the 700 cm core, samples (10g) were subjected to grounding (<40µm), mortaring and sieving, followed by oven drying. After preparation, the samples are injected into the machine where a liquid sample is atomized, and the ions were excited by an inductively coupled plasma (ICP) (at a temperature up to 10 000 K) for the emission of light. The emitted light was split by a monochromator and element-specific wavelengths measured through an emission spectrometer (OES) were detected. The intensity of emitted photons, Intensity (I), is directly proportional to the concentration (c) of the element. Elemental composition was then determined using ICP-OES (Varian 725-ES) after a modified microwave-assisted aqua regia digestion containing deionised water, HCl (30%) and HNO_3 (30%) in a ration of 1:2:4. Biogenic silica was also measured with ICP-OES following the procedures described by Ohlendorf and Sturm (2008), without pre-treatment with H_2O_2 and HCl, and no centrifuging after NaOH leaching.

4.2.8. CNS analysis

CNS analysis was conducted using CNS element analyser, Elementar Analysensysteme GmbH at Friedrich Schiller University. Samples were collected at every 8 cm depth and 20 mg of each sample was packed in

an airtight container for combustion with Tungsten Oxide added as a catalyst in order to measure Total Carbon (TC), Total Nitrogen (TN) and Total Sulfur (TS). The samples were pre-treated with 10% HCl in order to remove carbonates prior to the determination of TOC, and Total inorganic Carbon (TIC) was calculated as a difference between Total Carbon (TC) and TOC. Molar TOC/TN ratios were calculated using measured TOC and TN values.

To investigate relationships between the geochemical data, correlations were calculated using Pearson correlation coefficients (r-values) with a p-value set to 0.05.

Chapter 5: Results

5.1. Core Photographs

The sediment core is composed of two main sedimentary units; namely unit A, a compacted sandy layer and unit B, a 287 cm long sequence of soft organic-rich silt that was deposited on unit A (Figure 12). This transition coincides with a change in colour from grey to dark brown, changes in texture from sandy to silty, and a decrease in sediment density from high to low (Figure 14). Photographs of the cores are shown below with colour correction.

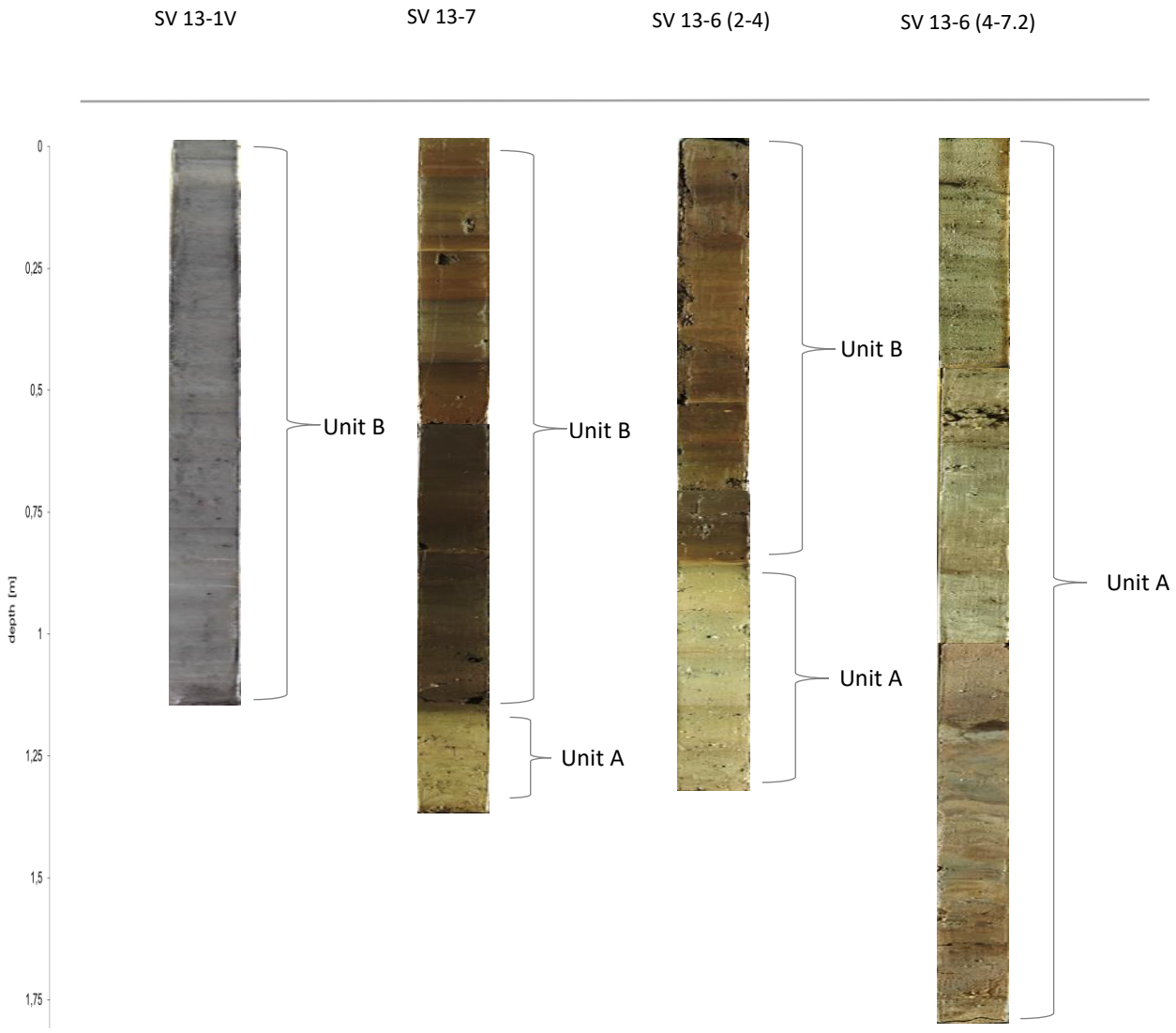

Figure 12: Photographs of Swartvlei cores SV 13-1V, SV 13-6 and SV 13-7 with colour correction

5.2. Chronology

The age model has a basal age of 8630 cal BP at 700 cm sediment depth. Radiocarbon ages were calibrated using Calib software (http://calib.org/calib/calib.html). Age-depth model was developed based on ^{14}C ages as modelled by Bacon Version 2.2 on the R software package Version 3.4.2 (http://chrono.qub.ac.uk/blaauw/bacon.html), and four ages that were not in stratigraphic order were excluded by the model (Figure 10). The average accumulation rate is 0.8 mm yr^{-1} (Figure 11). The accumulation rate is constant from 700 cm to 210 cm at 0.08 cm yr^{-1} and increases to 0.12 cm yr^{-1} at 200 cm. The rate then decreases to 0.065 cm yr^{-1} until 80 cm depth, where it then rises to its highest range between 0.079 and 0.12 cm yr^{-1} until the surface.

Table 2: OSL and ^{14}C ages with errors and calibration curves used to create age model

Core	Sample Type	Measurement Method	Age (BP)	Error (BP)	Sediment Depth (cm)	Calibration	Δ R
SV13-1	TOC	AMS	920	+/- 30	75	SH13	n/a
SV13-1	TOC	AMS	1860	+/- 35	145	SH13	n/a
SV13-7 (1.5-3.5) A	TOC	AMS	2865	+/- 30	199	SH13	n/a
SV13-7 (1.5-3.5) A	wood	AMS	2420	+/- 35	199.5	SH13	n/a
SV13-6 (2-4) B	TOC	AMS	2245	+/- 35	206	SH13	n/a
SV13-6 (2-4) A	carbonates	AMS	6710	+/- 40	280.5	Marine13	187 +/- 18
SV13-7 (1.5-3.5) A	sand	OSL	3180	+/- 440	306	n/a	n/a
SV13-6 (6-7.2)	sand	OSL	15400	+/- 2600	689	n/a	n/a
SV13-6 (6-7.2)	shell	AMS	8310	+/- 50	694.5	Marine13	187 +/- 18
Ages excluded from the age model							
SV 13-6 (4-6) B	carbonates	AMS	9220	+/- 50	397.5	n/a	n/a
SV13-6 (4-6) A	carbonates	AMS	11260	+/- 60	472	n/a	n/a
SV13-6 (6-7.2)	carbonates	AMS	10160	+/- 70	630	n/a	n/a
SV 13-6 (6-7.2)	TOC	AMS	16840	+/- 100	685	n/a	n/a

E

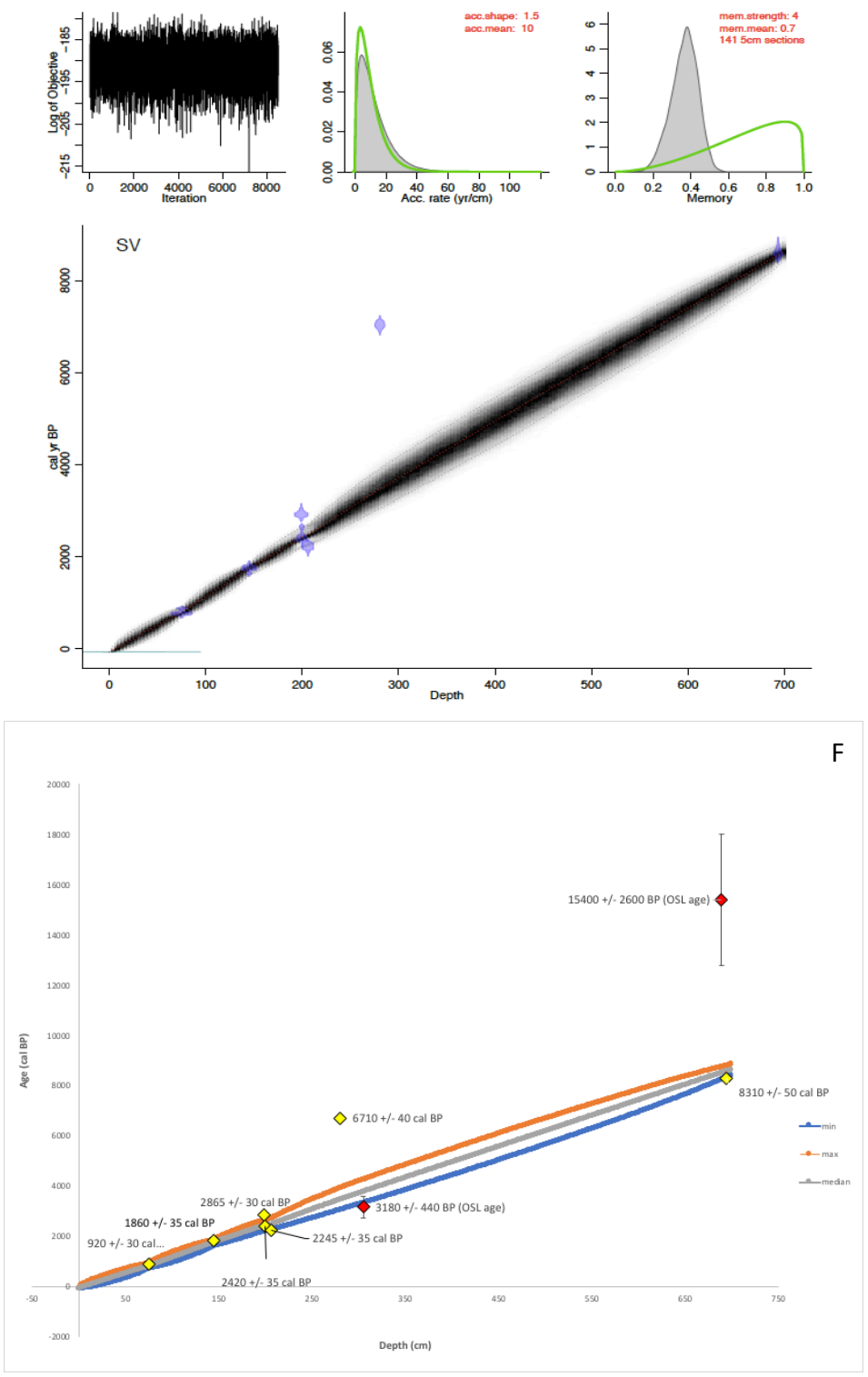

Figure 10: e) BACON age-depth model for SV 13 made using the seven ages in Table 2, f) ^{14}C and OSL ages with errors plotted along with BACON outputs of minimum, maximum and median ages

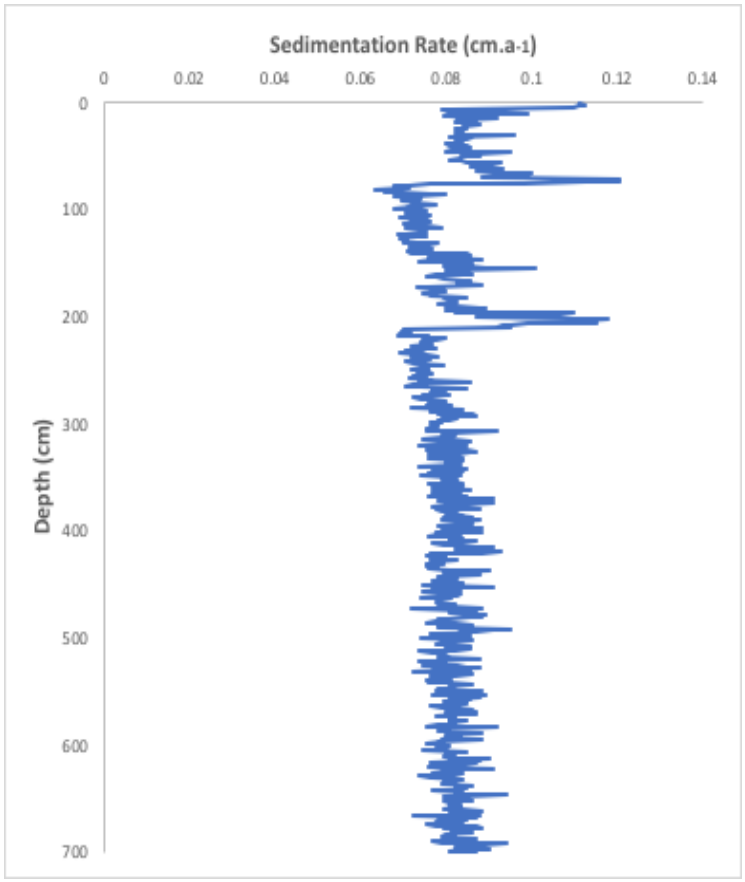

Figure 11: Sedimentation rates for SV 13 based on Bacon age-depth model

5.3. Particle size

5.3.1. Unit A (700 cm to 288 cm)

In Unit A, which ranges from 700 to 288 cm (8620 to 3550 cal BP), there are very low amounts of clay which lie between 1-5% (Figure 13). Thereafter, clay proportions increase gradually to 11% at 288 cm (3550 cal BP) with a peak (14.9%) at 425 cm (5250 cal BP). Silt occurs in slightly higher proportions than that of clay although the overall pattern is very similar. Silt fluctuates strongly, more so than clay, in the lower part of Unit A, where values vary from a low of 4.6% at 698 cm (8600 cal BP) to a high of 76% at 606 cm (7580 cal BP). From 598 cm (7480 cal BP) silt remains below 10% until a pronounced peak of 83% is observed at 425 cm (5240 cal BP) (Figure 3). From 425 cm (5240 cal BP) to the top of Unit A, silt increases with moderate degrees of variability. Sand, ranging between 60-95%, is dominant throughout Unit A, with a mean abundance of 80%. There are marked decreases in sand at 425 cm (5240 cal BP) (1.5%) and 606 cm (7480 cal BP) (18.2%) a gradually reduction from 425 cm (5240 cal BP) towards the top of Unit A, down to 20% at a depth of 288 cm (3550 cal BP).

The mean particle size, which is significantly larger in Unit A, ranges between 100 -300 μm, reflecting the larger proportion of sand in this part of the core. The mean grain size for Unit A starts at around 100 μm at 344 cm (4250 cal BP) before decreasing to a low of 19.3 μm at 288 cm (3550 cal BP) at the top of Unit A. Sorting values range between 3 and 6, meaning that the particles vary between poorly sorted (values 2 to 4) and very poorly sorted (4 to 16). Sediments range from being very finely skewed (<-1.3) to very coarse skewed (>1.30) throughout Unit A. Between 700 and 624 cm (8620 to 7700 cal BP), skewness is more variable, tending toward being very finely skewed, before trending to coarser skewness values up to 380 cm (4690 cal BP) where a gradual tendency towards finer skewness is seen at the top of Unit A. Kurtosis values range between 4 and 11, indicating that the sediments are leptokurtic (3.7 – 7.4) to very leptokurtic (>7.4).

5.3.2. Unit B (287 to 0 cm)

Unit B is far more uniform in the proportions of sand, silt and clay proportions compared to the underlying Unit A. Overall, there is significantly more silt found in this section, varying between 65 to 80% while the clay fraction ranges between 10 and 15%. The lower parts of Unit B are more sandy (~20%) but these

proportions decline to around 5% at 220 cm, whereafter such low values are maintained towards the top of the core.

The mean grain size in Unit A is smaller than in the underlying sediments, remaining well below 20 μm for the most part. Between 287 and 220 cm mean size is more variable, but declines from 20 μm to 7 μm. This trend is interrupted by a peak of 30 μm between 215 and 212 cm (2580 to 2540 cal BP), corresponding to an increase in sand content and, mean particle size reaches 40 μm accompanied by a decline in both silt and clay fractions. From 212 to 21 cm (2540 to 170 cal BP), mean particle size ranges between 6 and 9 μm and shifts to values below 6 μm from 15 cm through to the top of Unit B where sand is almost absent. Except for the peak at 215 – 212 cm (2580 to 2540 cal BP), which is very poorly sorted, the sediments of Unit B are poorly sorted (values 3 to 4). Skewness in the top 212 cm ranges between -0.4 and -0.09, which means that the distribution is symmetrical to coarsely skewed. Kurtosis is 5.3 at 284 cm (3500 cal BP) but values then drop to 2.2 at 252 cm (3500 cal BP to 3080 cal BP), indicating a shift from leptokurtic (3.7 - 7.4) to platykurtic (1.7 – 2.5) distribution. Kurtosis values remain between 2 and 2.5 through to the top of the core.

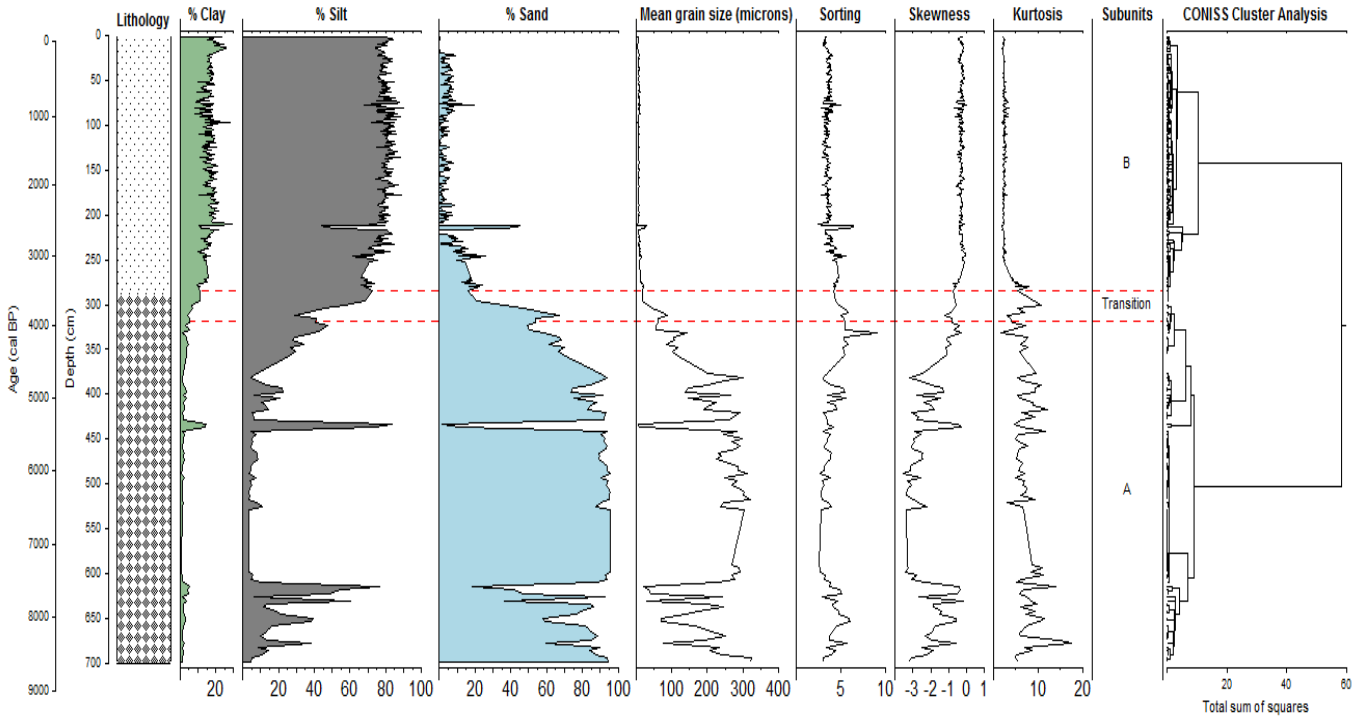

Figure 13: Particle size data for SV composite core against depth (cm) and age (cal BP), with the CONISS cluster analysis and demarcations for Unit A and Unit B

5.4. Magnetic susceptibility

In general, the magnetic susceptibility values are very low in the sediment record with the exception of the basal 80 cm which displays notable fluctuations in this parameter (Figure 14). Overall, magnetic susceptibility ranges between 0 and 550 *10^{-6} SI. Above 600 cm, the signal remains very low through to the surface.

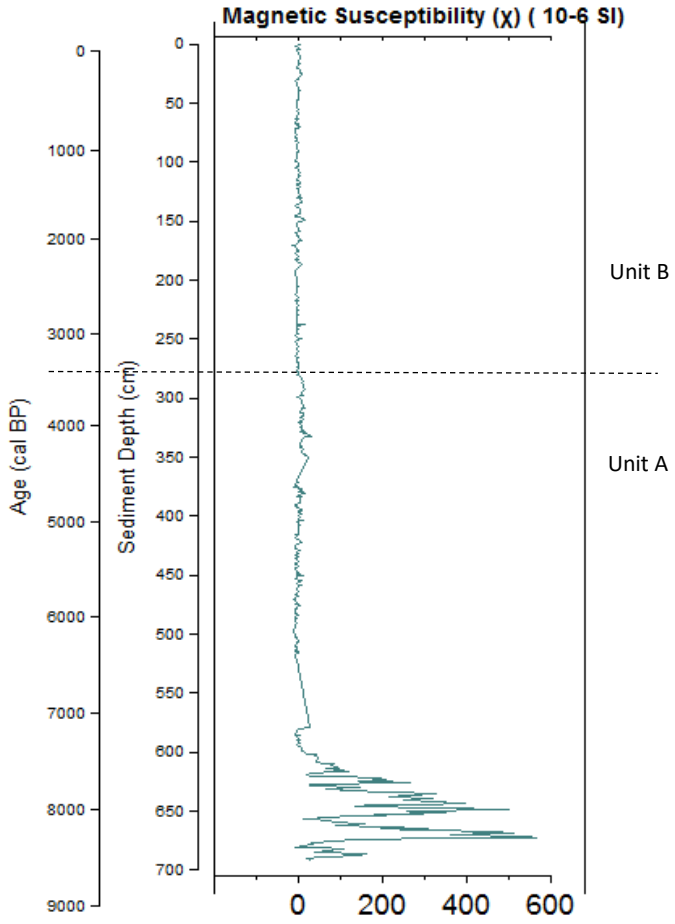

Figure 14: Bulk magnetic susceptibility against depth (cm) and age (cal BP)

5.5. Water content and sediment density

Sediments in Unit A have wet bulk density values that range between 1.8 g cm^{-3} and 2.4 g cm^{-3} from 700 cm to 320 cm (8620 to 3950 cal BP), with a slight decrease to 1.5 g cm^{-3} at 310 cm (3830 cal BP) (Figure 15). The wet bulk density then increases to 3 g cm^{-3} at 260 cm (3190 cal BP), before a marked reduction in values to oscillate around 1 g cm^{-3} at 200 cm (2410 cal BP); these levels are maintained throughout Unit

B. Overall, water loss ranges between 0 and 20% in Unit A, then transitions to higher values from about 300 cm (3700 cal BP). Above 300 cm (3700 cal BP), water loss values lie between 60 and 80% until 150 cm (1810 cal BP), where they decrease to below 60%.

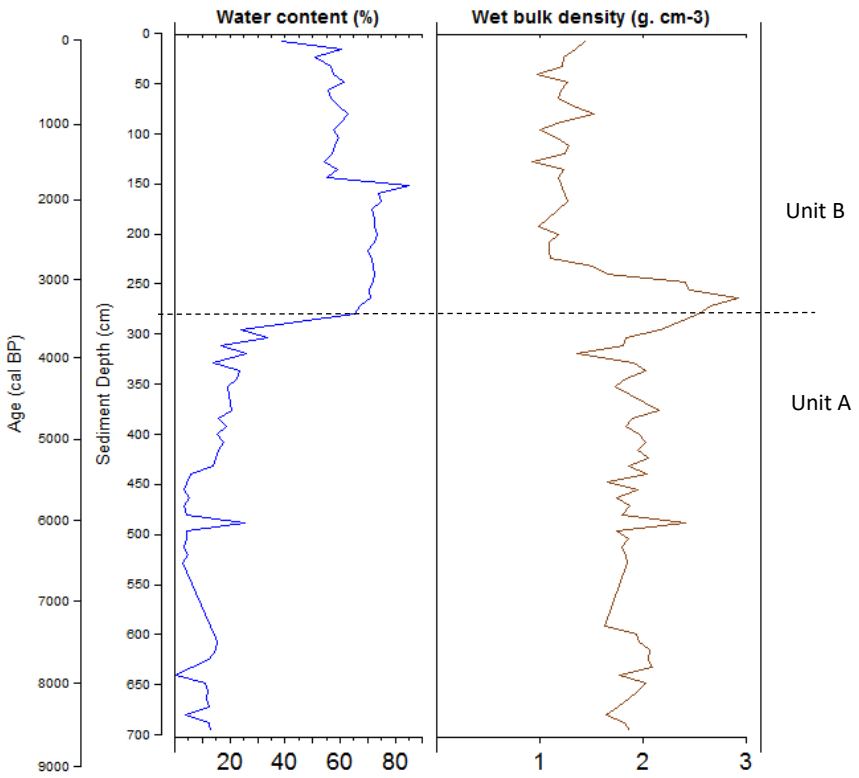

Figure 15: Graphs of wet bulk density (g cm-3) and water content (%) against depth (cm) and age (cal BP)

5.6. Geochemistry

Elements that exhibit significant variation in composition are described below.

5.6.1. Organic content

Markedly higher concentrations of total nitrogen (TN) and total organic carbon (TOC) occur in the Unit B than in Unit A. Overall, the organic content is low between 700 and 400 cm (8620 to 4940 cal BP) (Figure 16). A slight increase occurs between 400 and 300 cm (4940 to 3700 cal BP), followed by a steep rise to high but varying concentrations through to the surface. Both TN and TOC peak at 168 cm (2030 cal BP) (TN = 0.81% and TOC = 11.8%) followed by a return to slightly lower values at 120 cm (1410 cal BP) (where TN = 0.52% and TOC = 6.5%). Both TN and TOC increase again to a lower peak at 48 cm (490 cal BP) before approaching the lower values found at the top of the core.

Total Sulphur (TS) follows a similar trend to that of TN and TOC with higher values in Unit B, although they increase earlier (Figure 16). TS ranges between 0 and 0.50% in the section between 700 and 320 cm (8620 to 3950 cal BP), while reaching higher proportions (2.5-4.23%) in the upper part of Unit B from 272 cm (3340 cal BP) to the surface. The highest TS values are recorded between 200 cm and 176 cm (2410 to 2130 cal BP) (4.18 to 4.23%). TOC/TS ratios are low in Unit A (0.67 to 1.93) and high in Unit B (2.04 to 3.53) while TOC/TN ratios are more variable and higher in both units. TOC/TN ratios range from 1.59 to 9.88 in Unit A and lie between 11.17 and 14.6 in Unit B; both ratios peak at 392 cm (2840 cal BP). Extremely low quantities of P ranging from 33 to 90 ppm are observed from 700 to 456 cm (8620 to 5630 cal BP), thereafter, the concentration increases sharply to >1500 ppm in the upper part of the sequence. A sharp decline to lower concentrations however occurs at 176 cm (2130 cal BP), immediately followed by a consistent increase from 160 cm (1930 cal BP).

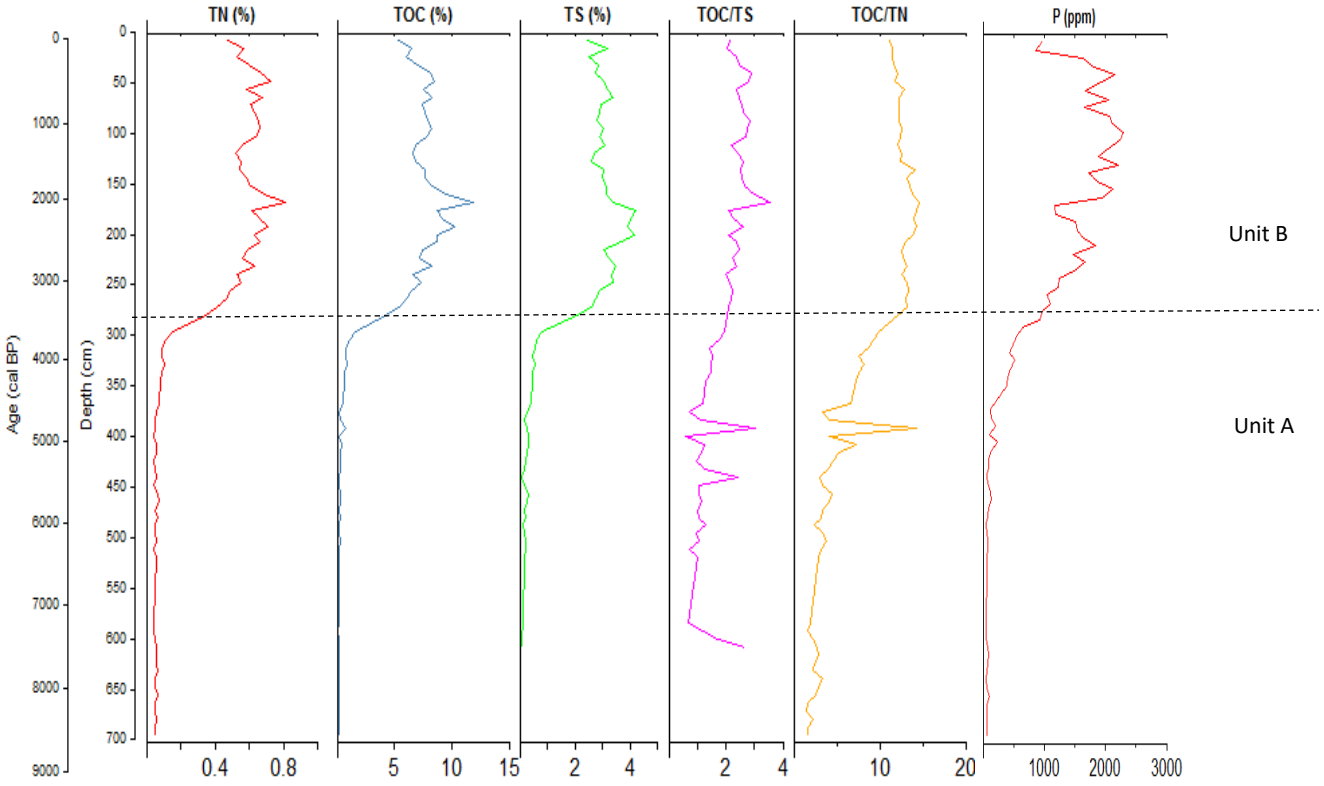

Figure 16: Plots of TOC, TN and TS (CNS), TOC/TS, TOC/TN and P (ICP-OES) against depth (cm) and age (cal BP)

BiSi concentrations are low in Unit A (between 0.13 and 1.43%) and high in Unit B (between 3.67 and 8.86%) with the exception of the top 16 cm (110 cal BP) where they decrease again to 0.89% (Figure 17). A profound peak to 8.86% occurs at 168 cm (2030 cal BP), followed by a sharp decrease to 4.44% at 168 cm (1830 cal BP).

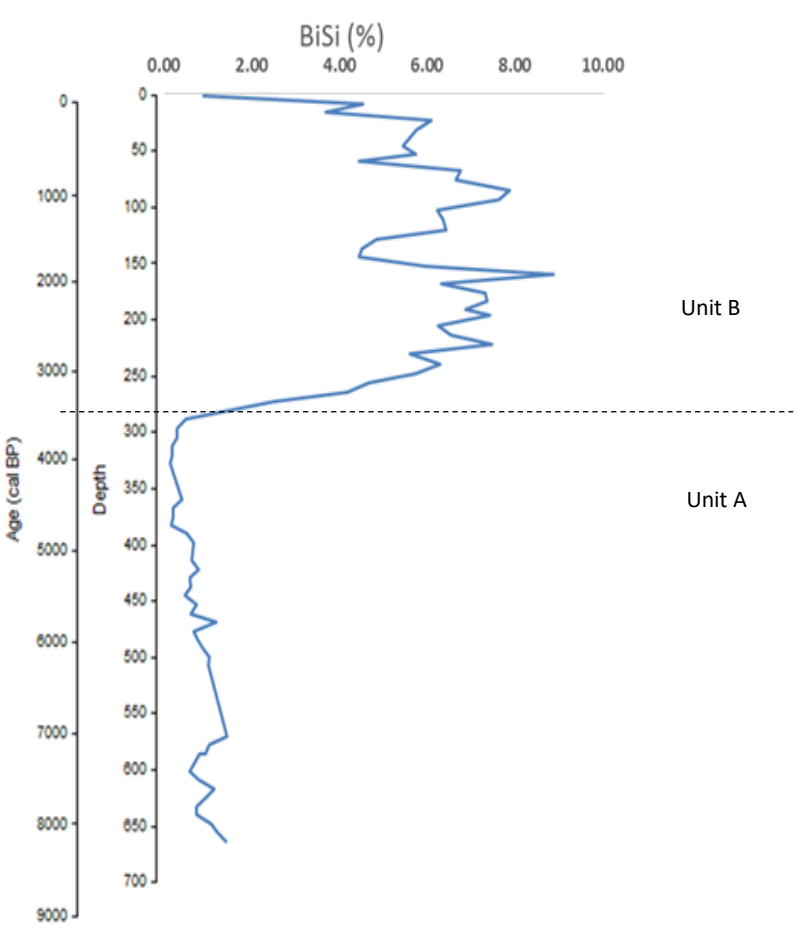

Figure 17: Biogenic silica (%) against depth (cm) and age (cal BP)

5.6.2. Calcium, Strontium and Total Inorganic Carbon (TIC)

Figure 18 indicates that the lowest concentrations of Ca, Sr and total inorganic carbon (TIC) are found at the base of the core although they exhibit a gradual increase between 696 to 624 cm (8580 to 7700 cal BP). From 472 cm (5830 cal BP), Ca and Sr levels vary greatly with reversals in the increasing trend at 440 cm (5430 cal BP), 400 cm (4940 cal BP) and 384 cm (4740 cal BP). The Ca and Sr levels then rapidly rise to the highest concentrations which are maintained between 344 cm and 296 cm (4548 - 3650 cal BP) where

the concentrations range between 88030 and 105 600 ppm. Above 296 cm (3650 cal BP), there is a sharp decline to lower values (e.g. 6220 ppm Ca at 232 cm (2810 cal BP)). Above 232 cm (2810 cal BP), Ca declines further and remains low. Sr concentrations fluctuate around 100 ppm from 232 cm (2810 cal BP) before declining to lower values in the last 400 years. TIC follows a similar trend in that concentrations are lower near the base of the core, increase sharply to higher values in the middle section and return to low values following the transition to Unit B. TIC values achieve maximum levels in the same section as Ca and Sr, ranging between 2.49% and 3.60% maintained over roughly 72 cm before dropping to relatively low values in the upper part of Unit B through to the surface.

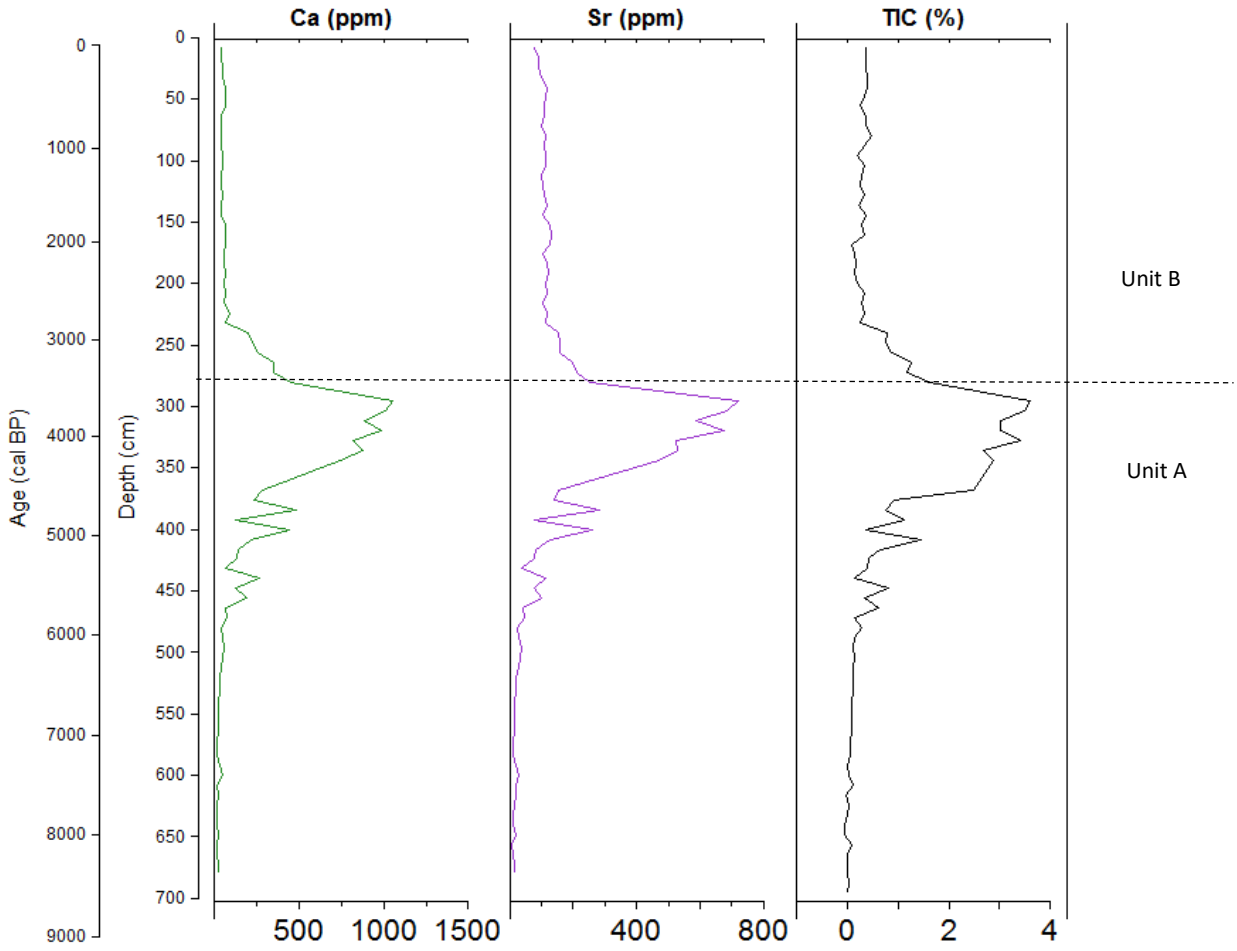

Figure 18: Plots of Ca, Sr (ICP-OES) and TIC (CNS) against depth (cm) and age (cal BP)

5.6.3. Minerogenic content

Between 700 and 600 cm, Al, K and Fe concentrations start very low but reach a minor peak at 608 cm (7510 cal BP) before declining to lower values (Figure 19). Above 312 cm (3850 cal BP), all three elements

increase markedly, and higher concentrations are maintained through to the present; K exhibits more variability than Fe. Fe/Al ratios show an inverse relationship to the Si/Al ratios where the signal is weak in unit A and strong in unit B. The negative correlation between Si/Al and Fe/Al (r = -0.601) is statistically significant at 1% (p-value = 0.0001).

Pb concentrations are low or below detectable levels prior to 272 cm (3340 cal BP) but gradually increase thereafter to 20 ppm until the present (Figure 19). Mn concentrations are very low from the base of the core and only increase slightly from 384 cm. A shift to higher values occurs at 240 cm and Mn concentrations vary thereafter, reaching peaks at 240 cm (2920 cal BP) (721 ppm) and 184 cm (2230 cal BP) (825.4 ppm) before a sudden decline at 128 cm (1520 cal BP) (251 ppm). Mn returns to high levels after 100 cm (1140 cal BP) and continues to increase until the surface of the core.

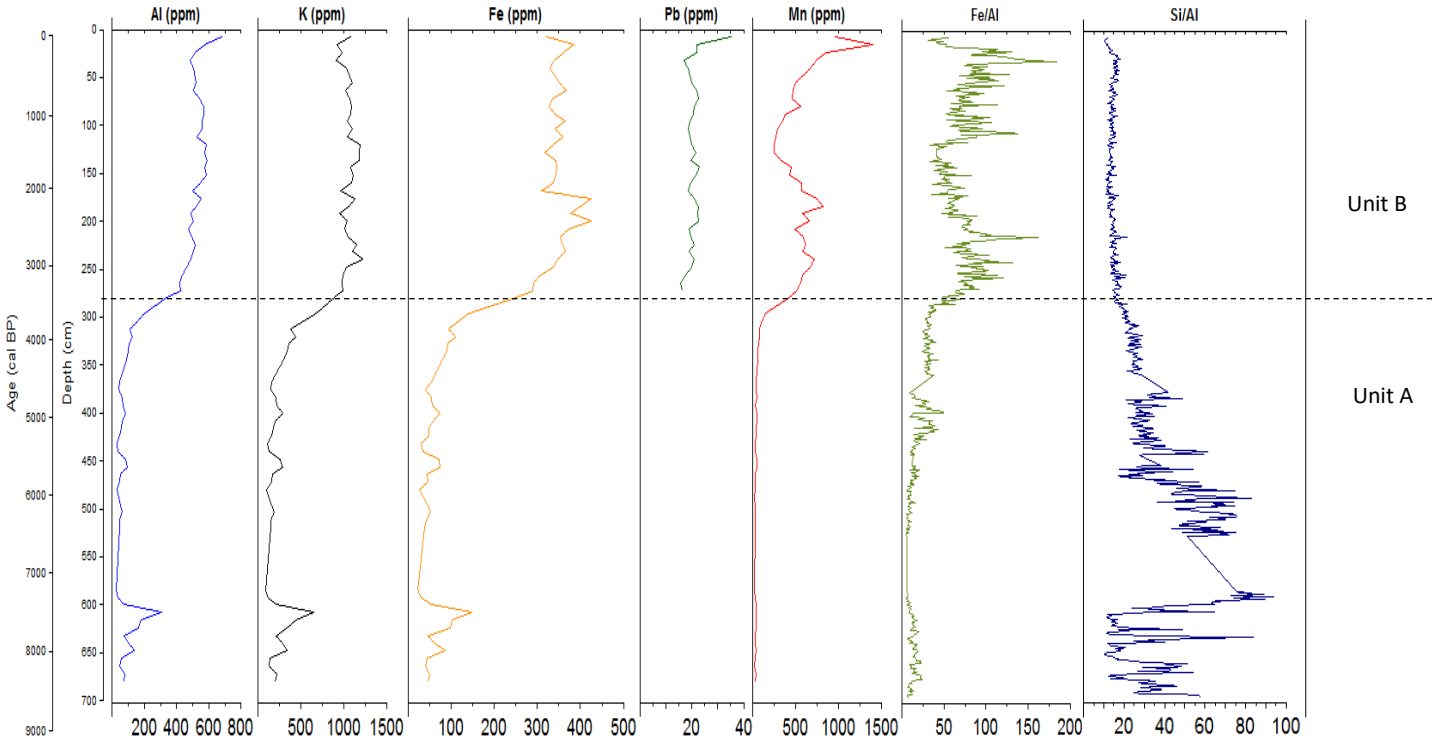

Figure 19: Plots of Aluminium (Al), Potassium (K), Iron (Fe), Lead (Pb), and Manganese (Mn) (all ICP-OES) and Fe/Al and Si/Al (XRF) against depth (cm) and age (cal BP)

Zr, Ti and Rb exhibit broadly similar trends, with variable values near the base followed by a shift to slightly lower but variable concentrations (Figure 20). Above 376 cm, Zr, Ti and Rb there are markedly higher concentrations in all three. Zr which oscillates around 25 ppm until a slight drop at 56 cm (23 ppm), followed by a peak to the highest in the record (27 ppm) at 16 cm. Si values have a markedly different

pattern, with relatively high counts in the lower parts of the sequence and, between 700 and 427 cm (8620 to 5270 cal BP), vary between 30 000 and 40 000 counts. Si then declines to lower counts of between 10 000 and 20 000 between 427 cm and 277 cm (5270 to 3410 cal BP), before declining to below 10 000 counts after 277 cm in Unit B. Si returns to >10 000 counts at 190 cm (2300 cal BP) until 112 cm (1300 cal BP), followed by a period with values that vary around 10 000 counts until the top 10 cm of Unit B where it peaks again.

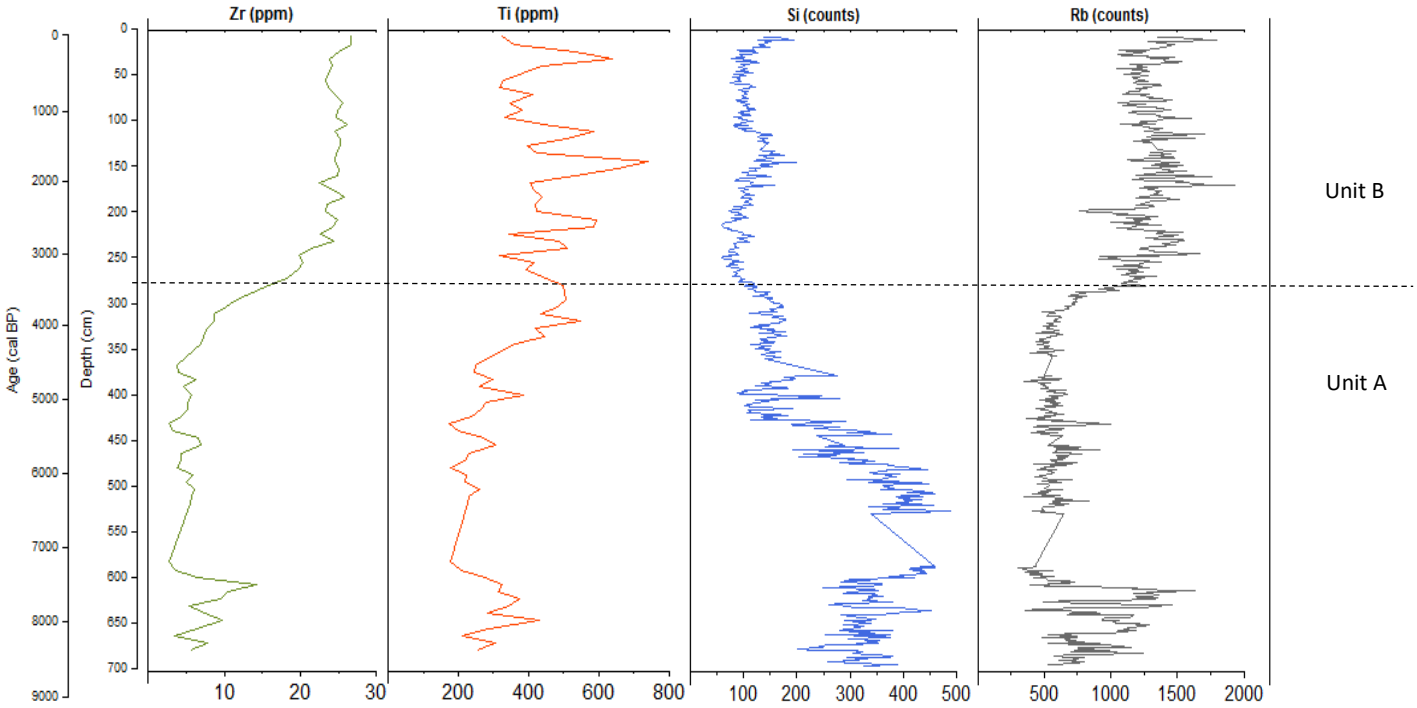

Figure 20: Plots of Zr, Ti (ICP-OES), Si, Rb (XRF) against depth (cm) and age (cal BP)

Chapter 6: Discussion

This chapter discusses the landscape modifications that were largely influenced by changes in sea-level and local dune morphology. This is followed by a discussion of the palaeoclimatic changes inferred from magnetic susceptibility, geochemical proxies, particle size data and organic matter accumulation in the lake. Each section contains a comparison of the Swartvlei record with those from surrounding sites. Sea-level changes are compared with those from local and regional curves.

6.1. Sea-level changes and landscape evolution

6.1.1. 8600 to 4500 cal BP

The higher Magnetic Susceptibility (χ) values that occur from 700 to 608 cm (8600 to 7600 cal BP) are indicative of the deposition of magnetisable material (Figure 14). The Table Mountain sandstones and beach sands can be excluded as a source of this due to their high SiO_2 content that is diamagnetic. The sediments could have emerged from the southern cape conductive belt (SCCB) that lies northward of Swartvlei and possesses a strong magnetic susceptibility signal due to the presence of magnetite in the basaltic rocks (de Beer, 1982). Through the hydration of olivines and pyroxenes into serpentine within the original basaltic rocks, iron is converted into magnetite which has a high magnetic susceptibility (de Beer, 1982). Thereafter, the sediments were likely eroded and transported into Swartvlei by aeolian processes. The deposition of sand during this time is likely from dominance of aeolian processes at Swartvlei as indicated by the absence of marine shell debris and the the measured OSL age of 15 400 +/- 2600 BP at a depth of 694.5 cm in the sediment core. Figure 21 below shows a comparison of grain size data from Swartvlei with those from surrounding areas. The data shows a similarity in the low distribution of silt and clay and the dominance of medium sized sand which constitutes >50% at all the localities. Although the mean grain size at Swartvlei (mean phi value = 1.385) indicates that the sediments were slightly coarser than those from the Wilderness dune cordon (mean phi value = 1.98), the similarity in the overall proportion of the grains suggests that the sand could have been sourced from surrounding dunes as reported by Bateman et al. (2004).

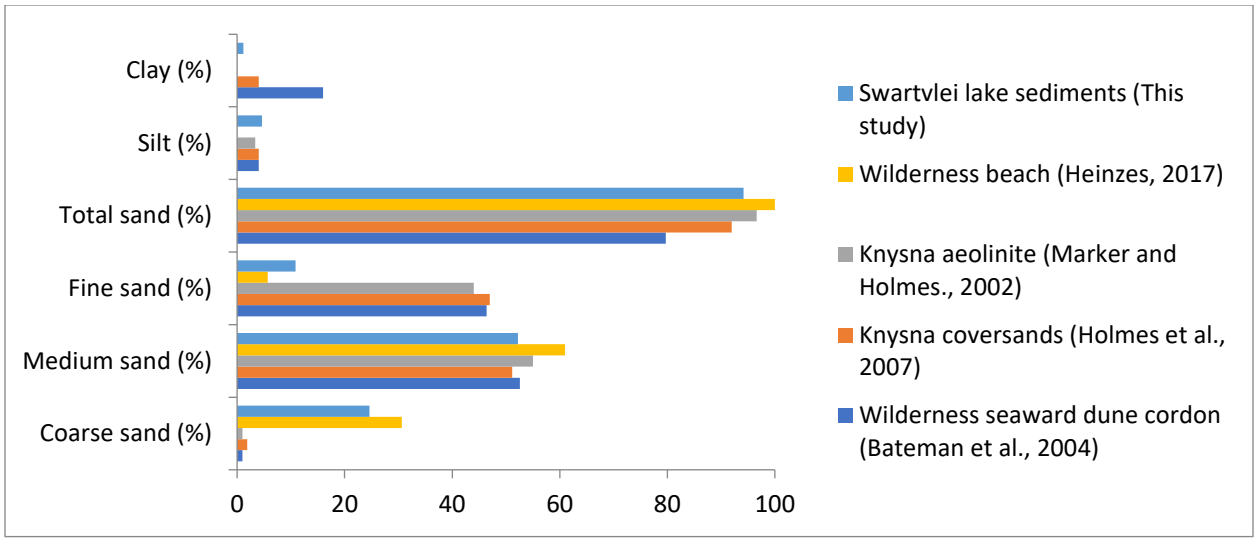

Figure 21: Grain size data comparison between Swartvlei and surrounding areas

Both Zr and Si are also prominent in this section of the core and are strongly correlated with each other (r = 0.77), but are negatively correlated with K, Al and Fe. This points to different source material or suggests that they were transported by different environmental processes. Si is common in the quartz-rich sandy material that could be detrital component of marine sand or derived from the erosion of the granites and sandstones in the river catchments or is from local dune sand (Willis, 1985). Although they were found to exist only in low densities, the common diatom *Coscinodiscus lineatus* was identified in Swartvlei by Robarts (1973) and could make a minor additional contribution to the silica content found in the sediment record. Zr is a robust element and contained in Cape Supergroup sandstone as shown in provenance studies by Bordy et al. (2016). The correlation of Zr with Si (0.77) however implies that some of the Si is sourced from the erosion of the underlying sandstones and transported to the site through aeolian processes. The strong correlation between Si and the larger sized particles of sand suggests that majority of Si content is carried in the coarse-grained sediment fraction through aeolian processes. Birch et al. (1978) also found that Zr occurred at the same depths as Si in earlier geochemical analyses at Swartvlei and suggested that Si and Zr are correlated and were deposited through aeolian processes when the climate was drier and windier.

Another possible source of the sediments found at the base of SV13 core is fluvial processes. The variation in minerogenic content (K, Al, Fe, Ti, Zr) is indicative of amplified riverine processes that eroded granite rocks in the catchment area during periods of increased precipitation. Furthermore, there is a

corresponding enrichment in the silt proportions at the same depth, which is mostly sourced from fluvial input. This evidence is described in detail in Section 6.2.

Mean grain size data between 8600 and 4500 cal BP reveal a dominance of sand (averaging 79%) indicating a marine influence, an interpretation that is supported by the high frequency of marine shell debris noted in the lithology. A transition to marine conditions following this period is also marked by a band of grey sand enriched with shell debris visible at 495 cm (6110 cal BP) (See Appendix A), which also coincides with a strong reflector visible on seismic profiles from Cawthra (2018) at the same depth (Figure 22). Below this strong reflector on the seismic profile (indicated by red line in the profile), there is a deeper river channel towards the right section of the seismic which was sub-aerially exposed when the lake was dry. Buried river channels at Swartvlei were also noted in earlier seismic investigations by Birch et al. (1978) although their precise location and depth were not indicated. Subsequent sand infilling of the flanks likely from aeolian deposition occurred and was later filled in with marine sediments resulting from over spillage when the sea-level rose. Ca concentrations began increasing gently from the same depth (Figure 18), providing evidence for the early stages of the marine intrusion. Furthermore, the high-density values and low water content indicate compacted, poorly sorted large sand grains. Berner and Raiswell (1984) recommended the use of TOC/S ratios as helpful indicators for paleosalinity, where marine sediments have low values (0.5-5) and freshwater sediments have high values (>10). The Swartvlei TOC/S ratios for this period are well below 5 (specifically, they lie between 0.59 and 3.53), indicating that Swartvlei experienced the deposition of marine sediments.

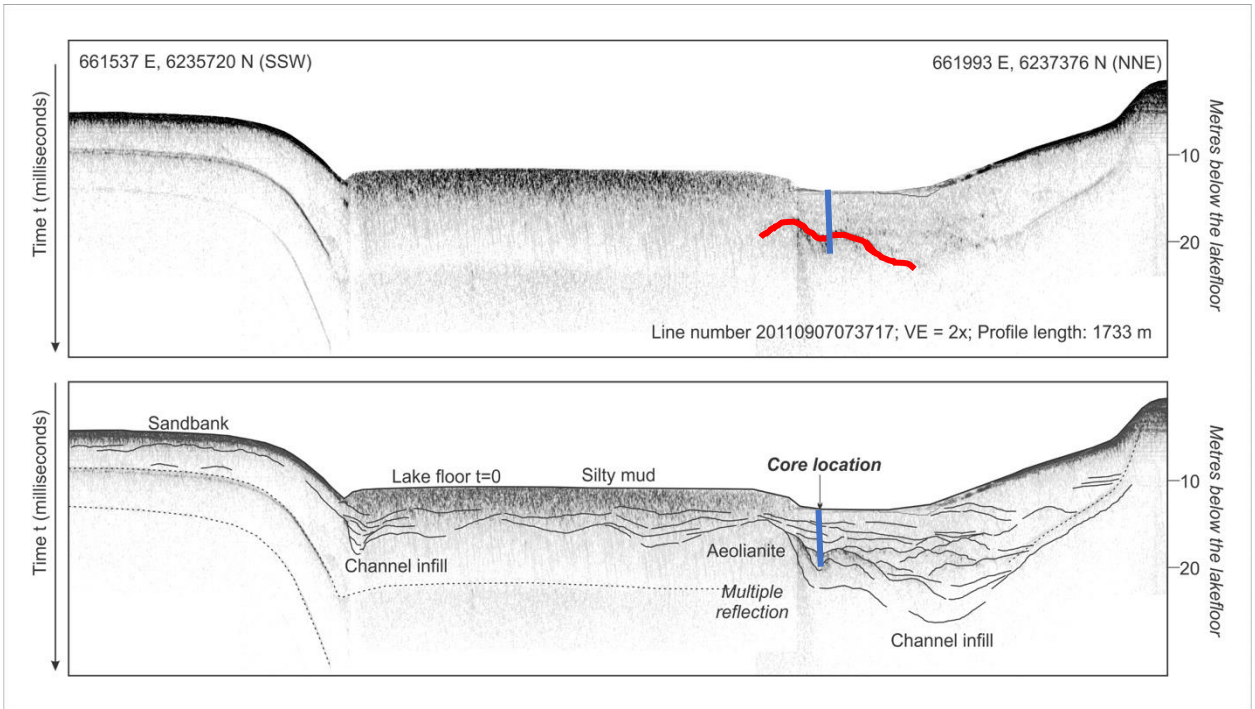

Figure 22: Seismic profile of Swartvlei taken by Cawthra et al. (2018) with a deeply incised river channel towards the right. Core location is overprinted with a blue line and the red line indicates a strong reflector

Extremely low quantities of TOC are found at the lake during this period (8600 to 4500 cal BP) (Figure 16). TOC concentrations are commonly used as an indicator of organic activity and palaeoproductivity in sedimentary environments e.g. Meyers (2003). High wave energy at Eilandvlei prevented good preservation of diatom frustules during the same period (Bennion et al., 2010; Kirsten et al. 2018). It is likely that a similar environment prevailed at Swartvlei and was not favourable to the accumulation of organic matter, thus the low TOC concentrations observed. Furthermore, molar TOC/TN ratios can be used as a proxy to distinguish between terrestrial and aquatic derived carbon. Aquatic organic matter is high in nitrogen and lacks cellulosic structures and therefore shifts TOC/TN ratios to lower values (Lamb et al., 2006). TOC/TN ratios for planktonic organisms are usually between 4 and 10 (Meyers, 2003). The molar TOC/TN values for Swartvlei range between 1.49 and 7.25 in Unit A (Figure 16) and therefore indicate that the accumulated organic matter was composed mostly of autochthonous planktonic organisms such as algae.

6.1.2. 4500 to 3500 cal BP

TIC and Ca concentrations peak between 4500 and 3500 cal BP and are strongly correlated (r=0.774). This indicates that most of the inorganic carbon is likely bound in $CaCO_3$. Terrestrial sediments are an additional possible source of Ca through the decomposition of organisms with calcified skeletons, although not mentioned in the literature to date. TIC and Ca are therefore taken here as a proxy for marine influence and indicate that the marine incursion into the lake probably occurred when the shoreline migrated landward between 4500 and 3500 cal BP due to sea-level rise. The marine transgression is broadly supported by evidence from sea-level reconstructions on the west and south coasts of South Africa (e.g. Miller et al., 1995; Ramsay, 1995; Baxter and Meadows, 1999; Compton, 2001) who postulated a marine transgression between 4400 and 3800 cal BP. Global isostatic models also report a mid-Holocene transgression (Clark et al., 1978). Ramsay (1995) estimated the mid-Holocene sea-level rise to have reached a maximum of 3.5 m above present sea-level. This marine transgression likely resulted in the deposition of the sandy unit identified by Cawthra et al. (2014) in the seismic survey at Swartvlei which was deposited during the mid-Holocene. The Groenvlei pollen record suggests that a marine phase occurred at the lake at around 7600 cal BP as indicated by increased *Chenopodiaceae* and *Restionaceae* (Martin, 1968). Completely marine conditions were found at Eilandvlei between 6400 and 4700 cal BP (Wündsch et al., 2018), while at Swartvlei the marine phase is dated between 4500 and 3500 cal BP (Figure 18).The onset of marine conditions at Swartvlei may have been delayed by physical barriers such as the rigid seaward dune cordon that lies in the south-west part of the lake; the delay was induced by the time needed for the transgression to breach the unconsolidated dune between Groenvlei and Swartvlei that constrained the width of the estuary mouth. Figure 23 compares the sea-level reconstruction from this study with those from nearby areas, showing consistency in mid-Holocene sea-level with Ramsay (1995). The west coast record by Compton (2006) does not show a distinct sea-level rise during the mid-Holocene but indicates an increase between 7000 and 6000 cal BP while Baxter and Meadows (1999) recorded it earlier at Verlorenvlei around 8000 cal BP, with a further transgressive phase at 4000 cal BP. The differences in the timing of the manifestation of sea-level at the west coast and the south coast is probably due to local differences in lake and lagoon morphology.

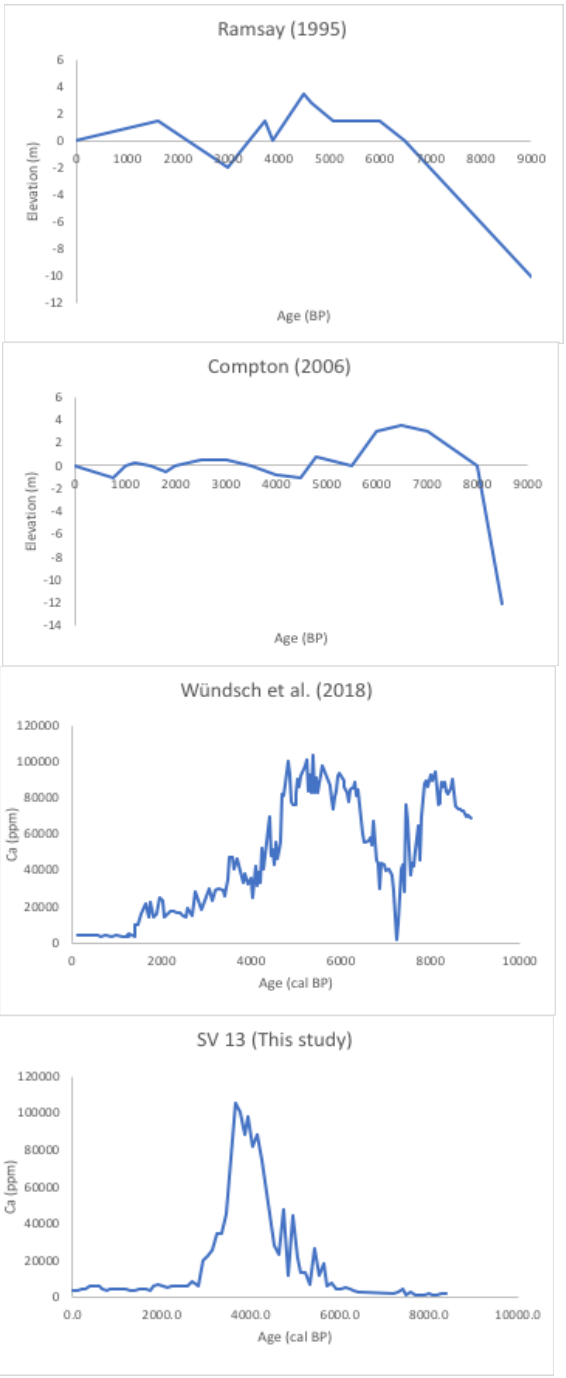

Figure 23: Comparison of Holocene Sea-level reconstruction for South Africa for the east coast (Ramsay, 1995), the west coast (Compton, 2006) and Ca concentrations at Eilandvlei (Wündsch et al., 2018) with this study

P concentrations in the lake sediments increased from 4200 cal BP, soon after the marine transgression, earlier than the other organic proxies. According to Liprot (1978), P concentrations in the Swartvlei estuary increased with increasing salinity and occurred in higher amounts closer to the seaward edge, signifying that sea-water contributes far more P than river water at Swartvlei modern sediments. Liprot (1978) further noted a high concentration of fine-grained sediments (<10 microns) in the areas where *Zostera capensis* grass grows. This suggests that macrophytes play a role in preserving the clay fraction in the lake. Therefore, the increase in the spread of emergent vegetation and terrestrial grasses around Swartvlei may explain the rise in the clay fraction in the sediment record after 3500 cal BP. *Ehrharta* and *Zostera* beds may act as sites for the sedimentation of P in the form of orthophosphate typically found adsorbed within clay-sized particles. Martin (1968) and Carr et al. (2006) proposed an elevation in the water table at Groenvlei due to higher sea-level after the marine phase, making a case for a second possible interpretation of elevated P levels, i.e. that they signify the intrusion of phosphate-rich groundwater into the lake.

Dune instability and increased aeolian activity took place in the Wilderness from about 3700 to 2400 cal BP (Bateman et al., 2011). It is proposed that the aeolian activity was driven by south-westerly winds which are dominant in the area even today, and transportation of sand through longshore drift (Whitfield et al., 1983), which possibly promoted sediment accretion that led to narrowing of the Swartvlei estuary mouth. Reconstructions by Whitfield et al. (2017) suggest that dune progradation occurred during this period on the section between Swartvlei estuary and Groenvlei (witnessed by the unconsolidated dune sediment) and led to their eventual separation. The idea of a constricted estuary mouth is supported by the low TIC and Ca concentrations in Unit B that indicate that the sea-water inflow was significantly reduced. Reduced sea-water inflow was also noted at Eilandvlei in reduced TIC, and lower abundances of ostracoda and marine diatoms as the lake took on a more strongly freshwater state (Kirsten et al., 2018). However, this process seems to have occurred earlier at Eilandvlei (shortly after 4700 cal BP) than at Swartvlei, which only became more lacustrine after 3500 cal BP. This delay in Swartvlei assuming a lagoonal state is likely due to its wider estuarine mouth that required more sediment to seal the mouth on Swartvlei's south eastern edge that then restricted sea-water incursions to the lake, as well as the robustness of the seaward dune on the south western margin of Swartvlei.

Whitfield et al. (1983) suggested that the estuary mouth was 2 km long at 6000 BP and by 4500 BP was 5km wide (Whitfield et al., 2017). This study suggests an estuary mouth that was >2 km and probably as wide as 5 km between 8600 and 7600 cal BP due to the high wave energy environment that breached the

southeastern dune barrier (Figure 24). While Swartvlei remained a marine inlet between 7600 and 4500 cal BP before the marine transgression, the estuary mouth did not widen further. Instead, the reduction in fluvial input during that time enhanced the marine influence at the site so that the deposition of marine sediments was maintained. Whitfield et al. (2017) have estimated the separation of Groenvlei and Swartvlei to have occurred between 4000 and 2000 BP and this study now provides a more precise estimate of the timing for Swartvlei assuming freshwater lacustrine status after the marine regression (3500 cal BP). Windier conditions after 3700 cal BP, as suggested Bateman et al. (2011), promoted vigorous dune building on the southeastern shore of Swartvlei adjacent to Groenvlei. After 3500 cal BP, the sea regressed and Swartvlei was converted into an estuarine lake with only limited sea-water entry. Low amplitude sea level fluctuations continued thereafter, as seen in other coastal lakes to the east, such as the Kariega Estuary where the amplitude of change was constrained within +/- 0.5m (Strachan et al., 2013). However, any sea-level changes after 3500 cal BP are not evident at Swartvlei as a result of the particular dune morphology (Whitfield et al., 2017). These changes in dune morphology and estuary mouth width in relation to sea-level are illustrated in a sketch on Figure 24 below.

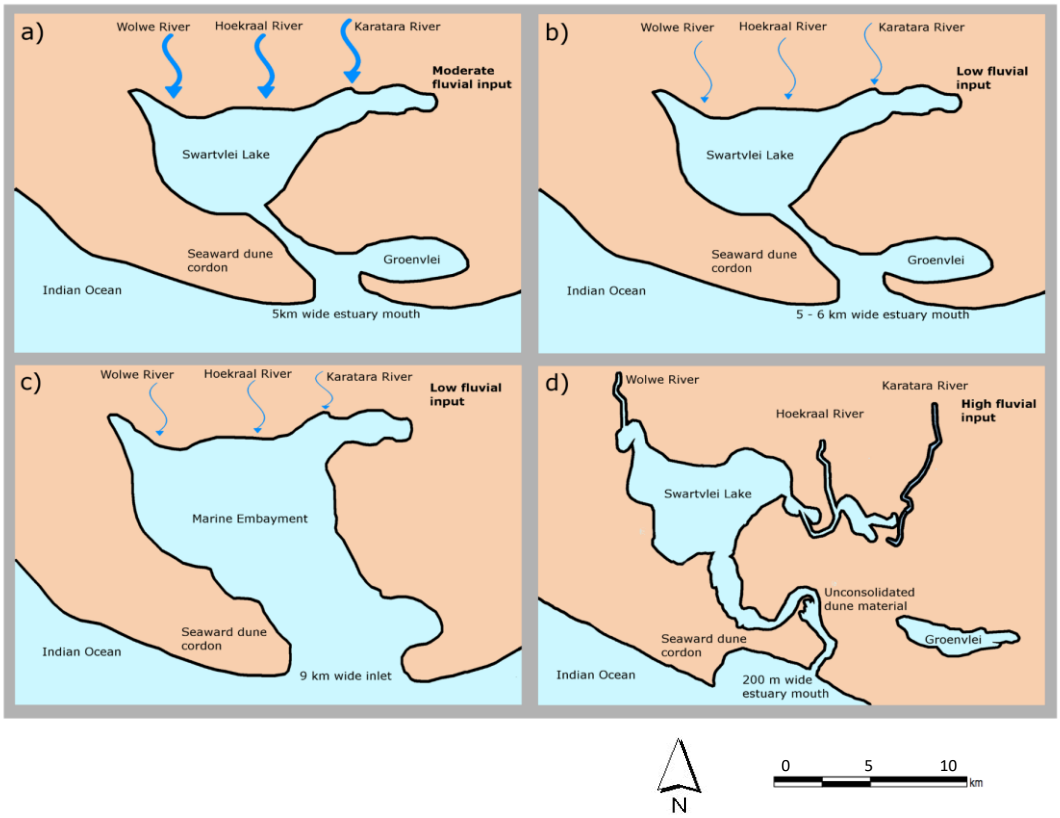

Figure 24: A sketch illustrating landscape modifications that took place at Swartvlei from 8600 to present relating to changes in the width of the estuary and timing of the separation between Swartvlei and Groenvlei a) 8600 to 7600 cal BP b) 7580 to 4500 cal BP c) 4500 to 3500 cal BP d) 3500 cal BP to present

6.1.3. Storm surge

The deposition of an event layer comprising very poorly sorted, coarse sand particles between 2580 and 2540 cal BP most likely results from an episodic in-wash of marine sand, probably during a storm surge (Figure 12). An increase in the degree of sorting and a decline in the skewness values in this layer reaffirm the introduction of marine sand in the lake during this period. The brief reappearance of marine influence after the transition into a freshwater lake was also noted by Kirsten (2018) at Eilandvlei at 3425 and 2900 cal BP indicating, even with lower sea levels, the situation remained dynamic and lake barriers were occasionally breached. A notable storm surge in the south coast occurred recently, in May 1992, due to strengthened westerly gale winds (speed >130 $km.h^{-1}$) that raised water levels in the Gamtoos Estuary by 1.15 m and resulted in the deposition of 30 000 m^3 of sand erosion from the surrounding dunes (Zhang and Schumann, 1995). It is possible that this was the kind of storm event that occurred at Swartvlei between 2580 and 2540 cal BP.

6.2. Palaeoclimatic Changes inferred from Swartvlei

6.2.1. 8600 to 4500 cal BP

Seismographs from Cawthra (2018) indicate an incised river channel beneath the SV13 core site. Cawthra et al. (2014) postulated that numerous rivers flowed through Swartvlei valley into the ocean when the sea was located 100 km away from the current location during the last glacial maximum (LGM), as suggested in the palaeo-shoreline reconstructions of Bateman et al. (2011). During Pleistocene deglaciation, the shoreline moved landward and these pre-existing river channels were drowned by marine waters. River(s) continued flowing into Swartvlei at this time with alternating wet and dry phases indicated by the highly varied fine-grained silt percentages ranging between 3 and 76% between 8600 and 7580 cal BP that suggests erratic river inflow due to irregular runoff. The silt proportions are higher, hence suggest wet phases from 8070 cal BP to 7980 cal BP and 7680 cal BP to 7580 cal BP, with intervening drier phases. Furthermore, notable variation in the geochemical proxies (K, Fe, Al) observed in the sediment record during the same period were likely sourced from greater erosion of clay minerals from the granite rock underlying the Wolwe River catchment and transported during periods of increased precipitation. The existence of a more humid phase during this period is supported by the palynological record of Quick et

al. (2015), which indicates high productivity corresponding to greater moisture availability at Still Bay from 9000 to 6000 cal BP. On the other hand, Wündsch et al. (2018) noted a period of reduced river discharge indicated by low concentrations of terrigenous elements such as Fe at Eilandvlei between 8900 and 7900 cal BP. The Groenvlei pollen record suggests dry climate conditions to have prevailed between 8000 and 7200 BP based on the spread of Asteraceae pollen due to lower rainfall, followed by moister conditions as the dry heath was replaced by mesic vegetation by 7000 BP driven by a westward shift of 60-100 km in the 400 mm isohyets (Martin, 1968). Although Swartvlei, Groenvlei, Eilandvlei and Still Bay all lie within the YRZ, these opposing palaeoenvironmental reconstructions of moisture may arise from local differences, indicate a particularly dynamic transitional phase, or are a result of dating imprecision.

Extremely low silt proportions (consistently <10%) in the upper part of Unit A from 7500 to 5000 cal BP, along with low TOC concentrations, indicate that the lake was receiving less runoff than before. Declines in concentrations of F, K, Al show reduced fluvial input, suggesting more arid conditions in the area. Stable isotope evidence from rock hyrax middens at Seweweekspoort (Chase et al., 2013) revealed the period between 7000 and 5000 cal BP to have been drier, while Quick et al. (2015) also found low productivity around this time based on evidence of lower organic matter preservation levels at Still Bay. The Eilandvlei pollen record, however, indicates humid conditions during this period based on the increase in Afrotemperate forest taxa (Quick et al., 2018). The dry conditions experienced during between 7500 and 5000 cal BP at Swartvlei, Seweweekespoort and Still Bay occurred concurrently with warmer temperatures as recorded at Cango Cave (Talma and Vogel, 1992). Moreover, the aridity was coupled with decreases in δDwax values at Vankervelsvlei between 6800 and 4700 cal BP that suggest decreased evaporation at the peat during this time (Strobel et al., 2019). According to Cohen and Tyson (1995), the warm and dry conditions correspond with periods of lower SST's in the southern Cape, increased local upwelling and weaker westerly influence on the YRZ. The importance of westerlies in controlling southern cape precipitation has been established (Chase and Meadows, 2007), and as originally proposed by Tyson (1986), evidence from Seweweekspoort best illustrates how a southward displacement in the westerly storm track leads to arid conditions in the area (Chase et al., 2013), and reduced Antarctic sea ice extent as recorded in sea-salt concentrations by Fischer et al. (2007) and Wolff et al. (2010). The southward displacement of westerlies during the mid-Holocene therefore explains the aridity experienced at Swartvlei during this period and was also observed by Hahn et al. (2016) in a study of an off-shore marine core from the Agulhas Bank.

Palaeoenvironmental interpretations from geomorphological evidence in the Wilderness (Bateman et al., 2011) and recent studies by Chase and Quick (2018) highlight the importance of the Agulhas current as an additional system that influences southern Cape palaeoclimate. The carbonate-poor sediments on the sea-ward dune cordon are in part a result of increased deposition of terrigenous clastic sediment by fluvial processes on the landward side (Bateman et al., 2004), although riverine input is responsible for only 17.9% of the overall sediment supply in the southern cape (Dingle et al., 1987). Bateman et al. (2011) presented a second explanation for the dearth of carbonates; that it results from changes in the strength and position of the Benguela and Agulhas currents. These currents bring more nutrients and carbonate producing biota, which would influence carbonate content in the sediments deposited by the sea. The Agulhas current has indeed been suggested as a key vector of climate change for the coastal margin of the southern Cape by Chase and Quick (2018), whereby moisture transport by the current brings wetter conditions for the southern near-shore sites and the southern and central parts of the SRZ. The Agulhas current transports warm waters on the east coast and propagates moist air onshore (Jury et al., 1993), as such projects a tropical climate signal (Chase and Quick, 2018). Furthermore, under a wetter climate post the mid-Holocene marine transgression, increased evaporation was also inferred from δDwax data at Vankervelsvlei after 4700 cal BP (Strobel et al., 2019). This wind-driven evaporation therefore supports Bateman et al.'s (2011) suggestion that the moister conditions and stronger southwesterlies assisted with dune building around the edges of Swartvlei during this period.

6.2.2. Flooding event from 5400 to 5350 cal BP

A flooding event possibly occurred at 5400 to 5350 cal BP where silt and clay percentages increased abruptly. The event coincides with a peak in TOC/TN and TOC/TS ratios, a minor peak in Fe/Al, and a decline in Ca and TIC at roughly the same depth. This shows that the fluvial input exceeded the marine input during this brief event. The cause of this flooding event cannot be explained using data from this study, however, the shift to less negative skewness values at the same depth indicates an enrichment in the fine grain component, which are likely sourced from the Wolwe river catchment that flows over the Cape Granite rock which mostly weathers into fine grains. The Wolwe River that flows over the Cape granite was found to carry a higher silt load than the other two river systems which increases during flooding events (Whitfield et al., 1983), and was therefore likely responsible for the increase in fines during the flooding event at 5400 cal BP. Severe floods in 1982 led to the delivery of silt-laden waters to Eilandvlei

from the Diuwe River (Weisser et al., 1992) and supports the suggestion of the Wolwe River transporting similar sediment content to Swartvlei.

6.2.3. 3500 cal BP to 1400 cal BP

The last 3500 cal BP have been relatively stable, characterized by higher moisture availability and significant reduction in sea-water ingress via the estuary mouth. In Unit B (3500 cal BP to present), the lithology indicates a change towards smaller mean grain size, while the statistical parameters indicate a shift to poorly sorted sediments which result from the deposition of variably sized particles carried through inland rivers. There is a shift in skewness to the less negative domain due to dominance of finer grains. Unit B contains dark brown clayey-silt, suggesting the reduced influence of wave-transported sediments and a generally quieter depositional environment within the lake. The greater silt fraction also suggests that a larger portion of the sediments is derived from the inland rivers during periods of increased regional moisture. Enrichment in the finer silt fraction in this unit may have occurred as a result of changes in the hydrodynamic conditions of the rivers including widening of the channel, extension of the tributaries and increased flow velocity due to increasing gradient of the river channels. Sedimentation rates increase from 0.08 cm yr^{-1} in the early Holocene to an average of 0.1 cm yr^{-1} as higher volumes of fluvial sediments were supplied after 3500 cal BP (Figure 11). Increased moisture after 3500 cal BP can be explained by variations in seasonal insolation in the southern Cape. According to Berger and Loutre (1991), summer insolation progressively increased after the mid-Holocene near 34°S. Higher summer insolation would lead to an increase in the SSTs on the Agulhas Bank and higher evaporation which could bring more rainfall to the area. SSTs on the Aguhlas Bank were higher between 4000 and 2000 BP (Cohen and Tyson, 1995), and possibly afterwards and may have introduced higher rainfall at the site.

Changes in the minerogenic component result from variations in the transfer of terrestrial sediments sourced from eroded rocks exposed on the river catchment that collect in the lake basin. XRF data for sediments with large variations in organic matter require normalization with Al to overcome dilution effects as it is conservative element that is largely unaffected by biological and diagenic processes (Löwemark et al., 2011). Accordingly, Al has been used for normalization of Fe and Si XRF data in this study. Fe/Al ratios show an inverse relationship to the Si/Al ratios where the signal is low in Unit A and strong in Unit B. The high Fe/Al ratios since 3500 cal BP are taken as a proxy for terrigenous sediment input. Other geochemical proxies that exhibit higher values in this section, Ti, Rb, K and Mn, are strongly correlated, suggesting that they come from a common sedimentary environment. K is considered to be of detrital

origin because plants only contain it in trace concentrations when compared to clay minerals (López-Buendıa et al., 1999). The Fe enrichment observed in the sediment record may be from weathered granite rock minerals such as the Fe-rich mica. The increase in these geochemical proxies therefore may be considered as a palaeoprecipitation indicator and, as a result, of river discharge. Fe is commonly interpreted as a detrital source influenced by increased moisture, for example Naeher et al. (2012), Kasper et al. (2012) and Wündsch et al. (2018). In all three papers, elevated Fe from terrigenous sediment is thought to indicate increased humidity. Figure 25 shows late Holocene moisture availability through a comparison of Fe data between Swartvlei and Eilandvlei, while Figure 26 compares other proxy data from Swartvlei and other lakes in the surrounding areas. In addition, the increase in sedimentation rate upcore typically indicates an increase in the overall sediment input (Bennett and Buck, 2016). In this case, the increasing fluvial input contributed to an overall increase in the reconstructed sedimentation rates from lower values in the early and mid-Holocene. Pollen concentrations and charcoal assemblages at Norga Peat investigated by Scholtz (1986) showed that between 4000 and 2500 cal BP, Afromontane forest expansion occurred because of wetter conditions arising from increased summer rainfall. Further support for these results is from δ15N and δ13C records from Seweweekspoort which indicate a trend to significantly moister and warmer conditions in the late Holocene starting from 3500 cal BP (Chase et al., 2013).

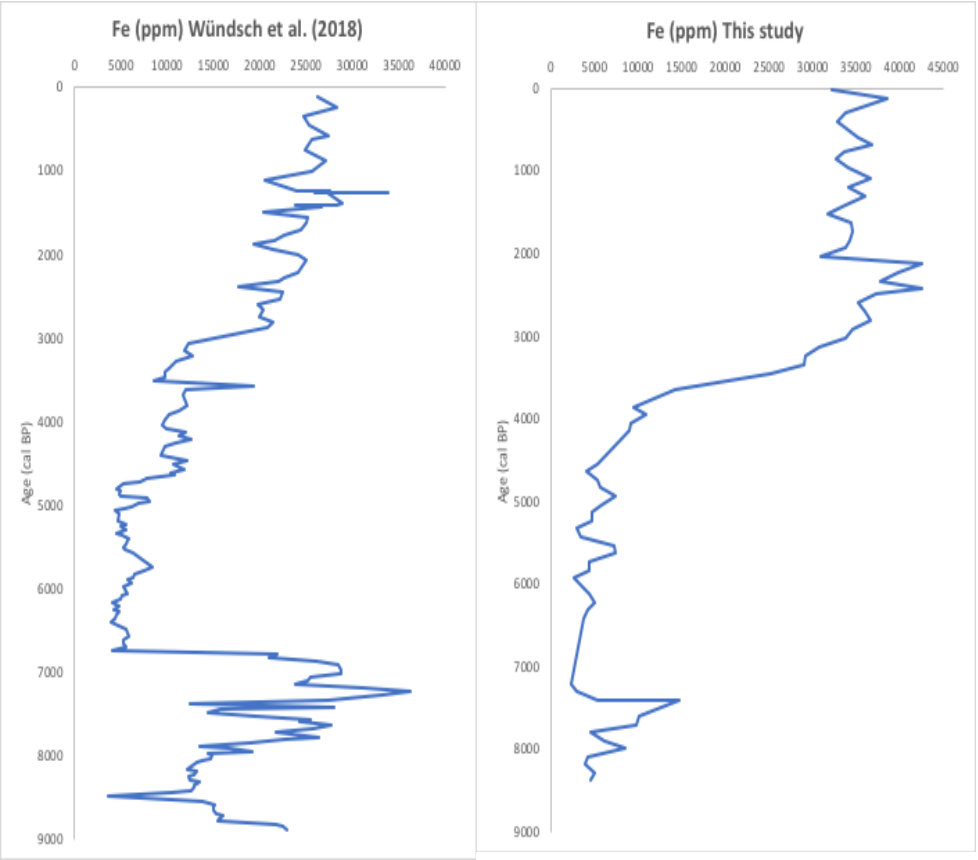

Figure 25: Comparison of Fe concentrations from Eilandvlei (Wündsch et al., 2018) and Swartvlei, where Fe serves as a proxy for moisture. Eilandvlei had increased riverine inputs from 3000 cal BP while Swartvlei received greater precipitation (seen in high Fe concentrations) after 3500 cal BP.

The shift to higher TOC/TN ratios (from 11.2 to 14.6 in Unit B) after 3500 cal BP which, according to Lamb (2006) indicates the input of terrestrially derived carbon sourced from allochthonous vascular vegetation due to its high lignin and cellulose content. Organic matter (TOC, TN, TS) accumulates principally from two sources, viz. aquatic productivity within the lake of photosynthetic macrophytes and algae, and from the in-wash of organic matter from the catchment area. A wetter climate can be inferred from the increase in terrestrial organic matter, as it points to increase in vegetation cover which also corresponds to a decrease in windblown sand due to dune stabilisation.

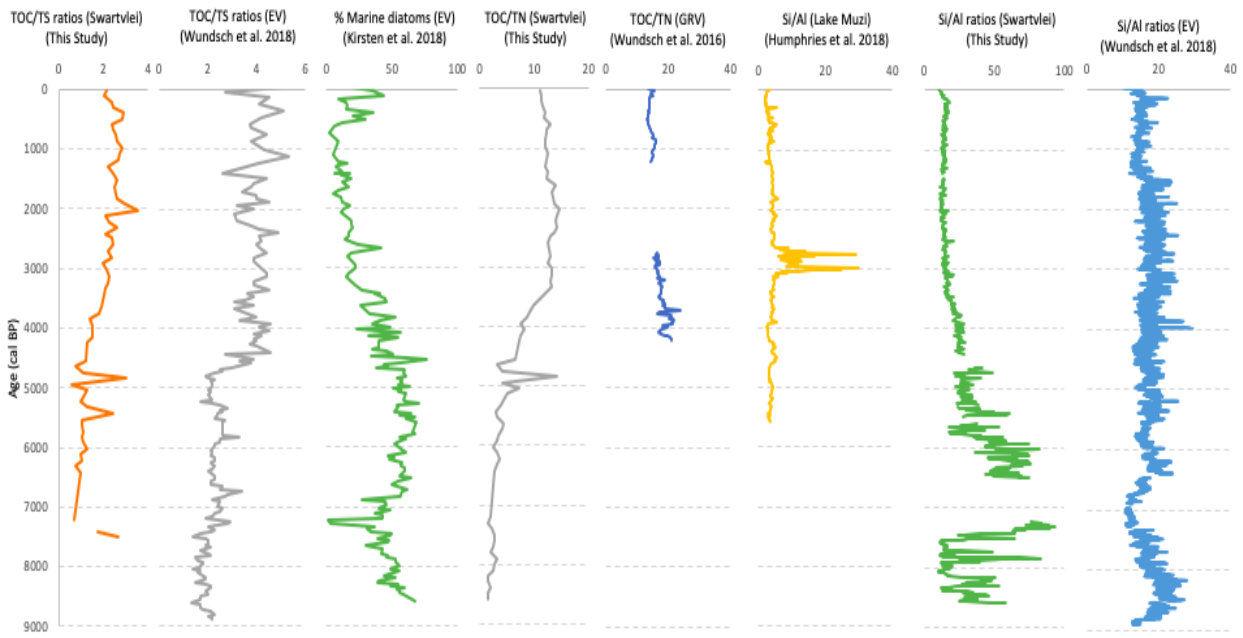

Figure 26: Composite plot of Swartvlei data for TOC/TS, TOC/TN and Si/AL in comparison with data from Eilandvlei, Groenvlei and Lake Muzi

The high water content in Unit B of 40-80% (Figure 14) suggests greater organic content in this lithological unit. Sediments with high organic matter or water content exhibit diamagnetism, which is seen through weak magnetic susceptibility values (Dearing, 1999). The low magnetic susceptibility values due to a diamagnetic effect in the latter part of SV13 are indicative of the dominant organic matter (Dearing, 1999; Dankoub et al., 2012). Other minerals that produce a diamagnetic signal include quartz (wind-blown from sand dunes and erosion of surrounding sandstone), feldspars (erosion of Cape granite), calcium carbonate (biogenic and clastic formation in marine environment) which are also deposited at Swartvlei during this time in large amounts through fluvial, marine and possibly aeolian transport mechanisms.

As in Wündsch et al. (2018), this study used TOC/S linear regression models to reconstruct the degree of euxinic conditions at Swartvlei. The equation for the linear regression model for S and TOC for Unit B is = 0.23*TOC + 1.36 (n = 35; r= 0.694; r^2 = 0.482) (Figure 27). The slope for this model is less than that of marine waters but greater than the slope for euxinic conditions observed at the Black Sea by Berner (1984) of 0.1*TOC + 0.9. Although both sedimentary units have semi-euxinic conditions, organic matter in Unit B was deposited in more euxinic conditions than Unit A which has a linear regression equation = 0.49*TOC + 0.09 (n = 30; r = 0.935; r^2 = 0.873). Freshwater from the rivers is less dense than sea-water due to its lower salinity and therefore accumulates at the surface before flowing into the estuary (Russell, 2016). A stronger freshwater influence arose after the mid-Holocene environmental changes that reduced sea-

water ingress to Swartvlei, possibly driven by weakened southwesterly winds which led to less turbulence, reduced mixing of the bottom deoxygenated waters with the surface water and creation of anoxic conditions at the base of the lake and an enhanced production of H_2S (Howard-Williams and Allanson, 1984). Furthermore, Berner and Raiswell (1984) recommended the use of TOC/S ratios as helpful indicators for paleosalinity, where marine sediments have low values (0.5-5) and freshwater sediments have high values (>10). The Swartvlei TOC/S ratios are well below 5 (specifically, they lie between 0.59 and 3.53) (Figure 16), and therefore indicative of a mix of marine and freshwater sediments into the lake, with a shift to a stronger freshwater influence in the late Holocene. The TOC/S ratios indeed reveal higher values in Unit B, indicating the increased contribution of freshwater derived sediments to the lake from 3500 cal BP.

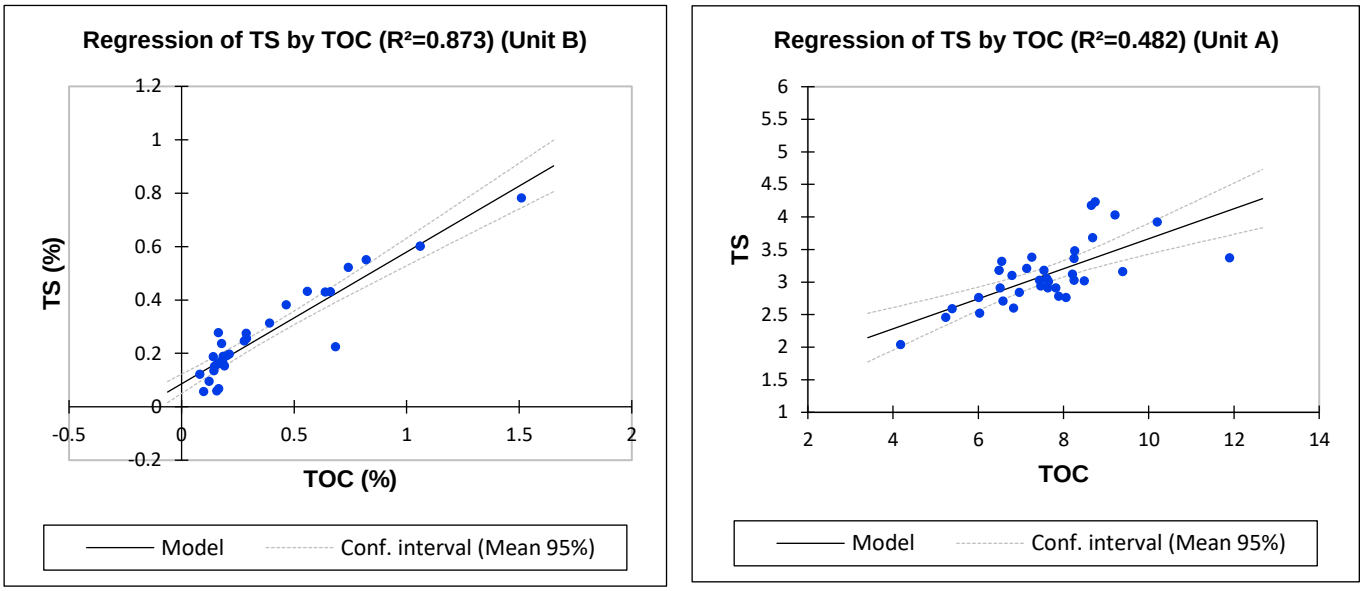

Figure 27: Regression cross plots showing the correlation of TS and TOC. The graph shows the semi-euxinic conditions that occurred at Swartvlei from (3500 cal BP to present).

The period 1800 to 1400 cal BP is characterised by relatively arid conditions as evidenced by the decrease in silt and lower TOC, TN and TS. The decrease in both fluvial and marine inputs at the lake may be interpreted as a decrease in the overall lake water levels resulting from regional aridity, since this period coincides with periods of decreased lake water levels at Eilandvlei based on diatoms (Kirsten et al., 2018) and the configuration of Groenvlei into a coastal lake as it became isolated from the sea (Martin, 1968; Wündsch et al., 2018).

6.2.4. 1400 cal BP to present

The high BiSi quantities from 1400 cal BP through to the present are indicative of increased lake productivity as BiSi can be used as a proxy for diatom abundance and productivity (Ragueneau et al., 1996). The notable decline in BiSi concentrations during the Medieval Climate Anomaly (MCA) (950 to 750 cal BP; Lüning et al., 2018) suggest reduced lake productivity or a stronger dilution by the allochthonous lithoclastics during this period (Ohlendorf and Stern, 2008). However, slight decreases are observed in the terrigenous sediment flux (K and Al) and the average silt proportions, suggesting a reduction in riverine input. Therefore, the Swartvlei record indicates climate conditions that were not conducive to the productivity or preservation of diatoms during the MCA. Hahn et al. (2017) found drier conditions to have prevailed in the WRZ during the MCA due to a reduction in the Atlantic westerlies, which possibly led to Swartvlei's aridity during this time. However, it was noted to be more humid than present at Groenvlei from 1200 cal BP until the present due to stronger influence of summer rainfall (Martin, 1968; Wündsch et al., 2016) even though the two systems are found within 3 km of one another and it is unclear from this data why these micro-climatic differences occurred. A finer resolution study of the palaeoecological record at Groenvlei could explain this climate reconstruction during the MCA. The dry conditions in the WRZ were contrasted by wetter conditions that prevailed in the rest of the country due to intensification of the easterlies (Lüning et al., 2018). One possible explanation for the differences is that Groenvlei could have benefited from moisture sourced from the easterlies as it lies to the east of Swartvlei, but this would need to be tested with more data.

High BiSi concentrations maintained during the Little Ice Age (LIA) between 680 and 300 cal BP indicate increased productivity in the lake. There was a corresponding increase in silt deposition from 700 to 500 cal BP followed by a decrease until 300 cal BP indicating that fluvial input was varied; high in the first half of the LIA and low in the latter part. A similar pattern is observed in TOC and TN concentrations as well as molar TOC/TN ratios with the decrease starting at 490 cal BP. Lake productivity therefore probably responded to a change in the temperature regime. Cooler conditions were recorded at Groenvlei during the LIA (Wündsch et al., 2016). Holocene vegetation changes observed by Zhao et al. (2016) suggested a cool LIA (700 – 200 cal BP) in both WRZ and SRZ, with significantly more precipitation in the WRZ while the SRZ was relatively dry.

In addition, enhanced sedimentation rates that peak in the top 19 cm (150 cal BP) of the SV record, possibly occurred due to accelerated soil erosion from anthropogenic activities such as farming and logging. Reinwarth et al. (2013) gave an account of anthropogenic activity at Eilandvlei using geochemical analyses on the lake sediments and showed that the arrival of Europeans since the late 19th century had fundamental changes on the southern Cape landscape.

Chapter 7: Conclusion

This study provides unique geochemical insights into the palaeoenvironmental changes within the year-round rainfall zone of South Africa. Swartvlei has been a great receptor of dynamic environmental changes during the Holocene that were documented by multiple proxies and thus helped to achieve the main aim of this study. The first objective of the study was achieved through the high-resolution radiocarbon and OSL dating that provided a reliable chronology against which the Holocene climatic and environmental changes could be interpreted. Si/Al ratios, magnetic susceptibility and particle size data indicate a shallow, aeolian dominated system from 8600 to 4500 cal BP, along with an arid climate during the mid-Holocene driven by the equatorward migration of the westerly storm track. While the initiation of a coastal lake with stronger marine signals occurred from 6100 cal BP, Ca, TIC data and accumulations of shell fragments suggest that Swartvlei was a marine embayment from 4500 to 3500 cal BP. Grain size data reveal that marine regression and barrier accretion after 3500 cal BP limited sea-water inflow and promoted the evolution of the lake into lacustrine conditions. A shift in molar TOC/TN ratios shows that the climate became significantly moister as freshwater inputs increased after 3500 cal BP, supported by higher Fe/Al ratios and deposition of fine fluvial sediments. Minor changes in particle size and biogenic silica data indicate humid conditions during the late Holocene linked with an intensified easterly flow. High sedimentation rates in the last 150 cal BP appear to have resulted from the interplay of natural and anthropogenic activity and these need to be investigated further in order to manage the recreational use of the lake and to monitor activity on the catchment. Integrated coastal management strategies can be developed with an improved understanding of variations in sea-water and freshwater inputs that can manifest in storm surges, flooding events and drought. Understanding of Wilderness lake systems over long-term periods is also critical to assessing current and future stressors on the system, and for ecological conservation.

The Swartvlei record has further proved to be a vital tool in understanding the evolution of Swartvlei and Groenvlei as indicates a more precise timing of separation of the two lakes. Comparison with nearby lakes indicates that the findings of this study are consistent with those from earlier studies, highlighting that coastal regions are fundamental in understanding long-term hydrological changes. The detailed geochemical and particle size analyses have thus helped to achieve the second and third objectives of this study as the landscape and palaeoclimatic changes in the region have been successfully elucidated and compared with those from the region. Future research conducted using palaeoecological proxies such as pollen and diatoms would help to enhance the reconstruction of regional palaeoclimatic changes.

Furthermore, an exploration into the evolution of the nearby Rondevlei would help to reveal the dynamics on the northwestern end of Swartvlei and add to the broader understanding of Wilderness Lakes during the Holocene.

References

Abell, P.I. and Plug, I., 2000. The Pleistocene/Holocene transition in South Africa: evidence for the Younger Dryas event. *Global and Planetary Change*. 26(1-3): 173-179.

Adachi, H., Yamano, H., Miyajima, T. & Nakaoka, M. 2010. A simple and robust procedure for coring unconsolidated sediment in shallow water. *Journal of Oceanography.* 66(6):865-872.

Agrawal, Y.C., Whitmire, A., Mikkelsen, O.A. & Pottsmith, H.C. 2008. Light scattering by random shaped particles and consequences on measuring suspended sediments by laser diffraction. *Journal of Geophysical Research: Oceans.* 113(C4)

Avery, D.M. 1982. The micromammalian fauna from border cave, Kwazulu, South Africa. *Journal of Archaeological Science.* 9(2):187-204.

Avery, D.M., 1993. Last Interglacial and Holocene altithermal environments in South Africa and Namibia: micromammalian evidence. Palaeogeography, Palaeoclimatology, Palaeoecology. 101(3-4): 221-228.

Avnimelech, Y., Ritvo, G., Meijer, L.E. & Kochba, M. 2001. Water content, organic carbon and dry bulk density in flooded sediments. *Aquacultural Engineering.* 25(1):25-33.

Bateman, M.D., Carr, A.S., Dunajko, A.C., Holmes, P.J., Roberts, D.L., McLaren, S.J., Bryant, R.G., Marker, M.E. and Murray-Wallace, C.V., 2011. The evolution of coastal barrier systems: a case study of the Middle-Late Pleistocene Wilderness barriers, South Africa. *Quaternary Science Reviews*. 30(1-2): 63-81.

Bateman, M.D., Holmes, P.J., Carr, A.S., Horton, B.P. & Jaiswal, M.K. 2004. Aeolianite and barrier dune construction spanning the last two glacial–interglacial cycles from the southern Cape coast, South Africa. Quaternary Science Reviews. 23(14-15):1681-1698.

Battarbee, R.W., Jones, V.J., Flower, R.J., Cameron, N.G., Bennion, H., Carvalho, L. and Juggins, S., 2002. Diatoms. In Tracking environmental change using lake sediments (pp. 155-202). Springer, Dordrecht.

Baxter, A.J. & Meadows, M.E. 1999. Evidence for Holocene sea level change at verlorenvlei, western cape, South Africa. *Quaternary International.* 56(1):65-79.

Bennett, K.D. & Buck, C.E. 2016. Interpretation of lake sediment accumulation rates. *The Holocene.* 26(7):1092-1102.

Bennion, H., Sayer, C.D., Tibby, J., Carrick, H.J. 2010. Diatoms as indicators of environmental change in shallow lakes. *The Diatoms: Applications for the Environmental and Earth Sciences.* :152.

Berger, A., Loutre, M. 1991. Insolation values for the climate of the last 10 million years. *Quaternary Science Reviews.* 10(4):297-317.

Berner, R.A. 1984. Sedimentary pyrite formation: an update. *Geochimica Et Cosmochimica Acta.* 48(4):605-615.

Berner, R.A. & Raiswell, R. 1984. C/S method for distinguishing freshwater from marine sedimentary rocks. *Geology.* 12(6):365-368.

Beuselinck, L., Govers, G., Poesen, J., Degraer, G. & Froyen, L. 1998. *Grain-size analysis by laser diffractometry: comparison with the sieve-pipette method.* Available: http://www.sciencedirect.com/science/article/pii/S0341816298000514 .

Birch, G.F. 1980. *Nearshore Quaternary sedimentation off the south coast of South Africa:(Cape Town to Port Elizabeth).* Government Printer.

Birch, G.F., Du Plessis, A. & Willis, J.P. 1978. Offshore and onland geological and geophysical investigations in the Wilderness Lakes region. *Transactions of the Geological Society of South Africa.* 81:339-352.

Blaauw, M. and Christen, J.A., 2011. Flexible paleoclimate age-depth models using an autoregressive gamma process. *Bayesian analysis*. 6(3): 457-474.

Blomqvist, S. 1991. Quantitative sampling of soft-bottom sediments: problems and solutions. *Marine Ecology Progress Series.* 295-304.

Blott, S.J. & Pye, K. 2001. GRADISTAT: a grain size distribution and statistics package for the analysis of unconsolidated sediments. *Earth Surface Processes and Landforms.* 26(11):1237-1248.

Bordy, E.M., Head, H. & Runds, M.J. 2016. Palaeoenvironment and provenance in the early Cape Basin of southwest Gondwana: sedimentology of the Lower Ordovician Piekenierskloof Formation, Cape Supergroup, South Africa. *South African Journal of Geology 2016.* 119(2):399-414.

Boyd, C.E. 2012. *Bottom soils, sediment, and pond aquaculture.* Springer Science & Business Media.

Braun, M., Hubay, K., Magyari, E., Veres, D., Papp, I. & Bálint, M. 2013. Using linear discriminant analysis (LDA) of bulk lake sediment geochemical data to reconstruct lateglacial climate changes in the South Carpathian Mountains. *Quaternary International.* 293:114-122.

Carr, A.S., Bateman, M.D., Roberts, D.L., Murray-Wallace, C.V., Jacobs, Z. and Holmes, P.J., 2010. The last interglacial sea-level high stand on the southern Cape coastline of South Africa. Quaternary Research, 73(2): 351-363.

Carr, A.S., Chase, B.M. & Mackay, A. 2016. Mid to Late Quaternary landscape and environmental dynamics in the Middle Stone Age of southern South Africa. In *Africa from MIS 6-2.* Springer. 23-47.

Cawthra, H.C., Bateman, M.D., Carr, A.S., Compton, J.S. & Holmes, P.J. 2014. Understanding Late Quaternary change at the land–ocean interface: a synthesis of the evolution of the Wilderness coastline, South Africa. *Quaternary Science Reviews.* 99:210-223.

Cawthra, H.C., Compton, J.S., Fisher, E.C., MacHutchon, M.R. & Marean, C.W. 2016. Submerged shorelines and landscape features offshore of Mossel Bay, South Africa. *Geological Society, London, Special Publications.* 411(1):219-233.

Chase, B.M., Boom, A., Carr, A.S., Meadows, M.E. and Reimer, P.J., 2013. Holocene climate change in southernmost South Africa: rock hyrax middens record shifts in the southern westerlies. *Quaternary Science Reviews*. 82: 199-205.

Chase, B.M., Chevalier, M., Boom, A. and Carr, A.S., 2017. The dynamic relationship between temperate and tropical circulation systems across South Africa since the Last Glacial Maximum. *Quaternary Science Reviews*. 174: 54-62.

Chase, B.M., Lim, S., Chevalier, M., Boom, A., Carr, A.S., Meadows, M.E. and Reimer, P.J., 2015. Influence of tropical easterlies in southern Africa's winter rainfall zone during the Holocene. *Quaternary Science Reviews*. 107: 138-148.

Chase, B.M. & Meadows, M.E. 2007. Late Quaternary dynamics of southern Africa's winter rainfall zone. *Earth-Science Reviews.* 84(3-4):103-138.

Chase, B.M. & Quick, L.J. 2018. Influence of Agulhas forcing of Holocene climate change in South Africa's southern Cape. *Quaternary Research.* 90(2):303-309.

Chase, B.M. & Thomas, D.S. 2007. Multiphase late Quaternary aeolian sediment accumulation in western South Africa: timing and relationship to palaeoclimatic changes inferred from the marine record. *Quaternary International.* 166(1):29-41.

Chevalier, M. & Chase, B.M. 2015. Southeast African records reveal a coherent shift from high-to low-latitude forcing mechanisms along the east African margin across last glacial–interglacial transition. *Quaternary Science Reviews.* 125:117-130.

Clark, J.A., Farrell, W.E. & Peltier, W.R. 1978. Global Changes in Postglacial Sea Level: A Numerical Calculation 1. *Quaternary Research.* 9(3):265-287.

Clausnitzer, S. 2011. Bathymetrische und flachseismische Auswertung hydroakustischer Profile der Seen Eilandvlei, Rondevlei und Swartvlei im Garden Route National Park Wilderness Coastal Section, Südafrika. Bachelor thesis. Friedrich Schiller University Jena.

Clift, P.D., Wan, S. & Blusztajn, J. 2014. Reconstructing chemical weathering, physical erosion and monsoon intensity since 25 Ma in the northern South China Sea: a review of competing proxies. *Earth-Science Reviews.* 130:86-102.

Coetzee, D.J. 1982. Stomach content analyses of Gilchristella aestuarius and Hepsetia breviceps from the Swartvlei system and Groenvlei, southern Cape. *African Zoology.* 17(2):59-66.

Cohen, A.L. & Tyson, P.D. 1995. Sea-surface temperature fluctuations during the Holocene off the south coast of Africa: implications for terrestrial climate and rainfall. *The Holocene.* 5(3):304-312.

Cohen, A.L. 1993. A Holocene sea surface temperature record in mollusc shells from the South African coast (Doctoral dissertation, University of Cape Town).

Compton, J.S. 2001. Holocene sea-level fluctuations inferred from the evolution of depositional environments of the southern Langebaan Lagoon salt marsh, South Africa. *The Holocene.* 11(4):395-405.

Compton, J.S. 2004. *The rocks and mountains of Cape Town.* Juta and Company Ltd.

Compton, J.S. 2006. The mid-Holocene sea-level highstand at Bogenfels Pan on the southwest coast of Namibia. *Quaternary Research.* 66(2):303-310.

Compton, J.S., 2011. Pleistocene sea-level fluctuations and human evolution on the southern coastal plain of South Africa. *Quaternary Science Reviews*. 30(5-6): 506-527.

Compton, J.S. & Wiltshire, J.G. 2009. Terrigenous sediment export from the western margin of South Africa on glacial to interglacial cycles. *Marine Geology.* 266(1-4):212-222.

Conley, D.J. & Schelske, C.L. 1993. Potential role of sponge spicules in influencing the silicon biogeochemistry of Florida lakes. *Canadian Journal of Fisheries and Aquatic Sciences.* 50(2):296-302.

Conley, D.J. & Schelske, C.L. 2002. Biogenic silica. In *Tracking environmental change using lake sediments.* Springer. 281-293.

Damm, B. and Hagedorn, J., 2010. Holocene floodplain formation in the southern Cape region, South Africa. *Geomorphology*. 122(3-4): 213-222.

Dankoub, Z., Khademi, H. & Ayoubi, S.H. 2012. Magnetic susceptibility and its relationship with the concentration of selected heavy metals and soil properties in surface soils of the Isfahan region. *Journal of Environmental Studies*. 38(63): 4-6

Davies, B.R. 1982. Studies on the zoobenthos of some southern Cape coastal lakes. Spatial and temporal changes in the benthos of Swartvlei, South Africa, in relation to changes in the submerged littoral macrophyte community. *Journal of the Limnological Society of Southern Africa.* 8(1):33-45.

De Beer, J.H., Van Zijl, J. & Gough, D.I. 1982. The southern cape conductive belt (South Africa): its composition, origin and tectonic significance. *Tectonophysics.* 83(3-4):205-225.

De Wit, M.J. & Ransome, I.G. 1992. Regional inversion tectonics along the southern margin of Gondwana. *Inversion Tectonics of the Cape Fold Belt, Karoo and Cretaceous Basins of Southern Africa.Balkema, Rotterdam.* 15:21.

Deacon, J. & Lancaster, N. 1988. *Late Quaternary palaeoenvironments of southern Africa.* Oxford University Press, USA.

Dearing, J. 1999. Magnetic susceptibility. *Environmental Magnetism: A Practical Guide.* 35-62.

Dellwig, O., Watermann, F., Brumsack, H. & Gerdes, G. 1999. High-resolution reconstruction of a Holocene coastal sequence (NW Germany) using inorganic geochemical data and diatom inventories. *Estuarine, Coastal and Shelf Science.* 48(6): 617-633.

Dingle, R.V., Birch, G.F., Bremner, J.M., De Decker, R.H., Du Plessis, A., Engelbrecht, J.C., Fincham, M.J., Fitton, T. et al. 1987. Deep-sea sedimentary environments around southern Africa (south-east Atlantic and south-west Indian oceans. *Annals of the South African Museum.* 98(1).

Du Plessis, A. & Birch, G.F. 1977. The nature of the sea floor south of Cape Seal in a block bound by the longitudes 23 15' E and 23 35' E and latitudes 34 10' S and 34 25' S: GSO/UCT Mar. Geol. Prog. *Bull.* (9):75-85.

Fairbanks, R.G. 1989. A 17,000-year glacio-eustatic sea level record: influence of glacial melting rates on the Younger Dryas event and deep-ocean circulation. *Nature.* 342(6250):637.

Fischer, H., Siggaard-Andersen, M., Ruth, U., Röthlisberger, R. & Wolff, E. 2007. Glacial/interglacial changes in mineral dust and sea-salt records in polar ice cores: Sources, transport, and deposition. *Reviews of Geophysics.* 45(1).

Fisher, E.C., Bar-Matthews, M., Jerardino, A. & Marean, C.W. 2010. Middle and Late Pleistocene paleoscape modeling along the southern coast of South Africa. *Quaternary Science Reviews.* 29(11-12):1382-1398.

Foster, I. & Walling, D.E. 1994. Using reservoir deposits to reconstruct changing sediment yields and sources in the catchment of the Old Mill Reservoir, South Devon, UK, over the past 50 years. *Hydrological Sciences Journal.* 39(4):347-368.

Frew, C. 2014. Coring Methods. In *Geomorphological Techniques.* British Society for Geomorphology.

Gabriel, M., Gałka, M., Pretorius, M.L. & Zeitz, J. 2017. The development pathways of two peatlands in South Africa over the last 6200 years: Implications for peat formation and palaeoclimatic research. *The Holocene.* 27(10):1499-1515.

Gingele, F.X., 1996. Holocene climatic optimum in Southwest Africa—evidence from the marine clay mineral record. *Palaeogeography, Palaeoclimatology, Palaeoecology*. 122(1-4): 77-87.

Glew, J., Smol, J. P. and Last, W. M. 2001. Sediment core collection and extrusion. In *Tracking environmental change using lake sediments volume 1: Basin analysis, coring, and chronological techniques. Developments in paleoenvironmental research.* Kluwer Academic Publishers.

Grimm, E.C. 1987. CONISS: a FORTRAN 77 program for stratigraphically constrained cluster analysis by the method of incremental sum of squares. *Computers & Geosciences.* 13(1):13-35.

Haberzettl, T., Baade, J., Compton, J., Daut, G., Dupont, L., Finch, J., Frenzel, P., Green, A. et al. 2014. Paleoenvironmental investigations using a combination of terrestrial and marine sediments from South Africa-The RAIN (Regional Archives for Integrated iNvestigations) approach. *Zentralblatt Für Geologie Und Paläontologie, Teil I.* 55-73.

Hahn, A., Compton, J.S., Meyer-Jacob, C., Kirsten, K.L., Lucasssen, F., Mayo, M.P., Schefuß, E. & Zabel, M. 2016. Holocene paleo-climatic record from the South African Namaqualand mudbelt: A source to sink approach. *Quaternary International.* 404:121-135.

Hahn, A., Schefuß, E., Andò, S., Cawthra, H.C., Frenzel, P., Kugel, M., Meschner, S., Mollenhauer, G. 2017. Southern Hemisphere anticyclonic circulation drives oceanic and climatic conditions in late Holocene southernmost Africa. *Climate of the Past.* 13(6):649-665.

Hogg, A.G., Hua, Q., Blackwell, P.G., Niu, M., Buck, C.E., Guilderson, T.P., Heaton, T.J., Palmer, J.G., Reimer, P.J., Reimer, R.W. and Turney, C.S., 2013. SHCal13 Southern Hemisphere calibration, 0–50,000 years cal BP. *Radiocarbon*. 55(4): 1889-1903.

Holmes, P.J., Bateman, M.D., Carr, A.S. & Marker, M.E. 2007. The place of aeolian coversands in the geomorphic evolution of the southern Cape coast, South Africa. *South African Journal of Geology.* 110(1):125-136.

Holmgren, K., Karlén, W., Lauritzen, S.E., Lee-Thorp, J.A., Partridge, T.C., Piketh, S., Repinski, P., Stevenson, C. et al. 1999. A 3000-year high-resolution stalagmitebased record of palaeoclimate for northeastern South Africa. *The Holocene.* 9(3):295-309.

Howard-Williams, C. & Allanson, B.R. 1979. *The ecology of Swartvlei: Research for planning and future management.* Water Research Commission.

Humphries, M.S., Benitez-Nelson, C.R., Bizimis, M. & Finch, J.M. 2017. An aeolian sediment reconstruction of regional wind intensity and links to larger scale climate variability since the last deglaciation from the east coast of southern Africa. *Global and Planetary Change.* 156:59-67.

Humphries, M.S., Green, A.N. & Finch, J.M. 2016. Evidence of El Niño driven desiccation cycles in a shallow estuarine lake: The evolution and fate of Africa's largest estuarine system, Lake St Lucia. *Global and Planetary Change.* 147:97-105.

Illenberger, W.K. 1996. The geomorphologic evolution of the Wilderness dune cordons, South Africa. *Quaternary International.* 33:11-20.

James, N.C. & Harrison, T.D. 2008. A preliminary survey of the estuaries on the south coast of South Africa, Cape St Blaize, Mossel Bay—Robberg Peninsula, Plettenberg Bay, with particular reference to the fish fauna. *Transactions of the Royal Society of South Africa.* 63(2):111-127.

Jury, M.R., Valentine, H.R. & Lutjeharms, J.R. 1993. Influence of the Agulhas Current on summer rainfall along the southeast coast of South Africa. *Journal of Applied Meteorology.* 32(7):1282-1287.

Kasper, T., Haberzettl, T., Doberschütz, S., Daut, G., Wang, J., Zhu, L., Nowaczyk, N. & Mäusbacher, R. 2012. Indian Ocean Summer Monsoon (IOSM)-dynamics within the past 4 ka recorded in the sediments of Lake Nam Co, central Tibetan Plateau (China). *Quaternary Science Reviews.* 39:73-85.

Kirst, G.J., Schneider, R.R., Müller, P.J., von Storch, I. & Wefer, G. 1999. Late Quaternary temperature variability in the Benguela Current System derived from alkenones. *Quaternary Research.* 52(1):92-103.

Kirsten K. Holocene environmental change at Groenvlei, Knysna, South Africa: evidence from diatoms (Doctoral dissertation, University of Cape Town).

Kirsten, K.L., Haberzettl, T., Wündsch, M., Frenzel, P., Meschner, S., Smit, A.J., Quick, L.J., Mäusbacher, R. et al. 2018. A multiproxy study of the ocean-atmospheric forcing and the impact of sea-level changes on the southern Cape coast, South Africa during the Holocene. *Palaeogeography, Palaeoclimatology, Palaeoecology.* 496: 282-291.

Klute, A. & Dinauer, R.C. 1986. Physical and mineralogical methods. *Planning.* 8:79.

Kok, H.M. & Whitfield, A.K. 1986. The influence of open and closed mouth phases on the marine fish fauna of the Swartvlei estuary. *African Zoology.* 21(4):309-315.

Kylander, M.E., Ampel, L., Wohlfarth, B. & Veres, D. 2011. High-resolution X-ray fluorescence core scanning analysis of Les Echets (France) sedimentary sequence: new insights from chemical proxies. *Journal of Quaternary Science.* 26(1):109-117.

Lamb, A.L., Wilson, G.P. & Leng, M.J. 2006. A review of coastal palaeoclimate and relative sea-level reconstructions using δ13C and C/N ratios in organic material. *Earth-Science Reviews.* 75(1-4):29-57.

Last, W.M. & Smol, J.P. 2001. *Tracking environmental change using lake sediments. Vol. 1, Basin analysis, coring, and chronological techniques.* Kluwer Academic Publishers.

Lee-Thorp, J.A., Holmgren, K., Lauritzen, S., Linge, H., Moberg, A., Partridge, T.C., Stevenson, C. & Tyson, P.D. 2001. Rapid climate shifts in the southern African interior throughout the mid to late Holocene. *Geophysical Research Letters.* 28(23):4507-4510.

Lewin, J. 1978. Floodplain geomorphology. *Progress in Physical Geography.* 2(3):408-437.

Liptrot, M.R. Community metabolism and phosphorus dynamics in a seasonally closed South African estuary (Doctoral dissertation, Rhodes University).

Loftus, E., Sealy, J., Leng, M.J. & Lee-Thorp, J.A. 2017. A late Quaternary record of seasonal sea surface temperatures off southern Africa. *Quaternary Science Reviews.* 171:73-84.

López-Buendıa, A.M., Bastida, J., Querol, X. & Whateley, M. 1999. Geochemical data as indicators of palaeosalinity in coastal organic-rich sediments. *Chemical Geology.* 157(3-4):235-254.

Lowe, J.J. & Walker, M.J.C. 2015. *Reconstructing quaternary environments.* 3. ed. London: Routledge.

Löwemark, L., Chen, H., Yang, T., Kylander, M., Yu, E., Hsu, Y., Lee, T., Song, S. et al. 2011. Normalizing XRF-scanner data: a cautionary note on the interpretation of high-resolution records from organic-rich lakes. *Journal of Asian Earth Sciences.* 40(6):1250-1256.

Lüning, S., Gałka, M., Danladi, I.B., Adagunodo, T.A. & Vahrenholt, F. 2018. Hydroclimate in Africa during the medieval climate anomaly. *Palaeogeography, Palaeoclimatology, Palaeoecology.*

Ma, X., Zuo, H., Tian, M., Zhang, L., Meng, J., Zhou, X., Min, N., Chang, X. et al. 2016. Assessment of heavy metals contamination in sediments from three adjacent regions of the Yellow River using metal chemical fractions and multivariate analysis techniques. *Chemosphere.* 144:264-272.

Maboya, M.L., Meadows, M.E., Reimer, P.J., Backeberg, B.C. & Haberzettl, T. 2017. Late Holocene marine radiocarbon reservoir correction for the southern and eastern coasts of South Africa. *Radiocarbon.* :1-12.

Marker, M.E. 1997. Evidence for a Holocene low sea level at Knysna. *South African Geographical Journal.* 79(2):106-107.

Marker, M.E. & Holmes, P.J. 2005. Landscape evolution and landscape sensitivity: the case of the southern Cape. *South African Journal of Science.* 101(1-2):53-60.

Martin, A. 1962. Evidence relating to the Quaternary history of the Wilderness lakes. *South African Journal of Geology.* 65(Transactions 1962, Part 1):19-42.

Martin, A. 1968. Pollen analysis of Groenvlei lake sediments, Knysna (South Africa). *Review of Palaeobotany and Palynology.* 7(2):107-144.

Mayewski, P.A., Rohling, E.E., Stager, J.C., Karlén, W., Maasch, K.A., Meeker, L.D., Meyerson, E.A., Gasse, F. et al. 2004. Holocene climate variability. *Quaternary Research.* 62(3):243-255.

McCarty, R. & Schwandes, L. 2006. Biogenic silica as an environmental indicator. In *First Floridians and Last Mastodons: The Page-Ladson Site in the Aucilla River.* Springer. 471-491.

Baxter, A.J. and Meadows, M.E., 1999. Evidence for Holocene sea level change at verlorenvlei, western cape, South Africa. *Quaternary International*. 56(1): 65-79.

Meadows, M.E., Baxter, A.J. & Parkington, J. 1996. Late Holocene environments at Verlorenvlei, Western Cape Province, South Africa. *Quaternary International.* 33:81-95.

Meadows, M.E., Rogers, J., Lee, J.A., Bateman, M.D. & Dingle, R.V. 2002. Holocene geochronology of a continentalshelf mudbelt off southwestern Africa. *The Holocene.* 12(1):59-67.

Meyers, P.A. 1997. Organic geochemical proxies of paleoceanographic, paleolimnologic, and paleoclimatic processes. *Organic Geochemistry.* 27(5-6):213-250.

Meyers, P.A. 2003. Applications of organic geochemistry to paleolimnological reconstructions: a summary of examples from the Laurentian Great Lakes. *Organic Geochemistry.* 34(2):261-289.

Meyers, P.A. & Lallier-Vergès, E. 1999. Lacustrine sedimentary organic matter records of Late Quaternary paleoclimates. *Journal of Paleolimnology.* 21(3):345-372.

Miller, D.E., Yates, R.J., Jerardino, A. & Parkington, J.E. 1995. Late Holocene coastal change in the southwestern Cape, South Africa. *Quaternary International.* 29:3-10.

Mucina, L. & Rutherford, M.C. 2006. *The vegetation of South Africa, Lesotho and Swaziland.* South African National Biodiversity Institute.

Mulenga, H.M., Rouault, M., Reason, C.J.C. 2003. Dry summers over northeastern South Africa and associated circulation anomalies. *Climate Research*. 25(1): 29-41

Naeher, S., Smittenberg, R.H., Gilli, A., Kirilova, E.P., Lotter, A.F. & Schubert, C.J. 2012. Impact of recent lake eutrophication on microbial community changes as revealed by high resolution lipid biomarkers in Rotsee (Switzerland). *Organic Geochemistry.* 49:86-95.

Nakagawa, T. 2007. Double-L channel: an amazingly non-destructive method of continuous sub-sampling from sediment cores. *Quaternary International.* 167(Supplement):298.

Niang, I., Ruppel, O. & Abdrabo, M. 2014. WGII, Chapter 22: Africa. *IPCC, Fifth Assessment Report.Geneva, Switzerland.* 1-51.

Norström, E., Scott, L., Partridge, T.C., Risberg, J. & Holmgren, K. 2009. Reconstruction of environmental and climate changes at Braamhoek wetland, eastern escarpment South Africa, during the last 16,000Â years with emphasis on the Pleistocene*. Holocene transition.*

Ohlendorf, C. & Sturm, M. 2008. A modified method for biogenic silica determination. *Journal of Paleolimnology.* 39(1):137-142.

Parsons, R.P. 2014. No title. *Quantifying the Role of Groundwater in Sustaining Groenvlei, a Shallow Lake in the Southern Cape Region of South Africa.*

Parkington, M., 2000. Palaeovegetation at the last glacial maximum in the western Cape, South Africa: wood charcoal and pollen evidence from Elands Bay Cave. *South African Journal of Science*. 96(11-12): 543-546.

Partridge, T.C., Avery, D.M., Botha, G.A., Brink, J.S., Deacon, J., Herbert, R.S., Maud, R.R., Scholtz, A. et al. 1990. Late pleistocene and holocene climatic-change in Southern Africa. *South African Journal of Science.* 86(7-10):302-306.

Partridge, T.C., Scott, L. and Hamilton, J.E., 1999. Synthetic reconstructions of southern African environments during the Last Glacial Maximum (21–18 kyr) and the Holocene Altithermal (8–6 kyr). *Quaternary International*. 57: 207-214.

Pasquini, L., Cowling, R.M. & Ziervogel, G. 2013. Facing the heat: Barriers to mainstreaming climate change adaptation in local government in the Western Cape Province, South Africa. *Habitat International.* 40:225-232.

Pye, K. and Blott, S.J., 2004. Particle size analysis of sediments, soils and related particulate materials for forensic purposes using laser granulometry. *Forensic Science International*. 144(1): 19-27.

Qiu, L., Williams, D.F., Gvorzdkov, A., Karabanov, E. & Shimaraeva, M. 1993. Biogenic silica accumulation and paleoproductivity in the northern basin of Lake Baikal during the Holocene. *Geology.* 21(1):25-28.

Quick, L.J., Carr, A.S., Meadows, M.E., Boom, A., Bateman, M.D., Roberts, D.L., Reimer, P.J. & Chase, B.M. 2015. A late Pleistocene–Holocene multi-proxy record of palaeoenvironmental change from Still Bay, southern Cape Coast, South Africa. *Journal of Quaternary Science.* 30(8):870-885.

Quick, L.J., Chase, B.M., Wündsch, M., Kirsten, K.L., Chevalier, M., Mäusbacher, R., Meadows, M.E. & Haberzettl, T. 2018. A high-resolution record of Holocene climate and vegetation dynamics from the southern Cape coast of South Africa: pollen and microcharcoal evidence from Eilandvlei. *Journal of Quaternary Science.*

Quick, L.J., Meadows, M.E., Bateman, M.D., Kirsten, K.L., Mäusbacher, R., Haberzettl, T. & Chase, B.M. 2016. Vegetation and climate dynamics during the last glacial period in the fynbos-afrotemperate forest ecotone, southern Cape, South Africa. *Quaternary International.* 404:136-149.

Ramsay, P.J. 1996. 9000 years of sea-level change along the southern African coastline. *Quaternary International.* 31:71-75.

Ramsay, P.J. & Cooper, J.A.G. 2002. Late Quaternary sea-level change in South Africa. *Quaternary Research.* 57(1):82-90.

Reimer, P.J., Bard, E., Bayliss, A., Beck, J.W., Blackwell, P.G., Ramsey, C.B., Buck, C.E., Cheng, H., Edwards, R.L., Friedrich, M. and Grootes, P.M., 2013. IntCal13 and Marine13 radiocarbon age calibration curves 0–50,000 years cal BP. *Radiocarbon*. 55(4): 1869-1887.

Robarts, R.D. 1973. *A contribution to the limnology of Swartvlei: The effect of physico-chemical factors upon primary and secondary production in the pelagic zone.* RD Robarts.

Robarts, R.D. 1976. Primary productivity of the upper reaches of a South African estuary (Swartvlei). *Journal of Experimental Marine Biology and Ecology.* 24(1):93-102.

Russell, I.A. 1999. Changes in the water quality of the Wilderness and Swartvlei Lake systems, South Africa. *Koedoe.* 42(1):57-72.

Russell, I.A. 2015. Spatio-temporal variability of five surface water quality parameters in the Swartvlei estuarine lake system, South Africa. *African Journal of Aquatic Science.* 40(2):119-131.

Sandgren, P. & Snowball, I. 2001. The Late Weichselian sea level history of the Kullen Peninsula in northwest Skåne, southern Sweden. *Boreas.* 30(2):115-130.

Sayer, C.D., Davidson, T.A., Jones, J.I. & Langdon, P.G. 2010. Combining contemporary ecology and palaeolimnology to understand shallow lake ecosystem change. *Freshwater Biology.* 55(3):487-499.

Schefuß, E., Kuhlmann, H., Mollenhauer, G., Prange, M. & Pätzold, J. 2011. Forcing of wet phases in southeast Africa over the past 17,000 years. *Nature.* 480(7378):509.

Schillereff, D.N., Chiverrell, R.C., Macdonald, N. & Hooke, J.M. 2014. Flood stratigraphies in lake sediments: a review. *Earth-Science Reviews.* 135:17-37.

Scholtz, A., 1986. Palynological and palaeobotanical studies in the southern Cape (Doctoral dissertation, Stellenbosch: University of Stellenbosch).

Schulze, B.R. 1947. The climates of South Africa according to the classifications of Köppen and Thornthwaite. *South African Geographical Journal.* 29(1):32-42.

Scott, L., Steenkamp, M. & Beaumont, P.B. 1995. Palaeoenvironmental conditions in South Africa at the Pleistocene-Holocene transition. *Quaternary Science Reviews.* 14(9):937-947.

Scott, L. & Lee-Thorp, J.A. 2004. Holocene climatic trends and rhythms in southern Africa. In *Past climate variability through Europe and Africa.* Springer. 69-91.

Stevenson, F.J., Stevenson, E.J. & Cole, M.A. 1999. *Cycles of soils: carbon, nitrogen, phosphorus, sulfur, micronutrients.* John Wiley & Sons.

Stowe, M.J. and Sealy, J., 2016. Terminal Pleistocene and Holocene dynamics of southern Africa's winter rainfall zone based on carbon and oxygen isotope analysis of bovid tooth enamel from Elands Bay Cave. *Quaternary International.* 404: 57-67.

Strachan, K.L., Finch, J.M., Hill, T. & Barnett, R.L. 2014. A late Holocene sea-level curve for the east coast of South Africa. *South African Journal of Science.* 110(1-2):1-9.

Strobel, P., Haberzettl, T., Frenzel, P., Schittek, K., Quick, L., Kasper, T., Schefuß, E., Kirsten, K. et al. 2018. Late Quaternary paleoenvironmental change in the year-round rainfall zone of South Africa derived from peat sediments from Vankervelsvlei. *EGU General Assembly Conference Abstracts.* 4908.

Talma, A.S. & Vogel, J.C. 1992. Late Quaternary paleotemperatures derived from a speleothem from Cango caves, Cape province, South Africa. *Quaternary Research.* 37(2):203-213.

Thackeray, J.F. & Avery, D.M. 1990. A comparison between temperature indices for Late Pleistocene sequences at Klasies River and Border Cave, South Africa. *Paleoecol.Afr.* 21:311-315.

Thompson, R., Battarbee, R.W., O'sullivan, P.E. & Oldfield, F. 1975. Magnetic susceptibility of lake sediments. *Limnology and Oceanography.* 20(5):687-698.

Thompson, S., Eglinton, G. 1978. The fractionation of a recent sediment for organic geochemical analysis. *Geochimica Et Cosmochimica Acta.* 42(2):199-207.

Truc, L., Chevalier, M., Favier, C., Cheddadi, R., Meadows, M.E., Scott, L., Carr, A.S., Smith, G.F. and Chase, B.M., 2013. Quantification of climate change for the last 20,000 years from Wonderkrater, South Africa: implications for the long-term dynamics of the Intertropical Convergence Zone. *Palaeogeography, Palaeoclimatology, Palaeoecology.* 386: 575-587.

Tyson, P.D. 1999. Late-Quaternary and Holocene palaeoclimates of southern Africa: a synthesis. *South African Journal of Geology.* 102(4):335-349.

Tyson, P.D. & Preston-Whyte, R.A. 2000. *Weather and climate of southern Africa.* Oxford University Press.

Uncles, R.J. & Mitchell, S.B. 2017. Estuarine and Coastal Hydrography and Sediment Transport. In *Estuarine and Coastal Hydrography and Sediment Transport.* Cambridge: Cambridge University Press. 1-34.

Walker, M. 2005. *Quaternary Dating Methods.* 1st ed. New York: John Wiley & Sons, Incorporated. Available: http://lib.myilibrary.com?ID=23880.

Watling, R.J. 1977. Trace metal distribution in the Wilderness-lakes. *CSIR Special Report FIS.* 147.

Weisser, P.J., Whitfield, A.K. & Hall, C.M. 1992. The recovery and dynamics of submerged aquatic macrophyte vegetation in the Wilderness lakes, southern Cape. *Bothalia.* 22(2):283-288.

Whitfield, A.K. & Cowley, P.D. 2010. The status of fish conservation in South African estuaries. *Journal of Fish Biology.* 76(9):2067-2089.

Whitfield, A.K. 1988. The fish community of the Swartvlei estuary and the influence of food availability on resource utilization. *Estuaries.* 11(3):160-170.

Whitfield, A.K., Allanson, B.R. & Heinecken, T. 1983. *Swartvlei (CMS11).* CSIR, National Research Institute for Oceanology.

Whitfield, A.K., Weerts, S.P. & Weyl, O.L. 2017. A review of the influence of biogeography, riverine linkages, and marine connectivity on fish assemblages in evolving lagoons and lakes of coastal southern Africa. *Ecology and Evolution.* 7(18):7382-7398.

Willis, J.P. 1985a. The bathymetry, environmental parameters and sediments of the Bot River estuary, SW Cape Province. *Transactions of the Royal Society of South Africa.* 45(3-4):253-283.

Willis, J.P. 1985b. The bathymetry, environmental parameters and sediments of the Bot River estuary, SW Cape Province. *Transactions of the Royal Society of South Africa.* 45(3-4):253-283.

Wolff, E.W., Chappellaz, J., Blunier, T., Rasmussen, S.O. & Svensson, A. 2010. Millennial-scale variability during the last glacial: The ice core record. *Quaternary Science Reviews.* 29(21-22):2828-2838.

Wolin, J.A. & Duthie, H.C. 1999. Diatoms as indicators of water level change in freshwater lakes. *The Diatoms: Applications for the Environmental and Earth Sciences.* 183-202.

Wright, H.E. 1993. Core compression1. *Limnology and Oceanography.* 38(3):699-701.

Wündsch, M., Haberzettl, T., Kirsten, K.L., Meschner, S., Frenzel, P., Baade, J., Daut, G., Mäusbacher, R., Kasper, T., Quick, L.J. and Meadows, M., 2016. A 4.2 ka palaeosalinity record derived from lacustrine sediments from Groenvlei, wilderness embayment, South Africa. *Quaternary International*. 404: 182-183.

Wündsch, M., Haberzettl, T., Cawthra, H.C., Kirsten, K.L., Quick, L.J., Zabel, M., Frenzel, P., Hahn, A., Baade, J., Daut, G. and Kasper, T., 2018. Holocene environmental change along the southern Cape coast of South Africa–Insights from the Eilandvlei sediment record spanning the last 8.9 kyr. *Global and Planetary Change*. 163: 51-66.

Zhang, Q., Holmgren, K. & Sundqvist, H. 2015. Decadal rainfall dipole oscillation over southern Africa modulated by variation of austral summer Land–Sea contrast along the East Coast of Africa. *Journal of the Atmospheric Sciences.* 72(5):1827-1836.

Zhao, X., Dupont, L., Schefuß, E., Meadows, M.E., Hahn, A. & Wefer, G. 2016. Holocene vegetation and climate variability in the winter and summer rainfall zones of South Africa. *The Holocene.* 26(6):843-857.

Ziervogel, G., New, M., Archer van Garderen, E., Midgley, G., Taylor, A., Hamann, R., Stuart-Hill, S., Myers, J. et al. 2014. Climate change impacts and adaptation in South Africa. *Wiley Interdisciplinary Reviews: Climate Change.* 5(5):605-620.

APPENDIX A

Core description

Core ID[1]: SV13- 7 (1.5 – 3.5m) A
Water depth: 19
Opening date: 18.09.2017
Examiner: Lillian Maboya / Torsten Haberzettl
Core type: Piston
Fotos: Digi
Multisensor: Suszi
Remarks: 99.8cm length

[1]Example: RAL 01/1-1
Lake code Year Core No. Section No.

Lake: Swartvlei

Description guidelines
1.Sediment class Clastic, chemical or biogenic.
2.Grain size gravel (>2mm), sand (2mm-63µm), silt (63-2µm), clay (<2µm). Modifiers: fine, middle and coarse or eg. sandy silt etc.
3.Color eg. brownish grey (=main color is grey).
4.Structure e.g. laminated, homogenous, bioturbated, etc.
5.Organics e.g. terrestrial plant remains, diatoms, ostracods, etc.
6.Additions e.g. high water, or organic content consolidated, well rounded grains, Type of minerals (e.g. carbonate, feldspar, quartz, mica).
Example: 12-25cm: Clastic sandy silt, brownish grey, laminated, with terrestrial plant remains. Organic content increases towards top of the section, Sand grains=mainly quartz.

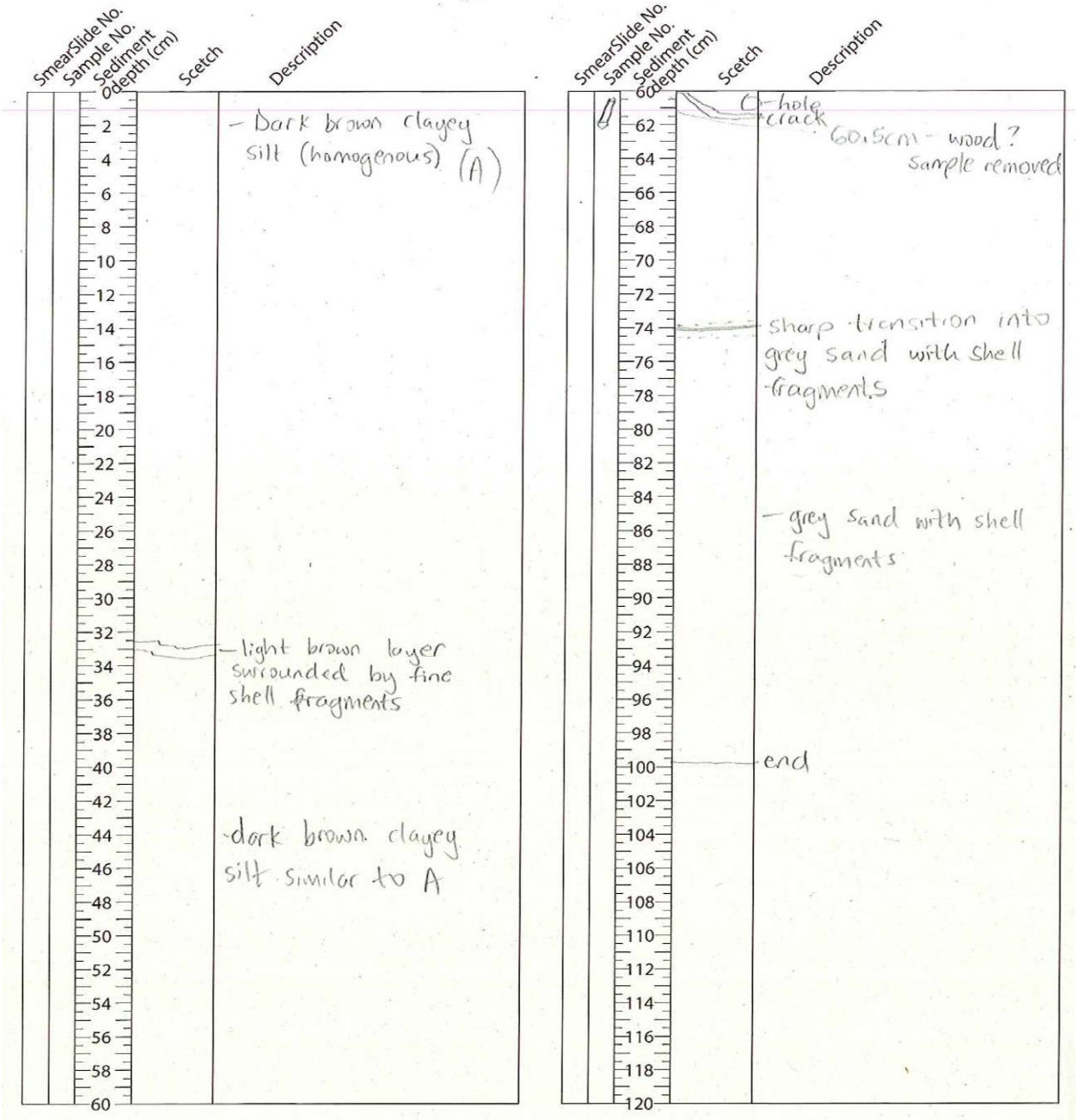

Core description

Lake: Swartvlei

Core ID[1]: SV13- 7 (1.5-3.5m) B
Water depth: 19
Opening date: 18.09.2017
Examiner: Lillian Maboya / Torsten Haberzettl
Core type: Piston
Fotos: Digi
Multisensor: Suszi
Remarks: -69.5cm length

[1]Example: RAL 01/1-1
Lake code Year Core No. Section No.

Description guidelines
1. Sediment class Clastic, chemical or biogenic.
2. Grain size gravel (>2mm), sand (2mm-63µm), silt (63-2µm), clay (<2µm). Modifiers: fine, middle and coarse or eg. sandy silt etc.
3. Color eg. brownish grey (=main color is grey).
4. Structure e.g. laminated, homogenous, bioturbated, etc.
5. Organics e.g. terrestrial plant remains, diatoms, ostracods, etc.
6. Additions e.g. high water, or organic content consolidated, well rounded grains, Type of minerals (e.g. carbonate, feldspar, quartz, mica).

Example: 12-25cm: Clastic sandy silt, brownish grey, laminated, with terrestrial plant remains. Organic content increases towards top of the section, Sand grains=mainly quartz.

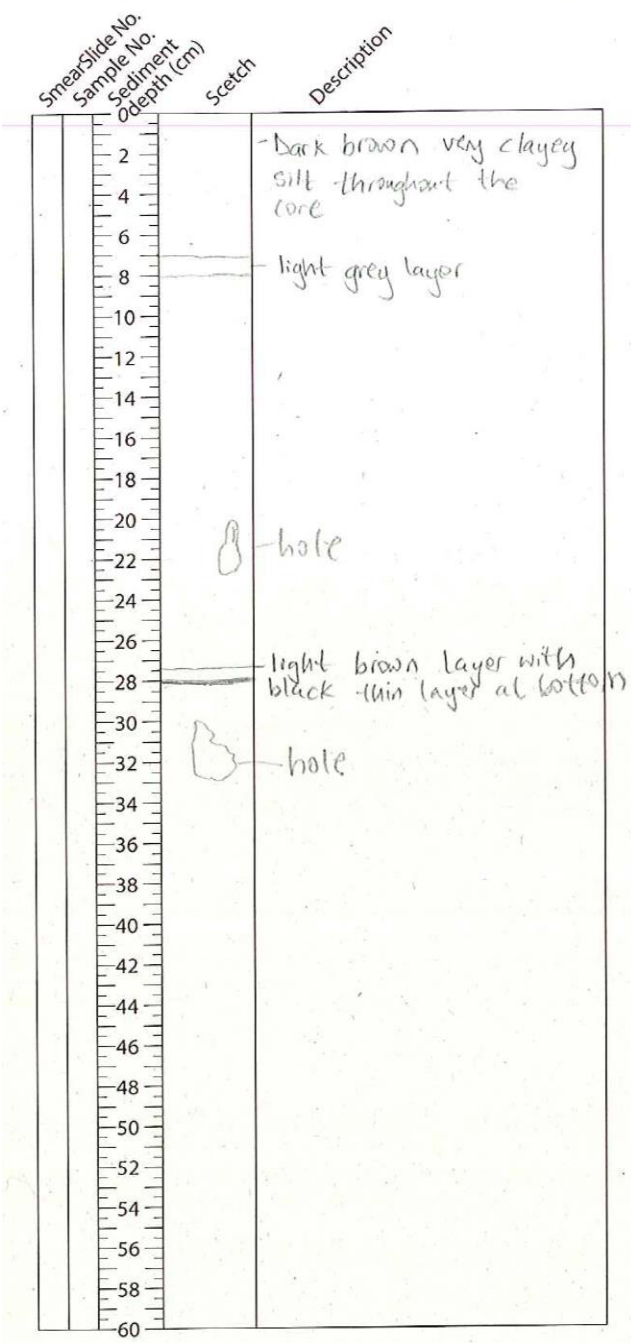

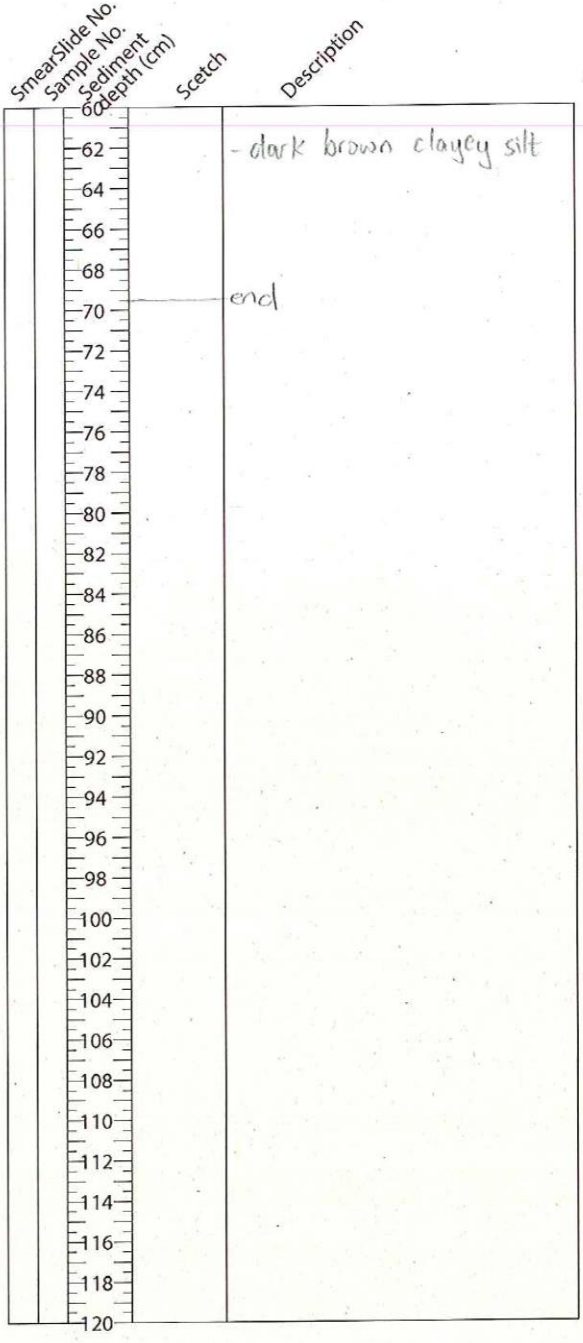

Core description

Lake: Swartvlei

Core ID[1]: SV13-5 (0-2m) B
Water depth: 20
Opening date: 18.09.2017
Examiner: Lillian Maboya / Torsten Haberzettl
Core type: Piston
Fotos: Digi
Multisensor: Suszi
Remarks: 90cm length
high water content
unconsolidated

[1]Example: BAL 01/1-1
Lake code Year Core No. Section No.

Description guidelines
1.Sediment class Clastic, chemical or biogenic.
2.Grain size gravel (>2mm), sand (2mm-63µm), silt (63-2µm), clay (<2µm). Modifiers: fine, middle and coarse or eg. sandy silt etc.
3.Color eg. brownish grey (=main color is grey).
4.Structure e.g. laminated, homogenous, bioturbated, etc.
5.Organics e.g. terrestrial plant remains, diatoms, ostracods, etc.
6.Additions e.g. high water, or organic content consolidated, well rounded grains, Type of minerals (e.g. carbonate, feldspar, quartz, mica).
Example: 12-25cm: Clastic sandy silt, brownish grey, laminated, with terrestrial plant remains. Organic content increases towards top of the section, Sand grains=mainly quartz.

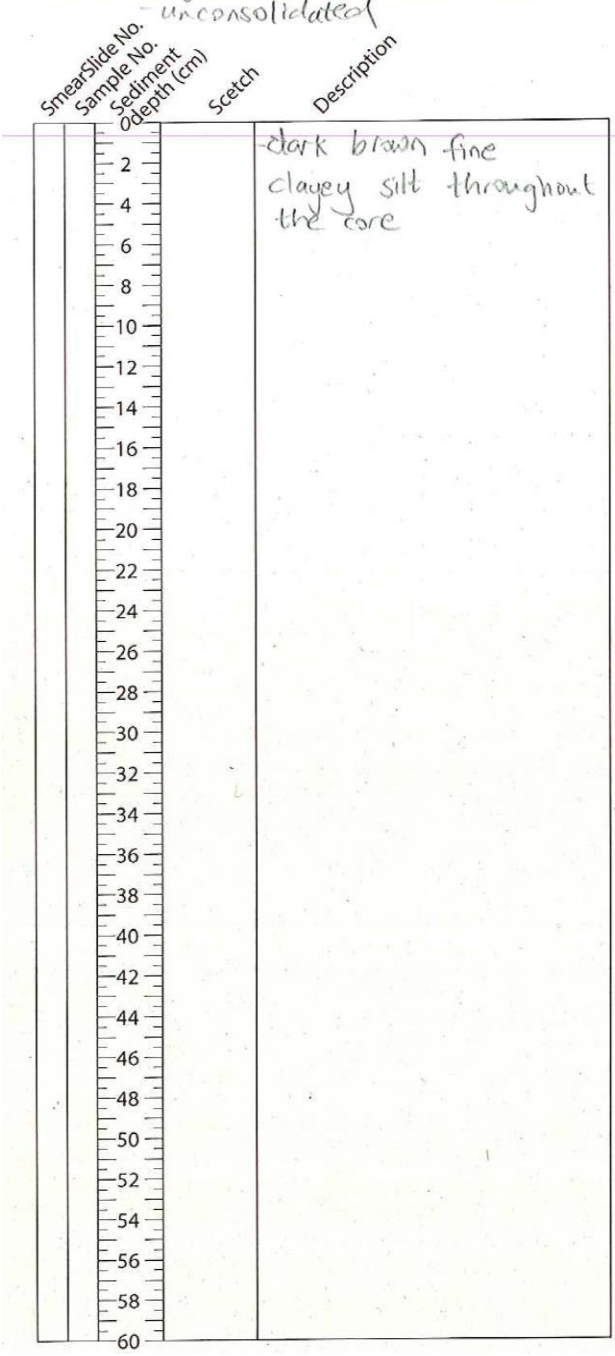

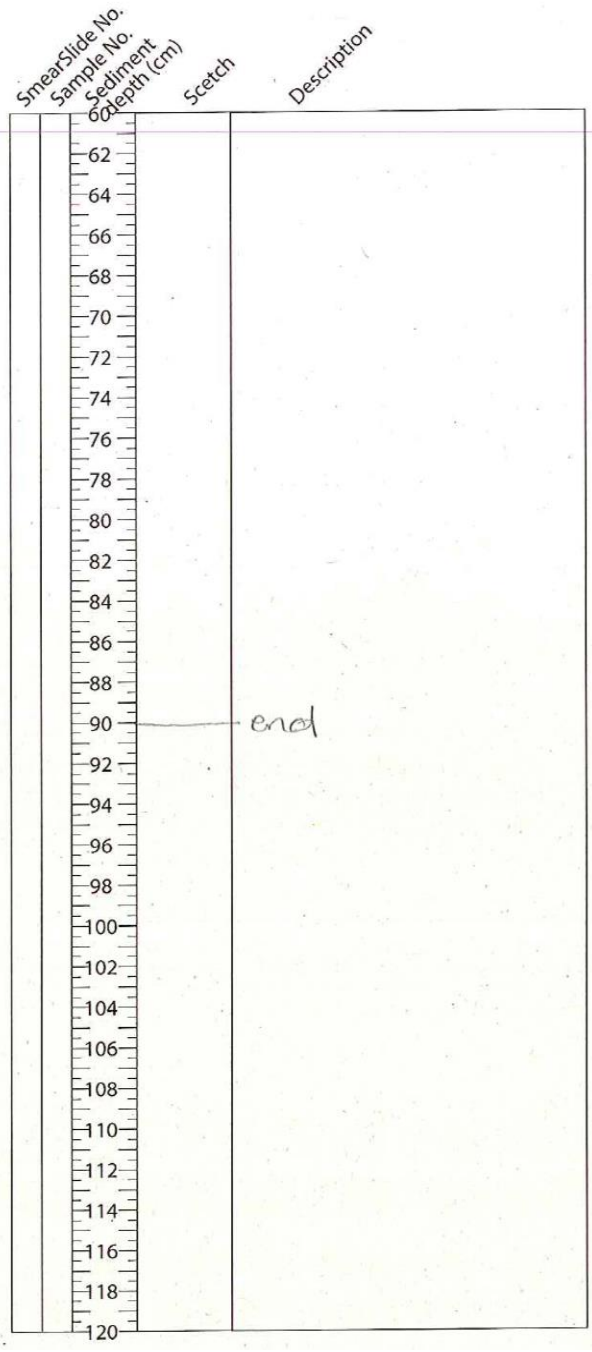

Core description

Lake: Swartvlei

Core ID[1]: SV13- 5 (0-2m)A
Water depth: 20
Opening date: 18.09.2017
Examiner: Lillian Maboya / Torsten Haberzettl
Core type: Piston
Fotos: Digi
Multisensor: Suszi
Remarks: - 99.8cm length

[1]Example: BAL 01/1-1
Lake code Year Core No. Section No.

Description guidelines
1. Sediment class Clastic, chemical or biogenic.
2. Grain size gravel (>2mm), sand (2mm-63µm), silt (63-2µm), clay (<2µm). Modifiers: fine, middle and coarse or eg. sandy silt etc.
3. Color eg. brownish grey (=main color is grey).
4. Structure e.g. laminated, homogenous, bioturbated, etc.
5. Organics e.g. terrestrial plant remains, diatoms, ostracods, etc.
6. Additions e.g. high water, or organic content consolidated, well rounded grains, Type of minerals (e.g. carbonate, feldspar, quartz, mica).

Example: 12-25cm: Clastic sandy silt, brownish grey, laminated, with terrestrial plant remains. Organic content increases towards top of the section, Sand grains=mainly quartz.

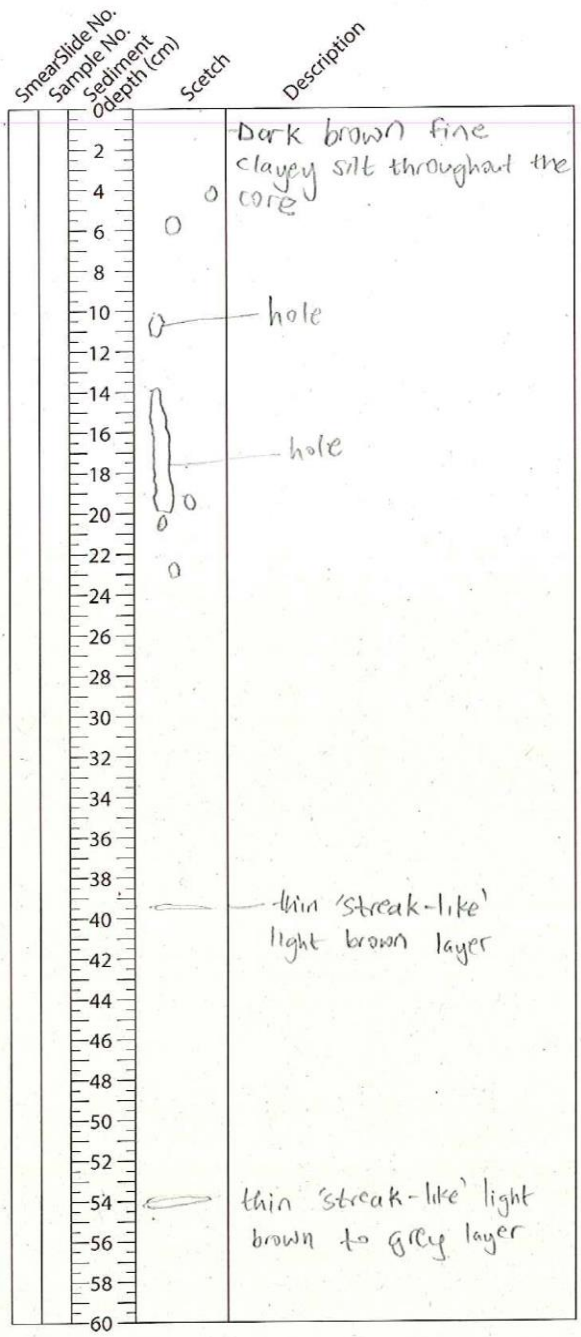

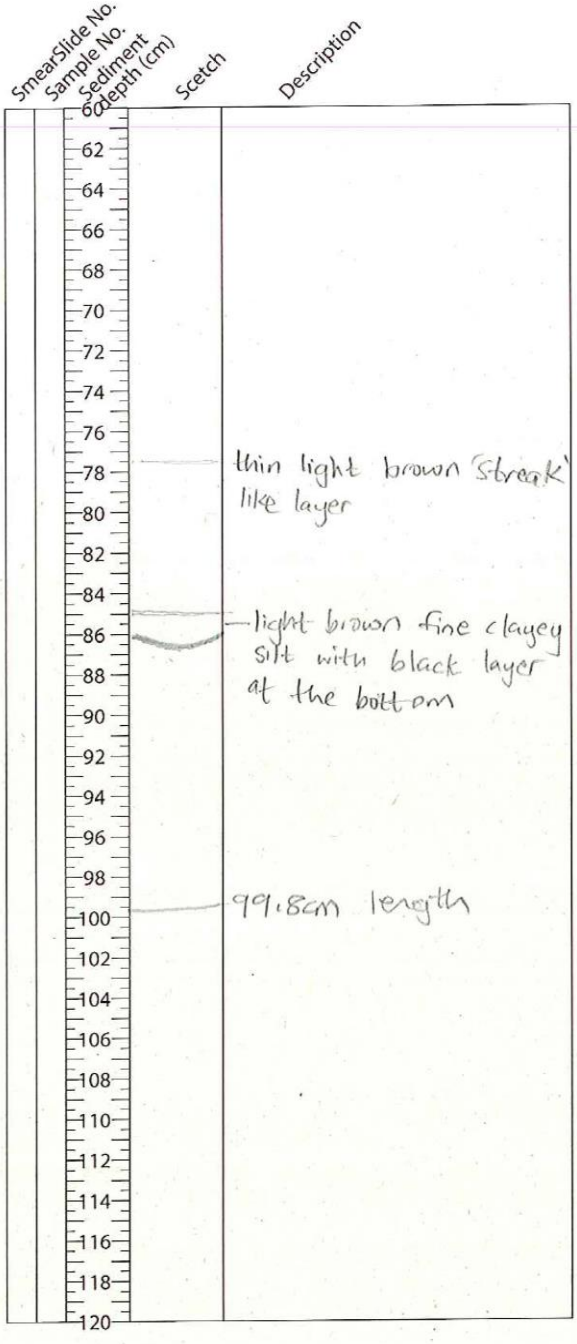

Core description

Lake: Swartvlei

Core ID[1]: SV13- 5 (4) (2 - 2 m)
Water depth: 20
Opening date: 18.09.2017
Examiner: Lillian Maboya / Torsten Haberzettl
Core type: Piston
Fotos: Digi
Multisensor: Suszi
Remarks: - 131cm length.
- slightly consolidated

[1]Example: BAL 01/1-1
Lake code Year Core No. Section No.

Description guidelines
1. Sediment class Clastic, chemical or biogenic.
2. Grain size gravel (>2mm), sand (2mm-63µm), silt (63-2µm), clay (<2µm). Modifiers: fine, middle and coarse or eg. sandy silt etc.
3. Color eg. brownish grey (=main color is grey).
4. Structure e.g. laminated, homogenous, bioturbated, etc.
5. Organics e.g. terrestrial plant remains, diatoms, ostracods, etc.
6. Additions e.g. high water, or organic content consolidated, well rounded grains, Type of minerals (e.g. carbonate, feldspar, quartz, mica).

Example: 12-25cm: Clastic sandy silt, brownish grey, laminated, with terrestrial plant remains. Organic content increases towards top of the section, Sand grains=mainly quartz.

- bottom part is missing because of core catcher malfunction
- bivalve samples @

SmearSlide No. | Sample No. | Sediment depth (cm) | Scetch | Description

0 – 60: crack; dark brown silty clay (homogenous) (A)

60 – 120: crack; light brown transition zone?; more shell fragments in this section; dark brown, very fine silty clay, darker than A; @ small gastropod; light grey transition zone; bright grey sand, lighter than B; grey sand with more shell fragments (B)

Core description

Lake: Swartvlei

Core ID[1]: SV13-6 (4–6m) A
Water depth:
Opening date: 13.09.2017
Examiner: Lillian Maboya / Torsten Haberzettl
Core type: Piston
Fotos: Digi
Multisensor: Suszi
Remarks: - 99.5cm length
- large fossils removed

[1]Example: BAL_01/1-1 (Lake code, Year, Core No., Section No.)

Description guidelines
1. Sediment class Clastic, chemical or biogenic.
2. Grain size gravel (>2mm), sand (2mm-63µm), silt (63-2µm), clay (<2µm). Modifiers: fine, middle and coarse or eg. sandy silt etc.
3. Color eg. brownish grey (=main color is grey).
4. Structure e.g. laminated, homogenous, bioturbated, etc.
5. Organics e.g. terrestrial plant remains, diatoms, ostracods, etc.
6. Additions e.g. high water, or organic content consolidated, well rounded grains, Type of minerals (e.g. carbonate, feldspar, quartz, mica).

Example: 12-25cm: Clastic sandy silt, brownish grey, laminated, with terrestrial plant remains. Organic content increases towards top of the section, Sand grains=mainly quartz.

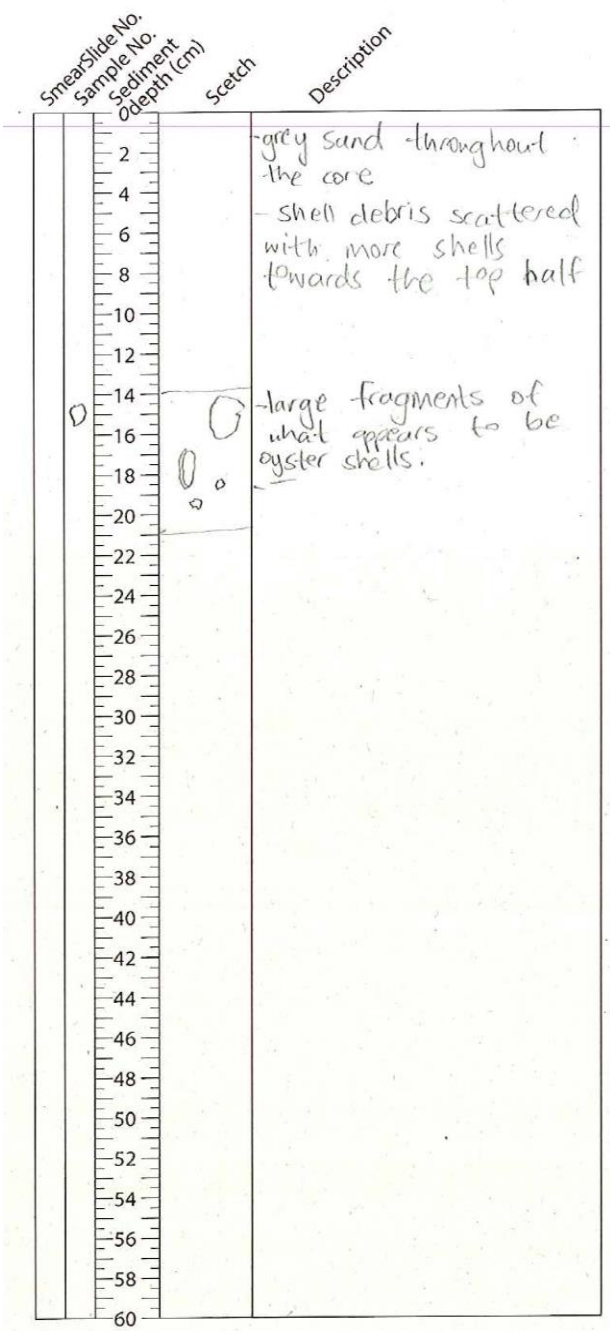

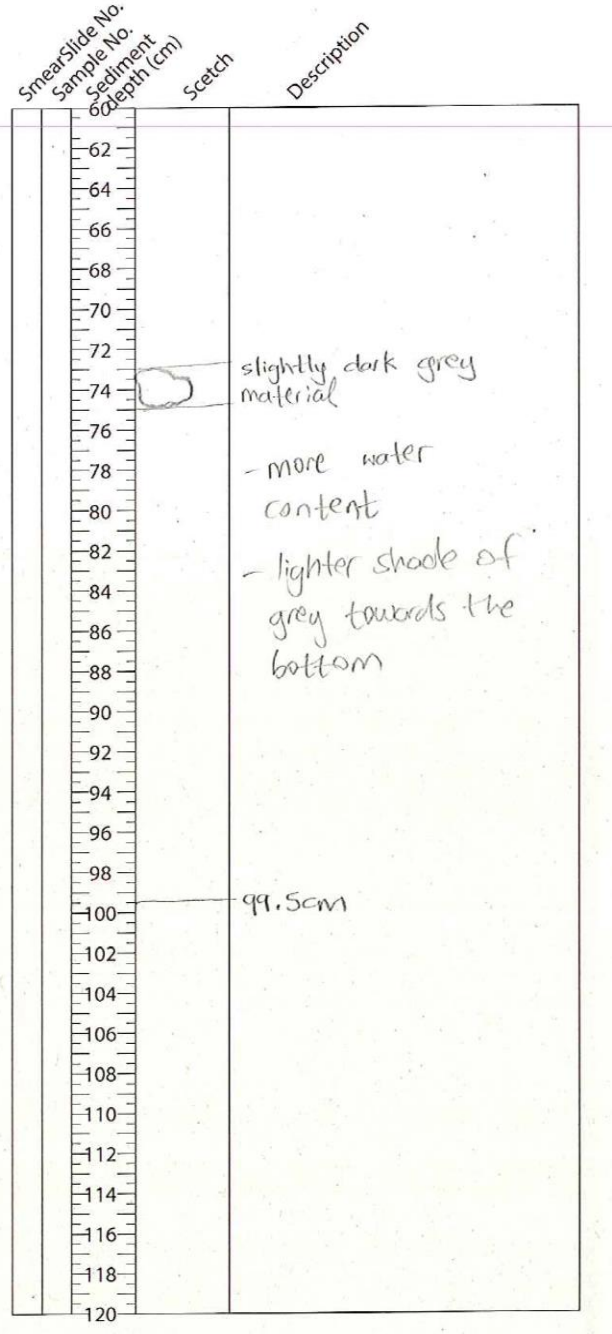

Core description

Lake: Swartvlei

Core ID[1]: SV13-6 (2-4m) A
Water depth:
Opening date: 13.09.2017
Examiner: Lillian Maboya / Torsten Haberzettl
Core type: Piston
Fotos: Digi
Multisensor: Suszi
Remarks: 97,5cm length
- sediment compression

[1]Example: BAL 07/1-1
Lake code Year Core No. Section No.

Description guidelines
1. Sediment class Clastic, chemical or biogenic.
2. Grain size gravel (>2mm), sand (2mm-63µm), silt (63-2µm), clay (<2µm). Modifiers: fine, middle and coarse or eg. sandy silt etc.
3. Color eg. brownish grey (=main color is grey).
4. Structure e.g. laminated, homogenous, bioturbated, etc.
5. Organics e.g. terrestrial plant remains, diatoms, ostracods, etc.
6. Additions e.g. high water, or organic content consolidated, well rounded grains, Type of minerals (e.g. carbonate, feldspar, quartz, mica).

Example: 12-25cm: Clastic sandy silt, brownish grey, laminated, with terrestrial plant remains. Organic content increases towards top of the section, Sand grains=mainly quartz.

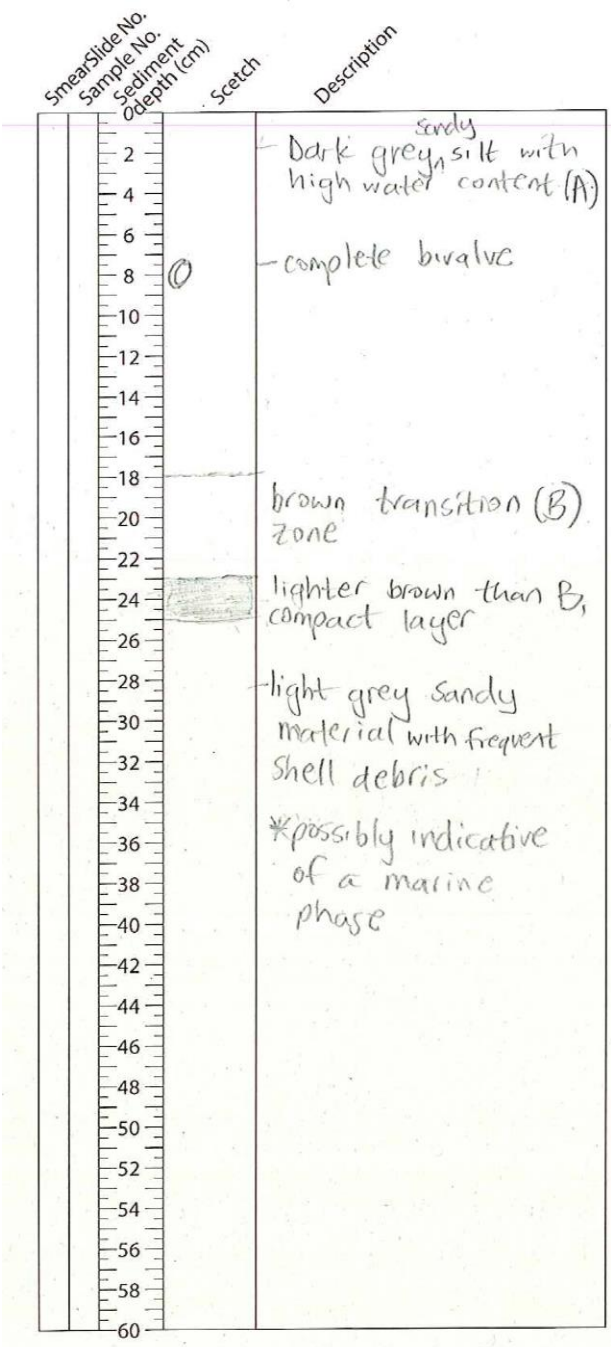

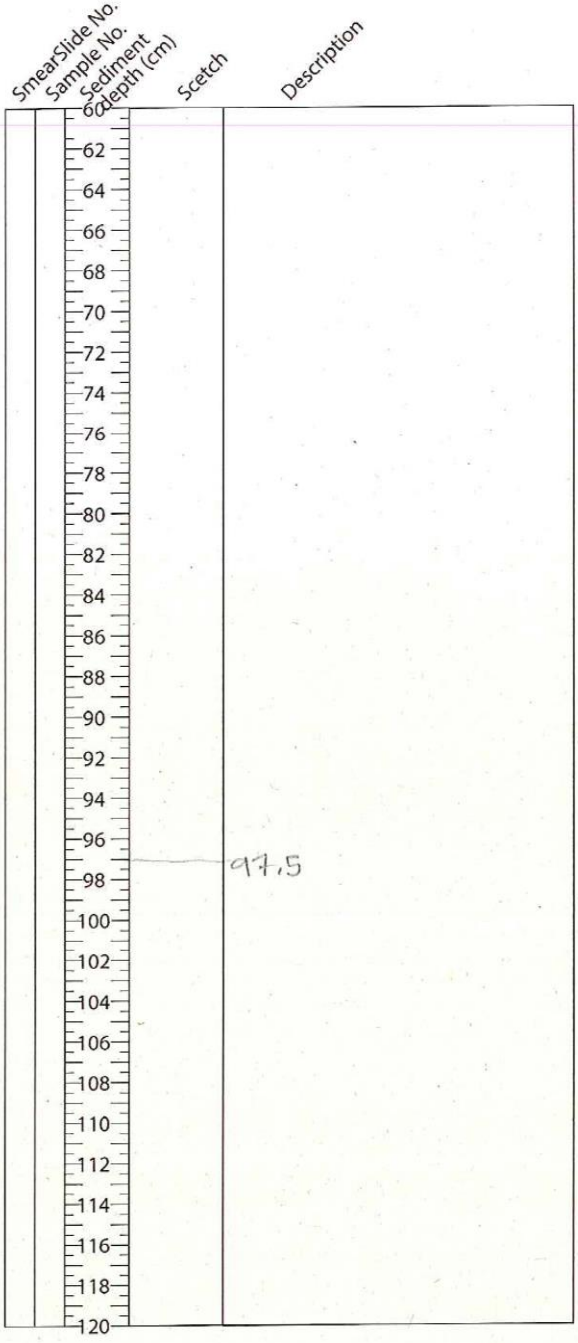

Core description

Lake: Swartvlei

Core ID[1]: SV13-6 (2-4m)B
Water depth:
Opening date: 13.09.2017
Examiner: Lillian Maboya / Torsten Haberzettl
Core type: Piston
Fotos: Digi
Multisensor: Suszi
Remarks: ~81cm length
- Sediment compression occured, leaving trapped air at top of sediment

[1]Example: BAL 07/1-1 (Lake code, Year, Core No., Section No.)

Description guidelines
1. Sediment class Clastic, chemical or biogenic.
2. Grain size gravel (>2mm), sand (2mm-63µm), silt (63-2µm), clay (<2µm). Modifiers: fine, middle and coarse or eg. sandy silt etc.
3. Color eg. brownish grey (=main color is grey).
4. Structure e.g. laminated, homogenous, bioturbated, etc.
5. Organics e.g. terrestrial plant remains, diatoms, ostracods, etc.
6. Additions e.g. high water, or organic content consolidated, well rounded grains, Type of minerals (e.g. carbonate, feldspar, quartz, mica).

Example: 12-25cm: Clastic sandy silt, brownish grey, laminated, with terrestrial plant remains. Organic content increases towards top of the section, Sand grains=mainly quartz.

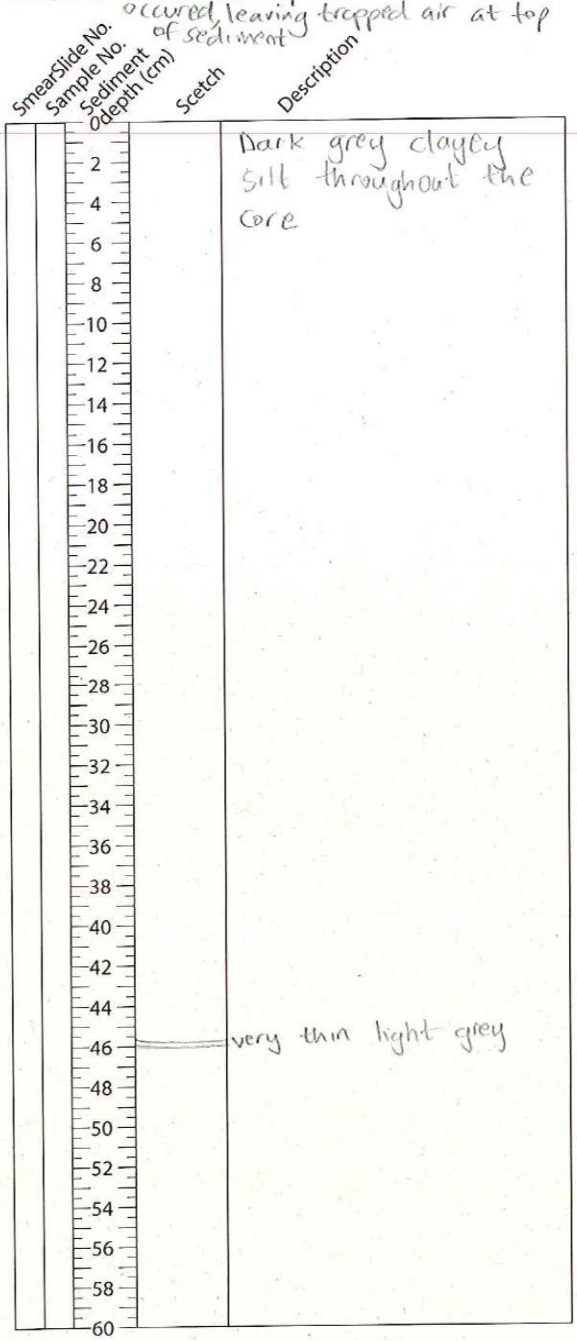

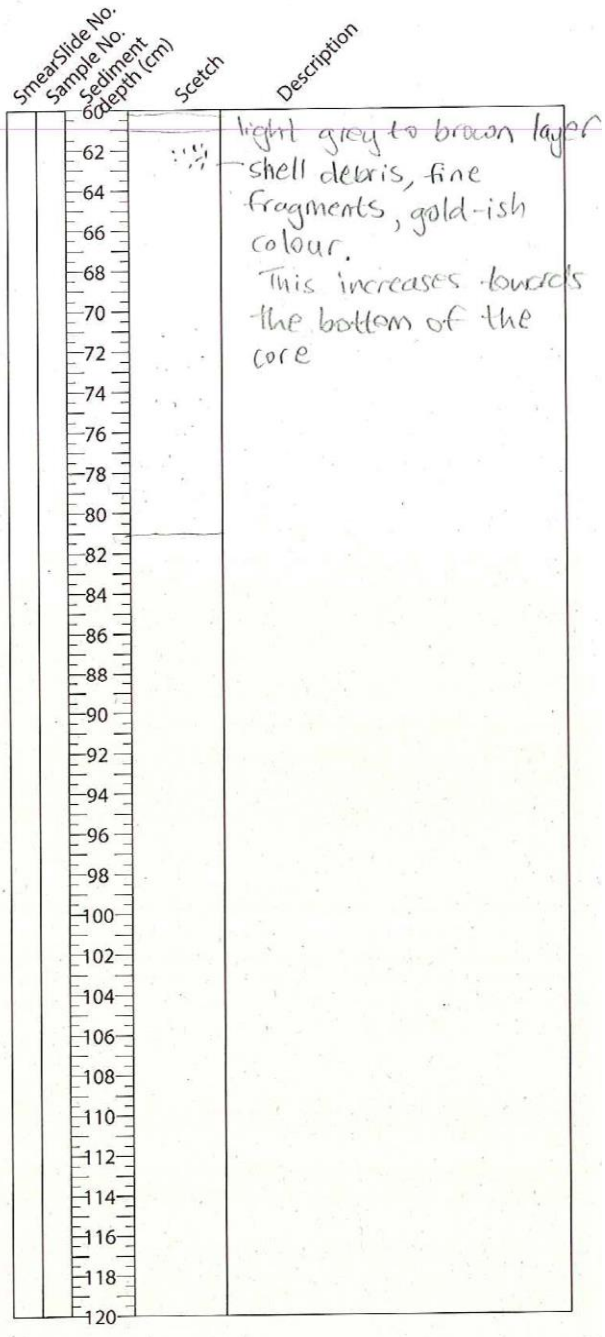

Core description

Lake: Swartvlei

Core ID[1]: SV13-6 (4-6m) B
Water depth:
Opening date: 13.09.2017
Examiner: Lillian Maboya / Torsten Haberzettl
Core type: Piston
Fotos: Digi
Multisensor: Suszi
Remarks: 54.5cm length

[1]Example: BAL 0121-1
Lake code Year Core No. Section No.

Description guidelines
1.Sediment class Clastic, chemical or biogenic.
2.Grain size gravel (>2mm), sand (2mm-63µm), silt (63-2µm), clay (<2µm). Modifiers: fine, middle and coarse or eg. sandy silt etc.
3.Color eg. brownish grey (=main color is grey).
4.Structure e.g. laminated, homogenous, bioturbated, etc.
5.Organics e.g. terrestrial plant remains, diatoms, ostracods, etc.
6.Additions e.g. high water, or organic content consolidated, well rounded grains, Type of minerals (e.g. carbonate, feldspar, quartz, mica).
Example: 12-25cm: Clastic sandy silt, brownish grey, laminated, with terrestrial plant remains. Organic content increases towards top of the section, Sand grains=mainly quartz.

40cm core loss

SmearSlide No. | Sample No. | Sediment depth (cm) | Scetch | Description

grey sandy material throught the core (A) with fragmanted shell debris

brown patch

bulging dark grey material. darker than A

light grey layer with shap transition into next layer

grey sandy material with similar colour to A

54.5cm

Core description

Lake: Swartvlei

Core ID[1]: SV13-6 (6-7.2m)
Water depth:
Opening date: 13.09.2017
Examiner: Lillian Maboya / Torsten Haberzettl
Core type: Piston
Fotos: Digi
Multisensor: Suzi
Remarks: -113.5cm length
-fossil removed from 82.5cm

[1]Example: BAL 01/1-1 (Lake code, Year, Core No., Section No.)

Description guidelines
1. Sediment class Clastic, chemical or biogenic.
2. Grain size gravel (>2mm), sand (2mm-63µm), silt (63-2µm), clay (<2µm). Modifiers: fine, middle and coarse or eg. sandy silt etc.
3. Color eg. brownish grey (=main color is grey).
4. Structure e.g. laminated, homogenous, bioturbated, etc.
5. Organics e.g. terrestrial plant remains, diatoms, ostracods, etc.
6. Additions e.g. high water, or organic content consolidated, well rounded grains, Type of minerals (e.g. carbonate, feldspar, quartz, mica).

Example: 12-25cm: Clastic sandy silt, brownish grey, laminated, with terrestrial plant remains. Organic content increases towards top of the section, Sand grains=mainly quartz.

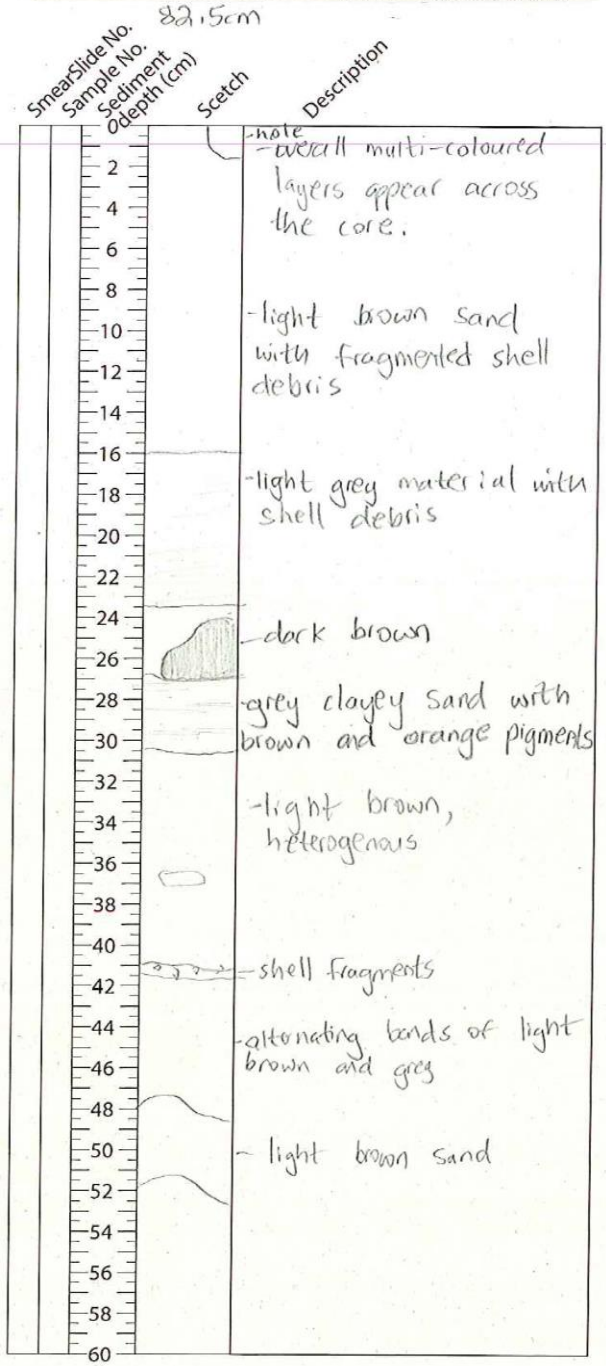

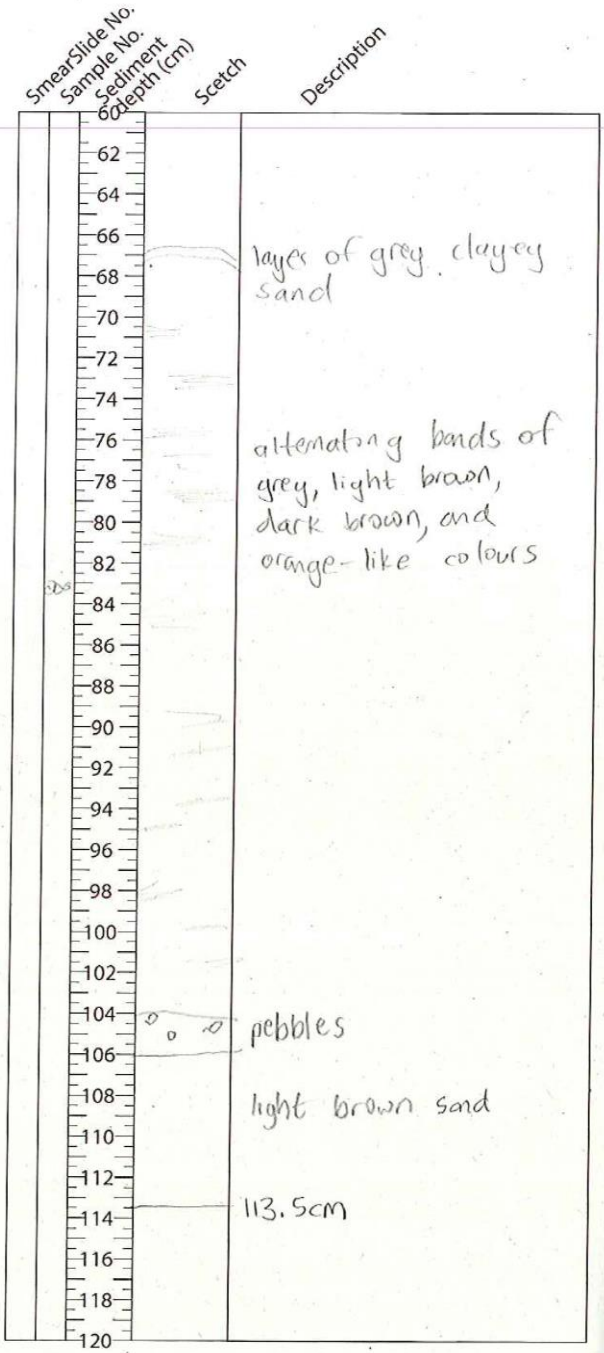

APPENDIX B

a) CNS data

Core name_depth	Composite Depth cm	14C ages cal BP	TN [%]	TC [%]	TOC [%]	TIC [%]	TS [%]
SV1_8	8	19.10	0.469	5.61	5.24	0.368	2.46
SV1_16	16	112.60	0.566	6.85	6.49	0.368	3.18
SV1_24	24	207.30	0.530	6.40	6.03	0.369	2.52
SV1_32	32	301.90	0.598	7.36	6.96	0.404	2.84
SV1_40	40	398.60	0.671	8.44	8.06	0.382	2.76
SV1_48	48	492.70	0.720	8.84	8.49	0.342	3.02
SV1_56	56	587.10	0.584	7.79	7.54	0.248	3.18
SV1_64	64	677.10	0.674	8.62	8.25	0.364	3.36
SV1_72	72	757.20	0.608	7.83	7.47	0.357	2.94
SV1_80	80	855.10	0.626	8.10	7.63	0.465	2.91
SV1_88	88	970.20	0.649	8.24	7.89	0.343	2.78
SV1_96	96	1079.80	0.659	8.46	8.25	0.207	3.03
SV1_104	104	1191.40	0.634	8.16	7.82	0.331	2.91
SV1_112	112	1300.70	0.561	7.07	6.79	0.276	3.10
SV1_120	120	1409.20	0.523	6.84	6.58	0.262	2.71
SV1_128	128	1520.80	0.551	7.17	6.83	0.341	2.60
SV1_136	136	1629.80	0.541	7.83	7.61	0.224	3.05
SV1_144	144	1734.30	0.580	8.01	7.65	0.366	3.01
SV7(1.5-3.5)B_13	152	1833.90	0.608	8.48	8.21	0.274	3.12
SV7(1.5-3.5)B_21	160	1927.30	0.680	9.71	9.39	0.323	3.16
SV7(1.5-3.5)B_29	168	2027.30	0.813	12.0	11.9	0.096	3.37
SV7(1.5-3.5)B_37	176	2128.60	0.611	8.87	8.74	0.137	4.23
SV7(1.5-3.5)B_45	184	2230.00	0.663	9.37	9.21	0.159	4.03
SV7(1.5-3.5)B_53	192	2327.20	0.711	10.3	10.2	0.136	3.92
SV7(1.5-3.5)B_61	200	2413.80	0.626	8.85	8.65	0.199	4.18

SV7(1.5-3.5)B_69	208	2489.50	0.664	9.03	8.68	0.345	3.68
SV7(1.5-3.5)A_8	216	2596.30	0.590	7.71	7.44	0.272	3.03
SV7(1.5-3.5)A_16	224	2702.90	0.560	7.47	7.14	0.327	3.21
SV7(1.5-3.5)A_24	232	2810.50	0.631	8.52	8.26	0.256	3.48
SV7(1.5-3.5)A_32	240	2919.40	0.524	7.34	6.55	0.790	3.32
SV7(1.5-3.5)A_40	248	3027.50	0.552	8.01	7.26	0.743	3.38
SV7(1.5-3.5)A_48	256	3134.80	0.486	7.38	6.51	0.874	2.91
SV7(1.5-3.5)A_56	264	3241.90	0.462	7.27	6.01	1.26	2.76
SV7(1.5-3.5)A_64	272	3344.20	0.409	6.56	5.39	1.17	2.59
SV7(1.5-3.5)A_72	280	3449.50	0.346	5.78	4.18	1.61	2.04
SV6(2-4)A_36	296	3650.30	0.153	5.12	**1.51**	3.60	0.782
SV6(2-4)A_44	304	3753.90	0.115	4.55	**1.06**	3.48	0.601
SV6(2-4)A_52	312	3853.20	0.0860	3.77	**0.740**	3.02	0.522
SV6(2-4)A_60	320	3954.00	0.0880	3.69	**0.661**	3.03	0.431
SV6(2-4)A_68	328	4052.70	0.101	4.24	**0.820**	3.42	0.551
SV6(2-4)A_76	336	4150.90	0.0850	3.32	**0.639**	2.68	0.429
SV6(2-4)A_84	344	4250.20	0.0780	3.45	**0.559**	2.89	0.432
SV6(2-4)A_92	368	4548.10	0.0710	2.95	**0.465**	2.49	0.381
SV6(4-6)B_1	376	4644.50	0.0540	1.09	*0.177*	0.912	**0.236**
SV6(4-6)B_9	384	4744.20	0.0450	0.925	*0.183*	0.742	**0.166**
SV6(4-6)B_17	392	4840.10	0.0480	1.80	**0.684**	1.12	**0.225**
SV6(4-6)B_25	400	4937.10	0.0400	**0.541**	*0.164*	0.377	**0.277**
SV6(4-6)B_33	408	5037.50	0.0540	1.84	**0.391**	1.44	0.313
SV6(4-6)B_41	416	5133.70	0.0540	0.929	**0.278**	0.651	**0.246**
SV6(4-6)B_49	424	5230.70	0.0410	**0.591**	*0.185*	0.406	**0.188**
SV6(4-6)A_3	432	5332.80	0.0480	**0.570**	*0.190*	0.380	**0.152**
SV6(4-6)A_11	440	5432.60	0.0550	**0.310**	*0.165*	0.145	**0.068**
SV6(4-6)A_19	448	5531.40	0.0440	**0.967**	*0.143*	0.824	**0.135**
SV6(4-6)A_27	456	5630.80	0.0650	**0.627**	**0.287**	0.340	**0.275**
SV6(4-6)A_35	464	5731.60	0.0700	0.891	**0.289**	0.602	**0.256**
SV6(4-6)A_43	472	5832.60	0.0520	**0.326**	*0.174*	0.152	**0.169**

SV6(4-6)A_51	480	5926.20	0.0670	**0.482**	*0.212*	0.270	**0.197**
SV6(4-6)A_59	488	6026.90	0.0510	**0.253**	*0.122*	0.131	**0.0950**
SV6(4-6)A_67	496	6122.20	0.0450	**0.246**	*0.147*	0.0988	**0.151**
SV6(4-6)A_75	504	6220.40	0.0540	**0.335**	*0.201*	0.134	**0.191**
SV6(4-6)A_83	512	6319.90	0.0440	**0.260**	*0.141*	0.119	**0.187**
SV6(4-6)A_91	520	6419.20	0.0570	**0.263**	*0.158*	0.105	**0.159**
SV6(4-6)A_99	584	7207.20	0.0420	**0.138**	*0.0807*	0.0573	**0.121**
SV6(6-7.2)_6	592	7305.40	0.0380	**0.0640**	*0.0566*	0.00743	
SV6(6-7.2)_14	600	7405.70	0.0450	**0.135**	*0.0987*	0.0363	**0.0570**
SV6(6-7.2)_22	608	7506.30	0.0580	**0.275**	*0.157*	0.118	**0.0590**
SV6(6-7.2)_30	616	7602.80	0.0530	**0.109**	*0.147*	-0.0379	
SV6(6-7.2)_38	624	7701.70	0.0570	**0.160**	*0.135*	0.0248	
SV6(6-7.2)_46	632	7802.50	0.0610	**0.132**	*0.129*	0.0031	
SV6(6-7.2)_54	640	7899.80	0.0460	**0.0910**	*0.153*	-0.0617	
SV6(6-7.2)_62	648	7996.10	0.0470	**0.0780**	*0.129*	-0.0507	
SV6(6-7.2)_70	656	8093.40	0.0640	**0.252**	*0.164*	0.0884	
SV6(6-7.2)_78	664	8190.20	0.0480	**0.0770**	*0.0776*	-0.00058	
SV6(6-7.2)_86	672	8288.30	0.0490	**0.0780**	*0.0707*	0.00733	
SV6(6-7.2)_94	680	8386.70	0.0580	**0.128**	*0.123*	0.00527	
SV6(6-7.2)_102	688	8484.00	0.0510	**0.0980**	*0.0812*	0.0168	
SV6(6-7.2)_110	696	8578.50	0.0450	**0.0750**	*0.0674*	0.00759	

b) ICP-OES data

Core Name	Composite Depth cm	14C ages cal BP	Al ppm	B ppm	Ba ppm	Ca ppm	Co ppm	Cr ppm	Cu ppm	Fe ppm	K ppm	Mg ppm	Mn ppm	Na ppm	Ni ppm	P ppm	Pb ppm	S ppm	Ti ppm
SV 13-1V	8	19.1	67930	56.6	163.6	3490	16.20	66.9	7.30	32150	10740	6430	966.40	17120	24.1	951	35.2	23431	324
SV 13-1V	16	112.6	57170	66.1	124.1	3860	15.20	63.4	6.53	38520	9200	7080	1405.00	20120	22.9	852	22.0	30599	357
SV 13-1V	24	207.3	51500	68.5	141.9	4280	11.82	66.0	8.11	36150	9740	6900	866.00	17190	22.9	1619	22.0	23760	534
SV 13-1V	32	301.9	48310	74.6	121.2	4440	9.62	64.6	7.81	33850	9030	7260	747.50	18780	22.0	1810	16.9	26398	637
SV 13-1V	40	398.6	50680	80.6	138.6	6300	8.05	67.0	9.21	32830	10270	8160	678.50	20020	21.1	2153	18.6	26421	438
SV 13-1V	56	587.1	52320	85.6	150.4	6370	11.15	64.2	7.61	35170	10940	7410	505.70	17560	21.9	1659	19.8	29350	327
SV 13-1V	64	677.1	50200	94.1	132.9	4120	7.99	66.7	8.22	36790	10160	7990	473.80	19340	22.3	2044	21.7	**31184**	319
SV 13-1V	72	757.2	54250	91.7	144.9	3730	11.05	66.9	8.05	33600	10710	7680	462.40	17790	21.6	1646	22.4	26695	411
SV 13-1V	80	855.1	56660	96.4	136.3	4160	11.38	66.9	8.28	32620	10820	8370	562.10	19260	20.2	2065	21.0	27107	348
SV 13-1V	88	970.2	57080	100.2	139.1	4030	9.70	68.6	9.60	34130	10770	8470	386.60	19900	19.8	2103	20.5	25803	380
SV 13-1V	96	1079.8	55830	100.6	128.7	4240	9.00	72.1	8.82	36580	10390	8470	352.90	19130	21.9	2299	19.1	27916	331
SV 13-1V	104	1191.4	55890	99.8	137.6	4380	8.86	74.0	10.27	34120	10990	8810	292.10	19580	23.3	2235	18.4	26233	443
SV 13-1V	112	1300.7	52410	94.6	132.7	3760	8.73	72.5	8.44	35950	10370	7780	272.00	15680	22.4	2035	19.3	27953	584
SV 13-1V	120	1409.2	58190	93.1	158.4	3900	8.56	79.1	10.27	33790	11840	8190	253.20	16270	26.7	1885	20.0	23977	507
SV 13-1V	128	1520.8	57650	95.1	153.0	4420	7.27	76.9	9.46	31700	11770	8650	251.40	16700	22.1	2213	21.6	22328	395
SV 13-1V	136	1629.8	58820	100.7	158.6	4050	9.86	70.0	9.94	34380	11740	8650	331.40	17170	22.1	1724	19.6	28004	422
SV 13-1V	144	1734.3	57520	100.4	141.5	3490	11.27	83.3	8.77	34540	10720	8210	453.10	16420	31.1	1866	22.7	26567	742
SV 13-7 (1.5-3.5) B	152	1833.9	58620	108.0	145.1	6060	8.15	70.3	9.32	34300	11070	8870	437.00	17210	21.4	2122	21.6	27712	654
SV 13-7 (1.5-3.5) B	160	1927.3	54700	107.2	134.6	6560	12.27	74.0	10.97	33770	10870	9290	576.40	19060	23.9	1940	19.6	28284	531
SV 13-7 (1.5-3.5) B	168	2027.3	49880	118.4	119.8	5970	12.24	61.9	9.02	30880	9570	8700	570.00	19380	19.8	1172	18.5	**30165**	403
SV 13-7 (1.5-3.5) B	176	2128.6	55000	101.2	144.8	5070	15.14	75.5	8.33	42450	11240	8260	756.70	16230	27.6	1186	21.0	**37435**	417
SV 13-7 (1.5-3.5) B	184	2230.0	52010	103.4	130.3	5850	13.05	64.3	7.63	39860	10530	8670	825.40	17530	17.6	1506	22.5	**35208**	440
SV 13-7 (1.5-3.5) B	192	2327.2	48820	115.5	119.3	5940	11.10	70.2	8.26	37790	9430	8500	584.80	17840	23.2	1534	22.3	**35475**	418

SV 13-7 (1.5-3.5) B	200	2413.8	50720	105.0	127.9	5790	13.03	87.4	8.42	42470	10340	8810	664.40	16780	32.9	1639	22.4	**36799**	422	
SV 13-7 (1.5-3.5) B	208	2489.5	47350	107.4	124.6	6020	11.50	77.1	7.92	37260	10070	8870	492.40	17510	24.4	1833	18.8	**32897**	595	
SV 13-7 (1.5-3.5) A	216	2596.3	49550	90.8	128.3	5780	11.25	73.9	8.68	35240	10450	8470	597.00	16450	22.2	1469	19.7	28009	584	
SV 13-7 (1.5-3.5) A	224	2702.9	51470	87.1	143.5	8770	12.14	80.5	9.64	35980	11480	8670	627.70	17600	27.4	1661	20.8	29228	345	
SV 13-7 (1.5-3.5) A	232	2810.5	50460	106.4	137.9	6220	11.00	77.7	9.53	36600	10910	8810	579.90	17620	25.2	1480	19.0	**31522**	488	
SV 13-7 (1.5-3.5) A	240	2919.4	48750	91.0	149.7	20030	12.72	71.7	9.97	34650	12190	8420	721.00	17800	27.1	1233	21.0	29854	510	
SV 13-7 (1.5-3.5) A	248	3027.5	46370	94.0	125.9	22600	9.78	71.5	8.45	33810	10280	8290	678.40	17720	25.6	1230	19.9	**29877**	316	
SV 13-7 (1.5-3.5) A	256	3134.8	43770	87.1	127.0	25600	8.87	75.9	9.18	30720	9870	7840	588.30	16370	29.0	1035	17.7	26222	414	
SV 13-7 (1.5-3.5) A	264	3241.9	41900	86.1	121.6	34680	7.83	70.6	8.11	29180	9760	7970	567.50	16650	25.9	1096	15.4	23883	393	
SV 13-7 (1.5-3.5) A	272	3344.2	42390	78.6	124.5	34720	8.36	77.8	9.35	28960	9850	7660	510.70	14460	30.5	970	16.3	22750	449	
SV 13-6 (2-4) A	288	3449.5	33780	62.4	114.4	45040	7.09	107.1	9.11	25190	8880	6930	438.50	12340	53.5	919		17912	499	
SV 13-6 (2-4) A	296	3650.3	20190	37.0	95.9	1E+05	3.31	43.9	4.33	14200	6740	6510	151.30	5940	17.3	643		6642	505	
SV 13-6 (2-4) A	304	3753.9	15750	29.2	79.3	1E+05	3.04	54.5	4.78	11800	5280	5520	114.70	4580	27.1	543		5187	484	
SV 13-6 (2-4) A	320	3853.2	11120	19.2	59.3	88560	3.24	92.5	2.65	9420	3790	4220	83.07	3230	55.9	431		3945	434	
SV 13-6 (2-4) A	328	3954.0	12750	23.3	66.1	98410	3.62	72.5	3.57	10870	4390	5080	87.24	3770	39.0	514		4804	549	
SV 13-6 (2-4) A	336	4052.7	10400	17.2	55.6	81760	3.25	75.8	3.70	9100	3540	3910	73.32	3030	44.9	433		3815	419	
SV 13-6 (2-4) A	344	4150.9	10080	17.0	54.9	88030	2.68	66.6	2.79	8980	3420	3810	68.22	3100	39.0	393		3951	445	
SV 13-6 (2-4) A	352	4250.2	8970	14.5	49.6	74390	2.54	76.6	3.83	8060	3020	3330	62.27	2630	46.4	382		3411	363	
SV 13-6 (4-6) B	376	4548.1	4730	4.9	33.2	28330	3.38	151.8	3.21	5340	1600	1410	40.47	2120	100.8	112		1825	250	
SV 13-6 (4-6) B	384	4644.5	4250	4.9	29.9	23380	2.66	121.9	2.73	4030	1440	1310	42.68	1410	80.8	123		1269	244	
SV 13-6 (4-6) B	392	4744.2	6090	8.0	37.7	47810	2.12	80.9		5350	2050	1860	55.85	2000	49.9	192		1853	298	
SV 13-6 (4-6) B	400	4840.1	6810	6.8	38.8	11910	1.98	73.0		5610	2170	1470	37.97	2120	46.2	95		2069	259	
SV 13-6 (4-6) B	408	4937.1	8460	11.2	46.7	44320	2.45	101.2	2.80	7380	2840	2590	58.16	2290	62.1	225		2754	384	
SV 13-6 (4-6) B	416	5037.5	6020	9.6	35.5	21450	4.11	176.8	3.32	5790	1970	1590	55.58	1670	117.2	126		1916	278	
SV 13-6 (4-6) B	424	5133.7	5530	7.3	32.7	13690	2.23	102.6	2.09	4750	1770	1290	42.77	1420	67.8	86		1429	264	
SV 13-6 (4-6) A	432	5230.7	4910	5.1	31.3	13110	4.25	204.7	3.73	4690	1590	1210	43.46	1460	138.7	80		1168	238	

SV 13-6 (4-6) A	440	5332.8	3180	1.8	23.5	6490	3.98	214.2	2.80	3020	1090	650	31.35	720	145.5	49		495	172
SV 13-6 (4-6) A	448	5432.6	3680	2.3	26.3	26700	1.85	120.0		3450	1240	1290	36.34	1330	69.2	70		1032	199
SV 13-6 (4-6) A	456	5531.4	8370	7.2	44.5	11960	4.35	180.6	3.07	7260	2580	1680	50.66	1780	119.3	116		2476	272
SV 13-6 (4-6) A	464	5630.8	9340	9.0	46.3	18560	4.40	175.2	2.89	7380	2850	1930	56.46	2080	113.8	124		2265	307
SV 13-6 (4-6) A	472	5731.6	5080	3.0	31.7	5980	2.64	144.2	3.05	4390	1630	960	33.82	1460	96.1	75		1336	230
SV 13-6 (4-6) A	480	5832.6	4870	3.6	30.5	7380	3.30	182.4	3.09	4470	1560	910	36.53	1280	123.6	68		1311	220
SV 13-6 (4-6) A	488	5926.2	2880	2.4	22.4	4080	3.02	173.4	2.89	2670	1020	530	34.75	940	119.7	44		534	178
SV 13-6 (4-6) A	496	6026.9	4060	5.5	27.0	4260	2.11	89.9		3620	1290	750	28.93	1080	51.3	50		1161	221
SV 13-6 (4-6) A	504	6122.2	4980	8.2	30.7	5280	2.36	113.9		4480	1600	910	31.06	1340	74.7	65		1552	217
SV 13-6 (4-6) A	512	6220.4	6140	7.7	35.9	4590	2.08	99.0		5090	1910	1060	36.86	1570	55.8	67		1600	259
SV 13-6 (4-6) A	520	6319.9	4740	6.1	30.4	3860	3.27	152.5	3.15	4220	1510	840	35.62	1220	102.1	54		1182	231
SV 13-6 (4-6) A	528	6419.2	4770	6.0	30.4	2960	1.55	72.8		3700	1510	780	33.21	1360	40.9	52		938	225
SV 13-6 (6-7.2)	592	7207.2	2710	3.0	22.2	1670	2.28	140.5	2.96	2260	880	420	29.49	1190	93.4	33		175	177
SV 13-6 (6-7.2)	600	7305.4	3700	4.1	26.3	2800	3.19	151.8	4.30	2980	1200	610	29.93	1480	101.7	44		313	207
SV 13-6 (6-7.2)	608	7405.7	7330	8.1	38.9	4420	4.98	200.6	3.94	5420	2070	1070	40.43	1420	132.2	69		447	277
SV 13-6 (6-7.2)	616	7506.3	30940	25.0	103.6	1240	3.73	78.3		14700	6480	2700	46.98	2300	33.8	86		197	324
SV 13-6 (6-7.2)	624	7602.8	18160	15.0	70.8	2510	3.73	112.1		10060	4380	1900	48.87	1600	64.4	63		99	312
SV 13-6 (6-7.2)	632	7701.7	16220	13.7	53.7	1090	3.93	131.3		9780	3360	1690	41.46	1420	69.6	58		75	373
SV 13-6 (6-7.2)	640	7802.5	7390	5.7	40.4	1350	2.89	113.5		4560	2060	850	36.85	1060	73.8	46			344
SV 13-6 (6-7.2)	648	7899.8	10770	11.3	52.3	1300	3.07	117.8		6150	2840	1120	38.19	1070	75.0	53			284
SV 13-6 (6-7.2)	656	7996.1	13770	13.9	56.4	2270	2.99	107.5		8540	3410	1520	44.59	1570	56.2	90		86	430
SV 13-6 (6-7.2)	664	8093.4	5540	4.8	26.8	1080	2.00	105.8		4320	1350	620	30.23	680	60.2	47			286
SV 13-6 (6-7.2)	672	8190.2	4790	3.9	26.7	1250	1.81	100.4		3880	1310	590	22.31	940	57.3	49		86	213
SV 13-6 (6-7.2)	688	8288.3	7880	6.6	39.0	1710	3.60	153.5	2.15	5060	2170	900	40.46	1100	98.8	58			307
SV 13-6 (6-7.2)	696	8386.7	7190	6.4	37.2	1940	2.68	118.6	2.23	4610	1980	880	30.83	1210	77.1	59			254

c) XRF data

Depth (cm)	^{14}C age (cal BP)	Fe (counts)	Br (counts)	Rb (counts)	Sr (counts)	Zr (counts)	Al (counts)	Si (counts)	K (counts)	Ca (counts)	Ti (counts)
1	-54	63562	2338	1355	1132	2587	1161	13914	6118	3162	5828
2	-45.1	56844	1834	1498	1164	2755	1489	16742	7464	2860	6261
3	-36.1	53317	1787	1587	1234	2505	1653	17249	8355	2821	6527
4	-27	57497	1715	1798	1251	3233	1883	19509	9324	2818	7252
5	-17.9	58075	2044	1700	1209	2420	1193	12675	6883	3149	5694
6	-5.6	56823	1875	1538	1168	2128	1403	15035	7211	3017	6243
7	7.1	58933	1681	1275	1205	2291	1314	15063	6755	2862	5828
8	19.1	63037	1690	1401	1156	2261	1188	14063	6022	2825	5824
9	30.6	61908	1960	1436	1131	2678	1193	13878	5826	3120	6190
10	40.7	53907	1890	1478	1158	2806	1040	12933	5428	2596	6011
11	53.1	69950	2008	1430	1207	2745	1007	13094	5473	2942	6290
12	65.7	83406	1976	1411	1279	2355	1223	14974	5793	2982	6445
13	78.1	104925	1868	1385	1177	2537	922	11775	5214	3133	5870
14	89.6	90674	1789	1355	1445	2875	821	11789	5084	2956	5946
15	100.5	89595	1721	1231	1307	2351	935	11997	5076	2976	5869
16	112.6	86787	1862	1064	1325	1926	663	8765	4144	2962	4741
17	124.7	86681	1775	1161	1356	2494	731	9516	4956	2790	4977
18	136.9	70638	1872	1259	1431	2603	833	11909	5418	2939	5121
19	148.4	65203	1692	1227	1417	2613	787	12599	5778	2949	5141
20	160	65185	1848	1119	1342	2667	635	10736	5295	2990	4877
21	171.4	68847	1853	1049	1464	2471	560	9198	4928	3060	4597
22	183.3	69384	1794	1085	1401	4246	549	9471	5040	3022	4591
23	195.1	81391	1849	1482	1588	2883	587	10265	5833	2983	5325
24	207.3	71222	2037	1271	1292	2579	508	9185	5173	3200	4575
25	219.4	81445	1714	1304	1287	2983	531	7788	5139	2933	4756

26	231.3	94877	1724	1429	1313	3188	515	8560	5617	2761	4914
27	243.5	76944	1996	1401	1556	3022	752	11247	6437	3022	5428
28	255.7	65997	1972	1402	1389	2717	527	8585	5562	3132	4871
29	267.5	67073	1817	1533	1396	2415	830	12336	6849	2819	5544
30	277.9	57405	2447	1498	1644	2787	777	12969	6518	3184	5092
31	290.3	51674	2417	1252	1469	2372	560	9415	5285	3242	4612
32	301.9	66985	2236	1143	1415	1987	663	10019	4960	3270	4405
33	313.7	58096	2373	1238	1626	1932	694	10218	5334	3424	4362
34	325.9	56136	2535	1197	1523	2000	575	9514	4932	3324	3982
35	337.8	55822	2399	1267	1593	2236	603	9117	5088	3455	4339
36	349.9	49154	2284	1209	1550	2383	595	10588	5360	3332	4361
37	361.9	58425	2443	1046	1507	2076	668	10629	5283	3526	4156
38	374.4	54597	2504	1264	1696	1963	662	10205	5265	3457	4268
39	386.8	64330	2331	1284	1510	2149	502	8638	5107	3490	4334
40	398.6	55266	2572	1267	1534	2037	602	10088	5637	3610	4526
41	410.3	53779	2536	1195	1588	2189	786	11679	5820	3483	4344
42	422.1	59309	2573	1098	1539	1983	573	8503	4930	3589	4233
43	434.3	60076	2421	1161	1578	1569	572	8103	4934	3442	4345
44	446.6	58798	2599	1281	1669	2066	759	10311	5513	3612	4477
45	459.1	50650	2555	1160	1528	2185	486	7984	4938	3511	4147
46	469.6	61937	2560	1190	1525	2302	539	9191	5225	3657	4124
47	481.1	51505	2653	1173	1585	1474	578	9217	5243	3685	4161
48	492.7	55789	2493	1171	1492	1994	613	8921	4905	3362	4257
49	504.1	54441	2692	1237	1582	1668	651	9162	5021	3622	4288
50	516.1	48791	2501	1277	1496	2094	736	9579	5276	3414	4336
51	528.1	53465	2621	1202	1478	2143	639	9111	5322	3486	4352
52	540.1	62723	2291	1172	1362	2090	514	7462	5187	3240	4097
53	552.5	61097	2421	1215	1508	1554	656	8877	5238	3212	4318
54	564.5	48055	2442	1368	1594	2371	714	10596	6062	3315	4684

55	576.3	50004	2285	1383	1517	2325	788	11623	5877	3412	4736
56	587.1	54821	2209	1240	1437	2490	798	11171	6078	3258	4953
57	598.3	51628	2219	1305	1711	2416	979	12257	6237	3399	4981
58	609.9	57602	2394	1251	1529	2429	653	10196	5282	3254	4486
59	621.6	55169	2515	1193	1532	2650	694	10687	5720	3250	4460
60	632.9	59486	2328	1227	1614	3013	613	9169	5332	3251	4465
61	643.7	51756	2445	1219	1615	2503	602	10141	5582	3575	4601
62	654.4	46584	2546	1137	1596	2714	723	10984	5654	3426	4583
63	665.6	62300	2370	1131	1540	2140	775	10105	5286	3420	4029
64	677.1	51934	2575	1089	1442	1797	760	10357	5271	3408	4159
65	688.1	55437	2490	1285	1489	2315	744	10724	5744	3634	4528
66	698.1	43254	2683	1223	1562	2028	640	9774	5255	3373	4195
67	708.3	48230	2706	1300	1598	2257	705	9971	5153	3082	4320
68	718.7	58088	2403	1314	1485	2141	739	10342	5618	3312	4456
69	729	61122	2183	1291	1399	2447	725	10143	5637	3213	4390
70	740.3	52738	2334	1325	1472	2180	902	10855	5911	3032	4603
71	748.6	49130	2225	1460	1439	2652	583	8608	5693	2935	4647
72	757.2	73503	2056	1390	1419	2631	644	8842	5407	2996	4681
73	765.5	52909	2438	1237	1552	2465	779	10701	5476	3382	4386
74	774.4	48313	2495	1055	1505	2066	713	9438	5052	3415	4148
75	784.6	49108	2167	1192	1537	2383	693	11057	5376	3305	4437
76	797.7	45697	2483	1259	1462	2132	793	11123	5353	3289	4357
77	811.7	46704	2515	1115	1599	2074	747	10386	5074	3474	4047
78	826.5	47361	2405	1085	1506	1984	633	9935	4957	3330	4136
79	841.1	46715	2330	1297	1578	2209	822	10976	5488	3251	4329
80	855.1	51817	2275	1401	1668	2141	847	10755	5559	3280	4591
81	870.9	47623	2371	1344	1621	2115	923	11850	6111	3459	4555
82	886	49578	2264	1452	1512	2361	861	12236	6614	3534	4812
83	901.3	56879	2265	1337	1660	2299	637	9560	4994	3150	4361

84	916	42719	2444	1184	1596	2391	672	11131	5320	3355	4266
85	929.1	64101	2489	1135	1602	2291	611	8968	4515	3378	3686
86	941.6	66042	2485	1243	1552	2062	738	9810	4951	3522	4137
87	955.4	58062	2571	1303	1533	1619	774	10904	5351	3320	4428
88	970.2	51449	2340	1369	1522	1810	961	11335	5723	3337	4736
89	983.8	62181	2283	1340	1563	2300	832	11029	6007	3247	4644
90	997.3	58150	2242	1358	1591	1966	547	8106	4967	3322	4298
91	1010.9	62071	2049	1605	1708	2258	733	9700	5691	3328	4926
92	1025.3	58489	2193	1416	1549	2350	666	9609	5442	3111	4503
93	1038.9	46464	2315	1382	1584	1911	737	9797	5355	3290	4613
94	1052.8	46647	2419	1325	1575	2297	814	11667	5858	3318	4675
95	1065.7	58377	2485	1235	1650	2079	750	11123	5514	3432	4323
96	1079.8	65801	2384	1220	1655	2046	784	10090	5412	3375	4244
97	1093.6	58555	2375	1333	1634	1937	614	8888	5146	3504	4237
98	1108.4	38622	2214	1069	1608	1848	576	8274	4505	3043	3591
99	1122.1	51616	2339	1235	1625	2336	737	10917	5442	3288	4189
100	1135.4	56778	2214	1179	2027	2554	606	8113	4793	3374	4093
101	1149.5	70089	2184	1286	1609	2201	540	8374	4814	3191	3808
102	1163.7	79200	1923	1292	1749	2008	576	9203	5154	2921	4272
103	1177.5	60257	2107	1388	1631	2257	859	11615	6456	3219	4788
104	1191.4	60551	2031	1354	1780	2108	689	9808	5259	3086	4060
105	1204.5	58325	2153	1286	2014	1547	662	10382	5679	4367	4196
106	1218.4	68574	2120	1256	1663	2112	779	11712	5978	2865	4483
107	1232.9	67262	2170	1375	1660	2338	985	12912	6568	2922	4903
108	1246.4	72640	2101	1541	1681	2645	1026	13662	6985	3134	5271
109	1259.7	67454	1818	1703	1471	2895	1202	15066	8303	2709	5936
110	1272.8	62696	2236	1448	1686	2498	1196	15497	8064	2980	5619
111	1286.6	54918	2095	1342	1462	2605	1007	13651	6997	2802	5368
112	1300.7	60647	1724	1274	1429	2689	770	12582	6188	2431	4990

113	1315	42901	1596	1322	1234	2251	986	13170	6699	2010	4727
114	1328.5	40938	1678	1635	1277	2378	1235	14576	7688	2092	5263
115	1341.8	56925	1899	1230	1451	1751	1072	13480	6597	2397	4839
116	1354.5	47597	1834	1287	1443	2530	1104	13971	6373	2384	5072
117	1368.7	41611	2019	1170	1377	2373	856	12730	6072	2248	4395
118	1382.3	46311	2215	1305	1556	2381	1127	14626	6594	2321	4841
119	1395.9										
120	1409.2										
121	1422.6										
122	1436.2										
123	1450.8										
124	1464.1										
125	1477.8										
126	1492.2	40463	2002	1355	1551	2052	984	13132	6251	2324	4844
127	1506.7	42262	1959	1428	1528	2146	957	13880	6571	2390	4944
128	1520.8	49604	2005	1486	1503	2532	1191	15783	7349	2558	5278
129	1535.1	53953	1834	1300	1529	2319	1157	15484	6992	2476	5241
130	1549.4	47324	1686	1453	1570	2278	1192	15045	6758	2228	4971
131	1562.2	39753	1649	1422	1406	2763	1223	16082	7750	2145	5361
132	1575.4	44471	1588	1387	1519	2718	1248	17624	7416	2003	5583
133	1589.1	55417	1831	1288	1612	2441	948	12993	6128	2332	4511
134	1602.8	54708	1909	1460	1554	2443	1071	14189	6908	2531	4918
135	1616.8	60428	1668	1477	1408	2331	1102	14509	7010	2392	5371
136	1629.8	54870	1829	1381	1422	2338	1371	15694	7877	2271	5597
137	1643.6	48008	2057	1123	1565	2340	836	13014	6600	2513	4638
138	1657.6	55826	2044	1169	1730	1990	858	12067	6184	2754	4401
139	1671.7	52268	2263	1237	1923	2629	923	13580	6762	2647	4887
140	1685.6	52849	1306	1515	1687	3012	1147	16885	7742	2297	5685
141	1697.4	54291	1758	1472	1771	2613	1442	19833	8744	2164	5834

142	1709.1	58420	2105	1337	1845	2532	1078	13407	7065	2709	5128
143	1721.1	48443	1916	1538	2304	2377	1011	13070	7686	3234	5484
144	1734.3	48658	2208	1309	1956	2456	1084	14226	7555	2699	5370
145	1747.2	60086	1989	1493	1850	2457	1351	15307	7977	2749	5839
146	1758.5	56650	2513	1246	1806	2693	690	11077	6172	2821	4677
147	1771.5	47517	1978	1323	1859	2332	911	12034	6641	4909	4772
148	1785.1	49349	1995	1439	2080	2698	995	12321	6838	5039	5094
149	1797.2	51461	2105	1429	1908	2351	1011	12440	6789	5389	5239
150	1808.8	51532	1923	1565	1963	2373	1103	12238	6799	5337	4903
151	1821.3	44221	2198	1383	2009	2688	791	9849	6101	5156	4954
152	1833.9	46376	2211	1371	1949	2494	908	10496	5973	5614	4615
153	1845.7	41746	2728	1317	2075	2548	784	10908	5861	5635	4516
154	1856.9	49813	2402	1191	1899	1981	842	10552	5838	5310	4147
155	1866.8	49787	2137	1499	1882	2773	1068	13627	7199	4976	5239
156	1879.3	46148	1794	1754	1924	2687	1284	15215	8306	4435	5752
157	1891.8	45694	2532	1217	1750	2106	797	9631	5301	4723	4222
158	1903.7	51364	1965	1273	1829	1556	845	9736	5110	4448	4203
159	1915.7	40441	2279	1159	1973	2408	620	8754	5128	5487	3874
160	1927.3	47238	2095	1328	2094	2613	637	8438	5341	5146	4384
161	1940.2	51598	2065	1501	1831	2304	940	10867	6067	4791	4727
162	1953.5	50146	2116	1579	1803	2061	934	11295	6551	4545	4671
163	1966.4	50921	2053	1486	1927	2428	940	11719	6714	4726	4752
164	1979	52506	2214	1686	1902	2295	967	11252	6697	4584	5027
165	1991.6	47079	2087	1701	1768	2658	866	11545	7089	4348	5233
166	2003.5	49020	1647	1928	1788	2977	1412	15796	8684	4026	6065
167	2015.2	43231	2816	1288	2038	2187	940	11856	5841	4797	4887
168	2027.3	41518	2287	1217	1982	2158	530	9053	4738	5053	4231
169	2039.4	49837	2182	1348	1959	2422	725	9674	5084	4975	4266
170	2050.7	49083	2242	1280	2035	2299	887	10983	5679	4922	4574

171	2063.9	40499	2533	1381	2074	2374	597	9438	5155	5064	3934
172	2077.6										
173	2090.6										
174	2103.3										
175	2115.8	43941	2236	1327	1989	2675	757	10480	5417	4800	4453
176	2128.6	55334	2175	1388	2001	2275	1018	11997	6588	4872	5066
177	2141.8	43134	2397	1364	2089	2459	710	10160	5327	5222	4415
178	2155.2	52582	2418	1230	1835	2003	846	10006	5239	5201	4285
179	2168	44021	2281	1188	1939	2243	726	9627	5164	5334	4347
180	2181.1	54441	2190	1369	2013	1801	902	11364	6132	5223	4799
181	2192.9	48255	2232	1518	1964	2682	950	11446	6493	5119	5049
182	2205.5	48580	2405	1332	1981	2000	733	10659	5199	5451	4543
183	2217.8	45057	2598	1325	2016	2460	680	10414	5370	5175	4074
184	2230	49430	2443	1268	1961	2320	749	10245	5658	5388	3999
185	2242.4	44318	2482	1274	2022	2250	793	10747	5806	5416	4464
186	2254.5	49466	2128	1255	2059	2244	822	11077	5826	5170	4382
187	2267.3	40986	2069	1193	2053	2958	879	11709	6089	5275	4306
188	2279.9	54945	2201	1319	2054	2560	887	11551	6080	5250	4575
189	2292.4	52073	2518	1321	2200	2023	584	8142	5049	5153	3833
190	2304.6	45961	2591	1255	2035	2259	832	10522	5838	5555	4092
191	2316	50450	2535	1177	2003	2144	748	9879	5120	5218	3994
192	2327.2	47608	2999	1178	2072	2307	621	9509	4623	5328	3825
193	2339.7	44148	3134	899	2126	1962	532	8472	3867	5250	3569
194	2351.1	41090	3093	764	2214	1587	500	7284	3231	5294	3097
195	2363.3	39525	3080	859	2201	1445	514	7963	3449	5289	3430
196	2372.4	48452	2837	903	2087	1565	602	8530	4005	5300	3523
197	2381.8	49911	2560	1123	1957	2051	646	9424	4464	5097	3698
198	2391.8	48326	2895	1045	2040	1934	593	8369	4529	5045	3631
199	2402.3	52266	2442	1163	2023	2048	719	9840	4992	5094	3965

200	2413.8	50506	2379	1350	2170	2284	713	10057	5407	5221	4218
201	2423	50839	2458	1243	2654	2176	718	10826	5446	6490	4081
202	2431.5	42385	2420	1116	2129	2410	550	7693	3868	6050	3463
203	2440.5	47272	2544	1209	2129	2170	611	8924	4870	5231	3891
204	2449.5	52330	2597	1299	1993	2211	717	9612	5264	5286	4281
205	2458.2	44818	2827	1180	1857	2114	530	8271	4706	4791	3787
206	2468.3	37625	2667	1213	1927	2038	468	7534	4619	4883	4000
207	2478.8	38670	2502	995	1794	1721	439	6905	4070	4938	3570
208	2489.5										
209	2500.4	45465	2178	1383	1862	1992	431	5976	4386	4517	3902
210	2510.9	41494	2186	1187	1891	2483	450	5876	4555	4312	3889
211	2525.2	45974	2204	1191	1863	2712	426	6138	4343	4492	3854
212	2539.1	47345	2255	1134	1972	3377	292	6330	4219	4678	3902
213	2553.5	53943	2307	1046	1865	2188	434	6697	4361	4755	3741
214	2567.9	49161	2538	1200	1876	2554	491	7698	4724	4515	3847
215	2581.8	49093	2266	1216	1924	2389	446	6951	4606	4876	3668
216	2596.3	48129	2337	1283	1939	2462	526	8087	5242	4850	4137
217	2610.9	51296	2355	1538	1736	1785	718	9714	6217	4240	4624
218	2624.1	47897	2314	1359	1818	2307	593	9590	5574	4534	4419
219	2637.5	45490	2274	1338	1914	2536	695	9953	5579	4789	4318
220	2650	51930	2123	1437	1603	2461	693	9664	5977	4217	4339
221	2662.9	50171	1872	1502	1769	2483	736	10591	6317	3972	4633
222	2675.9	47886	1840	1452	1737	1986	940	11907	6785	4581	4638
223	2689.4	46213	2182	1261	1818	2298	642	9769	5567	4857	4068
224	2702.9	44820	2003	1351	2017	2434	550	8818	5423	6834	4077
225	2715.9	45076	1975	1322	2179	2525	602	9291	5368	9500	3953
226	2729	54398	1849	1537	1914	2145	658	9779	6089	4329	4156
227	2742.9	47571	1838	1553	1822	2405	695	10388	6618	4823	4536
228	2756.7	45814	2000	1450	1915	2310	748	10994	6257	4311	4634

229	2769.6	48687	2118	1503	1853	2010	649	9582	5860	4276	4358
230	2782.9	48948	2312	1387	1860	2150	473	8108	5178	4553	4101
231	2796.3	47880	2341	1410	1940	1974	539	8283	5327	4551	3977
232	2810.5	47808	2293	1487	1838	2230	566	8371	5482	4583	4241
233	2824.4	45691	2556	1347	2091	2658	639	8441	5195	5173	3843
234	2838.9	49687	2659	1226	1929	2018	618	9088	5227	5020	3840
235	2852.5	54851	2494	1264	2021	2120	651	9092	5373	5995	4019
236	2865.8	51028	2486	1212	1949	2410	494	7606	4934	5497	3646
237	2878.6	50070	2402	1266	1962	2596	507	7725	5203	4283	3723
238	2892.5	53181	2526	1298	2062	1960	403	7244	4989	4786	3717
239	2906.3	46828	2503	1352	1980	1987	550	7328	4924	5133	3644
240	2919.4	46333	2196	1326	1989	2092	490	8221	5713	7392	3873
241	2933	42843	1873	1670	2396	2239	663	8723	6199	21107	3897
242	2947.2	47277	2524	1482	1873	2157	650	9135	6044	4263	3923
243	2961	45702	2362	1196	1947	1879	474	7226	4503	6321	3775
244	2973.6	44753	2424	1361	1886	2275	545	7608	4821	4723	4004
245	2987	39068	2892	915	1790	2302	419	6338	3490	4967	3378
246	3000.2	38760	2798	1047	1848	2027	379	5861	3612	4192	3183
247	3013.6	42083	2666	911	1844	2120	435	6280	3762	5033	3204
248	3027.5	42728	2185	951	2421	2297	428	7422	4503	15393	3423
249	3040.7	38791	1995	1194	2385	1850	587	8239	4958	17269	3786
250	3054.4	48601	1993	1382	1828	2023	731	9898	6120	5157	4502
251	3067.6	44328	2114	1275	2012	2259	528	8137	5038	7165	4108
252	3080.6	40710	2417	1213	2071	2239	357	7527	4548	7055	3536
253	3094.2	43182	2090	1219	2361	2846	584	8805	5257	11425	4113
254	3107.5	42214	2384	1169	2253	1914	466	7498	4611	10834	3633
255	3121.3	40184	2385	1019	2176	1779	333	6771	4306	11322	3369
256	3134.8	40572	2168	1188	2185	2459	419	7084	4682	11128	3744
257	3148.8	40881	1865	1288	2880	2976	563	8050	5150	16317	4126

258	3161.8	40797	1889	1124	2807	2649	603	9874	5530	20168	3991
259	3175.3	41174	1719	1045	2880	2642	588	9831	5185	20706	3837
260	3187	41299	1915	1211	2631	2788	541	9058	5313	17667	3949
261	3200.6	38779	1807	1152	2773	2664	519	8550	4985	16930	3833
262	3213.9	39348	1778	1243	2608	2684	470	8255	4876	16451	3789
263	3227.7	42225	1856	1156	2357	2624	574	8929	5319	11261	3979
264	3241.9	37988	1768	1078	2956	2283	443	8293	4762	19505	3486
265	3255.4	38485	1708	1128	2399	2859	477	8676	4699	17408	3829
266	3267.2	41502	1900	1144	2450	2231	455	8027	5170	15247	3712
267	3280.2	41801	1703	1338	2491	2388	566	9276	5660	15105	3925
268	3293.2	43812	1718	1179	2339	2488	681	9602	5673	15342	4037
269	3306.2	39508	1540	1228	2655	3021	627	9617	5651	17832	4013
270	3318.7	41629	1614	1205	2873	3081	644	10258	5942	18807	4149
271	3331.8	43787	1648	1135	2798	2555	619	9431	5722	17309	4018
272	3344.2	41116	1524	1195	3019	2575	555	9129	5218	18627	3726
273	3357.6	37980	1424	1105	3850	2568	621	11014	5941	30985	4027
274	3370.8	38683	1438	1084	4414	2732	809	11935	5931	28692	4098
275	3384.6	41572	1796	1162	3604	2266	773	11959	5978	30111	3867
276	3398.1	40302	1677	1172	3194	3258	688	10431	5850	24380	3840
277	3411.1	42581	1703	1265	3241	3206	617	10264	5997	23925	4501
278	3423.6	43452	1605	1064	3138	2548	730	12509	6720	23522	4349
279	3436.8	36169	1392	989	3554	2840	771	12522	6429	28354	4490
280	3449.5	35308	1342	906	4014	3081	696	10776	5713	29966	3719
281	3462.6	34563	1399	993	3878	2397	740	11637	5629	33359	3903
282	3474.9	36341	1187	1064	5934	3179	571	12320	6247	40056	4202
283	3488.2	32238	966	881	9180	2714	725	12318	6697	75425	3999
284	3501.2	25260	606	738	12244	2692	785	14929	7077	112381	3959
285	3515.1	30262	771	810	10537	3157	816	14552	7345	92698	3896
286	3527	25845	658	712	10778	2872	728	13418	6662	93519	3564

287	3539.5	25599	618	721	11455	3178	746	14428	6571	98462	3826
288	3552.6	23515	613	679	11466	2506	594	11710	5770	96724	3632
289	3565.1	23413	635	822	11527	3157	588	12400	6376	103257	3576
290	3577.9	24836	676	753	11113	2957	791	15402	7066	112407	3604
291	3589.5	25028	642	721	11350	2792	664	14477	6851	109250	3793
292	3601	25240	640	742	11695	2875	733	15491	6997	112991	3790
293	3613.7	25260	606	738	12244	2692	785	14929	7077	112381	3959
294	3625.8	24784	599	747	12416	3291	722	15165	7426	116531	3603
295	3637.9	24761	594	718	12356	2735	737	15510	7295	119922	3710
296	3650.3	24039	605	711	12658	2937	717	15715	7311	126617	3680
297	3663.1	24218	583	730	12276	3028	868	16526	7243	129731	3811
298	3675.8	24035	548	727	13197	2919	800	16863	7285	129875	3605
299	3688.9	23247	530	692	12729	2813	837	17322	6890	133415	3696
300	3701.7	22594	494	656	12964	3240	754	16762	7248	131689	3916
301	3714.7	22012	550	684	11660	3858	759	17516	7215	134088	3471
302	3727.8	22309	537	668	11278	3203	715	14932	6512	120639	3650
303	3740.6	23314	505	678	11420	3540	769	15633	7130	116354	3686
304	3753.9	22666	406	619	11975	4042	642	15171	6779	116517	3687
305	3767.1	19319	397	550	11124	3763	600	16232	6257	130265	3618
306	3780.4	18511	275	479	9124	5332	616	14714	5674	122558	3164
307	3791.3	13677	383	580	8032	3061	424	11058	3949	103001	2717
308	3803.6	17238	363	551	10583	4085	520	11949	4799	93632	2992
309	3815.7	18576	384	529	10981	2952	623	14487	5748	121140	3435
310	3828.4	20377	349	521	11033	3400	730	16457	6260	128872	3589
311	3840.6	20073	365	615	10297	4053	800	17422	6360	132314	3674
312	3853.2	18069	477	632	11095	3563	716	15468	5750	122339	3408
313	3865.8	22765	394	579	11690	3248	859	17798	7140	124518	3747
314	3879.2	21229	401	589	11482	3989	700	16784	6617	131356	3832
315	3891.5	20137	379	578	10752	4491	736	17880	6365	136520	3801

316	3903.2	18901	422	623	11612	3535	577	16706	6069	131986	3557
317	3915.8	20794	396	582	11402	3633	687	17224	6323	133106	3699
318	3928.6	20033	346	564	10668	3342	666	16064	6085	128644	3437
319	3942.2	19182	349	516	9327	4882	764	16706	6192	130706	3599
320	3954	17519	317	536	10797	3552	484	13615	5556	110638	3323
321	3966.3	17889	348	591	12199	3952	510	11916	5160	114558	3222
322	3979.1	18911	348	495	12927	3706	561	14803	5381	129616	3437
323	3992.4	16617	277	539	10541	4475	416	11381	4455	122445	3364
324	4004.2	18250	315	525	9332	5164	675	15552	5675	123914	3724
325	4015.7	16357	367	520	10055	4311	576	13067	5023	111208	3448
326	4027.4	17729	336	608	11110	3699	547	15303	5374	125119	3548
327	4039.5	19684	373	553	11533	3982	754	16418	6067	131296	3478
328	4052.7	19233	347	517	9417	4722	617	17773	5971	137659	3637
329	4064.9	16624	332	439	9836	4806	500	12978	5002	110951	3071
330	4077.2	18338	333	582	10121	3873	605	15678	5560	120825	3847
331	4089.1	18817	406	638	10367	3417	642	15940	5951	125228	3624
332	4102.3	21027	316	548	9683	5184	871	18110	6800	127754	3747
333	4114.2	18686	343	590	9152	4051	685	16479	6214	124128	3710
334	4126.3	18732	369	520	9338	3092	700	15746	5863	116252	3773
335	4138.8	18151	303	510	9071	3392	490	13067	5066	108982	3548
336	4150.9	17665	289	469	9021	5175	577	13937	5039	113905	3551
337	4163.1	16683	305	493	9787	3735	516	13470	4711	108922	3201
338	4175.1	18238	290	441	9160	4770	607	15944	5891	118575	3338
339	4188.7	17213	304	539	9866	4234	554	13841	4986	114755	3498
340	4200.8	18060	292	522	9411	4484	555	15630	5659	125040	3613
341	4213.8	17025	330	529	8666	4399	545	14651	5095	120838	3713
342	4225.6	16672	289	449	9165	5128	392	11425	4287	99952	3281
343	4238.3	17028	278	534	9161	3005	622	15149	5479	119323	3320
344	4250.2	17392	276	514	8530	5477	572	14160	5233	118798	3087

345	4262.4	16409	313	528	8935	3830	554	13645	5071	112450	3224
346	4275.6	17121	271	463	8151	4131	505	12244	4677	104272	3143
347	4287.6	17572	259	495	8853	4649	629	14909	5388	110128	3624
348	4301.1	16563	286	643	8916	3520	519	13992	5087	114820	3235
349	4313.4	18156	281	510	9109	3817	576	15437	5631	125183	3638
350	4325.6	18657	282	496	9087	5808	698	16996	6032	125557	3677
351	4338.3	17383	282	393	8652	4054	525	14981	5582	119508	3562
352	4350.4	17462	309	525	8934	5370	552	15181	5510	121655	3242
353	4362.7	17489	249	530	8408	6154	620	13469	5221	114294	3310
354	4375	16939	349	591	8751	5215	630	14914	5271	118575	3459
355	4386.9	18726	257	550	8864	4341	620	14860	5667	119919	3567
356	4400.1	19347	309	552	8238	4082	669	16956	6176	132464	4282
357	4412	18488					492	13983	5280	107715	3219
358	4423.9										
359	4436.5										
360	4449.5										
361	4461.2										
362	4473.5										
363	4485.7										
364	4498.7										
365	4510.7										
366	4523.1										
367	4536.3										
368	4548.1										
369	4560.8										
370	4571.8										
371	4584.6										
372	4596.4										
373	4608.9										

374	4619.9										
375	4632										
376	4644.5	5591	177	506	2105	3302	666	27575	3461	24041	2031
377	4657.5	6054	188	560	1683	3683	591	21581	3022	18119	1800
378	4670.1	6249	187	452	1323	5331	497	17590	2633	16273	1580
379	4681.5	9291	187	497	1690	4588	621	19683	3517	19858	2230
380	4694.4	8523	194	628	1674	3462	551	19566	3530	21283	2103
381	4707.1	7651	166	614	1166	3773	595	19297	3281	15209	1990
382	4719.6	5934	160	457	1137	4945	522	19212	2916	13284	1749
383	4731.7	5311	208	351	1598	4951	307	15014	2164	18632	1765
384	4744.2	19435	275	545	6896	7321	727	15139	5763	108688	3238
385	4756.1	14643	263	538	6726	7815	464	13311	4377	82736	3139
386	4768.2	13423	274	470	5642	6341	498	14380	4082	70656	3123
387	4779.8	12761	233	504	5201	7343	528	14960	4081	66897	2912
388	4792.4	15856	263	491	6452	7784	562	12296	4303	83324	3280
389	4805.1	15489	268	531	5918	5952	667	18041	4771	78745	3104
390	4816.5	8590	169	487	1341	4820	555	18441	3167	21910	2181
391	4828.5	8633	226	473	4897	4018	366	14928	2916	44504	2062
392	4840.1	15628	312	585	8352	4488	454	12238	4018	84847	2840
393	4852.3	14119	268	660	7715	4312	401	10274	3784	70918	2788
394	4865.1	11692	259	520	8051	5004	399	10704	2729	78734	2740
395	4877.8	13579	275	610	7312	5221	327	8911	3091	73813	2619
396	4890.5	16761	312	635	7395	6547	344	9992	4126	84044	2897
397	4901.8	17582	344	672	6965	4093	361	9402	4226	77051	2844
398	4914.1	9396	200	608	1637	4284	747	23352	3723	25239	2245
399	4925.8	9294	198	538	1369	4342	728	24636	4028	17441	2424
400	4937.1	9488	185	597	1168	5018	778	20315	4034	15555	2284
401	4950	7394	172	508	880	5735	808	28155	3885	10756	2084
402	4962.8	7563	194	605	2912	4154	599	17877	3608	21435	2332

403	4975.6	15248	275	556	5063	4318	559	12152	4645	66696	2793
404	4988.8	11190	218	468	4360	4206	609	16560	4239	63634	2757
405	5000.8	12964	257	543	5634	4318	437	13266	3755	65135	2720
406	5013.2	14436	239	615	5496	8757	402	13166	4281	68173	2747
407	5025.1	12219	240	546	4833	4887	385	12152	3570	61286	2642
408	5037.5	15044	230	572	5199	6574	468	11131	3970	66658	2648
409	5049	15071	333	633	5757	5595	426	10082	3741	61921	2764
410	5060.9	15149	256	502	4534	5628	469	11086	3821	56104	2687
411	5073.9	14807	275	573	4055	4816	379	11025	4372	45332	2702
412	5086.5	16068	299	581	3161	5786	473	11464	4403	33296	2750
413	5098.7	8566	200	441	2388	4333	571	19292	3086	29695	2156
414	5110.8	10543	199	505	3472	6698	366	12487	3398	40305	2492
415	5121.8	13608	309	514	3550	4975	317	10852	3643	45596	2634
416	5133.7	14519	254	552	4107	5795	433	11383	4097	48066	2870
417	5145.9	13864	264	515	3682	3003	371	10575	3620	43381	2814
418	5157.2	14499	268	545	4350	5265	385	10785	4126	45027	2557
419	5168	11974	242	646	2893	2383	455	15597	3992	33312	2673
420	5179.3	7962	204	502	2033	7002	570	18365	2981	21704	1756
421	5192.4	13062	253	579	2206	5453	522	14173	3971	26855	2764
422	5204.9	11201	230	483	2233	5374	429	13283	3360	29963	2293
423	5218.2	12781	237	549	2223	13893	526	14607	4141	28303	3493
424	5230.7	6743	156	364	1113	5814	444	16329	2547	14957	1875
425	5243.2	14051	246	635	2088	6234	494	11233	4224	28070	2801
426	5256.3	8339	203	443	3306	3343	465	15884	3106	40164	2305
427	5268.4	10135	218	651	1528	4417	757	29096	4348	21670	2292
428	5281.4										
429	5294.1										
430	5306.7	16615	264	1003	2290	3775	786	19071	6547	38621	3285
431	5320	14848	264	625	2262	6019	778	19274	5295	32254	3241

432	5332.8	8167	174	451	2016	2947	592	23696	3802	22433	2189
433	5346.1	8899	192	499	1767	6252	687	26124	3510	23026	2717
434	5359.1	8455	231	422	1594	4404	696	27984	3748	25444	2254
435	5372.3	12321	211	648	2316	4242	788	23229	4649	35661	2735
436	5384.7	8756	159	627	1650	4805	758	28592	4148	24932	2507
437	5395.8	7198	172	517	1600	8813	594	29665	2810	19993	2285
438	5408.4	7404	199	489	1543	6546	656	32739	3017	19872	2640
439	5420.3	5603	145	401	1609	3810	569	34823	2235	14111	2300
440	5432.6	8860	156	599	2018	5969	650	29431	4431	27069	2297
441	5444	6038	182	474	1210	6654	635	37768	3117	14230	1869
442	5456.8	13266	246	608	3258	5504	888	27274	5693	46676	2738
443	5469.4	10694	146	639	2604	4272	864	23824	4892	31195	2319
444	5481.5										
445	5493.6										
446	5506.6										
447	5518.8										
448	5531.4										
449	5543.3										
450	5555.4										
451	5568.8										
452	5579.8										
453	5592.8	8556	200	526	1398	4143	757	28961	3345	17576	2620
454	5605.4	13429	226	598	1805	6118	851	26606	5742	25963	2709
455	5617.4	13058	223	777	2019	9845	971	25330	5645	20550	2898
456	5630.8	13421	211	573	1663	4011	837	25782	5372	23334	2844
457	5643.6	6171	153	603	1263	6232	727	39208	4216	11281	2268
458	5656.2	27183	416	920	3425	4910	1306	22778	8594	55242	3906
459	5668.2	13861	273	590	1871	7944	734	19150	5449	34008	2754
460	5680.3	12225	156	590	1466	5513	851	28733	4938	21119	2569

461	5693.1	7836	182	565	1316	5059	741	32463	3466	15393	2400
462	5706.6	13297	183	652	1471	8637	1003	27003	5631	23536	2896
463	5718.9	14645	220	750	1575	7016	1018	28148	6090	26626	3383
464	5731.6	24474	305	779	2045	8044	1245	21381	8819	37825	4357
465	5744.4	11325	218	595	1440	4677	933	27425	4655	20803	2535
466	5757.3	18261	243	605	2192	4996	1115	20388	7059	39656	3703
467	5770.1	15393	253	671	2171	7260	936	23952	6336	31241	3421
468	5782.3	10651	233	652	1679	7652	829	28571	5046	30861	2811
469	5794.9	8142	166	549	1168	7920	827	33332	4072	16028	2720
470	5807.4	10110	215	641	1107	5946	848	29724	4503	15952	2610
471	5818.7	6212	159	560	1115	4418	609	34632	3494	12247	2149
472	5832.6	11692	206	605	1426	7914	853	31206	5080	17555	2610
473	5844.4	7090	170	749	1473	4568	730	28114	4597	13931	2135
474	5855.9	11456	189	695	1799	4725	821	31183	4959	23821	2478
475	5868	4197	117	417	1087	9242	636	37080	2581	9942	2149
476	5880.4	7105	182	660	1379	9210	690	37065	3966	18302	2758
477	5891.6	6364	169	502	1145	7468	679	39400	3525	12333	2364
478	5903.2	7561	161	540	1296	5648	860	39709	3855	15644	2732
479	5914.5	4466	170	492	1556	8259	738	42079	3386	19378	2186
480	5926.2	3536	131	444	576	3769	597	44610	2506	4574	1968
481	5938.6	7427	161	591	1075	5118	726	36755	4146	9696	2331
482	5951.4	7582	192	525	988	5353	793	36937	3530	12475	3018
483	5964.1	7193	132	561	1356	5410	771	33751	3967	15639	2379
484	5977	8609	199	571	1151	5177	773	33723	4632	15049	2724
485	5990.3	6438	162	559	2006	4904	730	34907	3567	26450	2295
486	6002.5	4545	150	534	1159	6152	639	39299	3020	11816	2070
487	6014.1	4432	155	501	1289	7066	531	36691	2400	13402	2273
488	6026.9	2724	112	429	619	4928	467	38667	2410	3881	1806
489	6039.2	5039	173	461	1066	8681	619	37782	3255	7330	1842

490	6052	6988	205	504	1086	5426	730	36813	3266	11300	2157
491	6062.5	6807	162	543	1080	5950	652	35520	3174	10577	1966
492	6073.5	13016	212	714	1470	4462	809	29316	5779	19751	3054
493	6085	3941	131	480	868	1282	527	39045	2552	8123	2052
494	6097	4983	139	630	973	10671	521	33371	2387	7408	2681
495	6109.1	4885	161	617	850	5606	651	42374	2547	5853	2503
496	6122.2	3903	161	444	586	5990	599	44721	2289	4556	1920
497	6133.9	4864	149	530	994	7247	637	40168	2692	9049	2005
498	6145.7	6086	171	536	977	7309	547	36261	2898	9011	2206
499	6158.9	6337	174	525	951	6930	821	37088	3536	9675	2908
500	6172.4	5905	167	527	947	6725	794	36510	3216	7773	2395
501	6184	5866	120	503	1035	6363	731	38174	3080	9360	2437
502	6195.6	5770	178	529	1306	8406	666	35813	3173	8876	2478
503	6207.8	7745	188	635	2203	7305	654	39298	3583	22642	2282
504	6220.4	3714	139	470	812	7865	597	43940	2633	5684	2133
505	6233.3	3078	131	531	681	4170	601	40760	2643	4970	2015
506	6246	4226	179	477	822	6567	606	45322	2597	6908	2231
507	6258.2	3650	154	427	762	8021	607	45964	2485	6082	2014
508	6269.9	4088	109	415	671	7867	608	45616	2721	4268	2022
509	6282.4	4007	182	621	861	7506	652	40477	3273	6543	2316
510	6294.1	3182	120	352	599	5161	553	38568	2302	4371	1930
511	6306.3	4067	145	515	767	7743	624	43760	2862	5173	2021
512	6319.9	8222	201	637	1031	8048	766	39122	3893	8661	2979
513	6332.9	4982	168	629	724	6922	665	40581	3663	7550	2694
514	6345.7	4585	105	582	622	5204	718	43345	3525	5956	2805
515	6358.2	5769	133	838	1020	6889	797	40171	5048	9661	2248
516	6370.8	6555	193	566	974	9522	871	41124	3409	9436	2600
517	6383.2	5158	127	566	802	7507	790	40843	3513	8651	2829
518	6396	7575	168	683	1175	5913	766	36142	4731	18763	3319

519	6407.4	4227	100	538	664	7130	615	41473	2616	5573	1996
520	6419.2	3753	115	649	447	4751	775	45707	3871	3414	2421
521	6432.1	6576	156	516	945	6710	763	33390	3490	17427	2419
522	6445.7	3677	100	490	573	6359	548	34846	2575	5485	1803
523	6458.2	3363	113	479	534	5597	566	39126	3706	3969	1958
524	6470.8	5994	140	480	1293	6650	738	36081	3001	15183	2330
525	6484.2	2599	98	482	518	6920	541	40658	2168	4280	1698
526	6496.3	3612	120	503	681	5546	704	47594	2865	9848	1937
527	6508.1	3434	119	407	535	8476	681	48863	2708	3497	2091
528	6519.5										
529	6532.5	3947	125	642	543	6258	661	33926	2897	5271	1763
530	6544.9										
531	6558.7										
532	6570.4										
533	6583.2										
534	6594.8										
535	6607										
536	6620.1										
537	6632.6										
538	6644.9										
539	6658.2										
540	6671.4										
541	6684										
542	6695.6										
543	6707.3										
544	6719.7										
545	6731.9										
546	6744.2										
547	6757										

548	6769.9
549	6781.2
550	6793.7
551	6805.4
552	6818.4
553	6829.6
554	6842
555	6853.4
556	6865.6
557	6877.3
558	6889.9
559	6901.7
560	6913.5
561	6925.4
562	6937.8
563	6950.9
564	6963.6
565	6975.7
566	6987.3
567	6999.2
568	7010.7
569	7023.2
570	7034.7
571	7046.7
572	7059.6
573	7071.8
574	7084
575	7096.4
576	7108.8

577	7120.6										
578	7132.9										
579	7145.3										
580	7157.5										
581	7170.3										
582	7183.6										
583	7194.5										
584	7207.2										
585	7219.9										
586	7232.7										
587	7245.1	3659	170	426	715	7182	607	45839	2165	2933	2149
588	7257.5	3454	189	441	467	10079	540	44846	2059	2016	2023
589	7268.8	3448	139	406	392	9311	539	41291	1674	1670	2239
590	7281.3	3378	158	299	542	9433	513	45810	1744	1752	2331
591	7293.4	3216	130	354	398	12117	568	41229	1894	1865	1967
592	7305.4	2962	147	377	341	7544	467	43767	1896	1359	2500
593	7317.8	3087	143	563	508	7328	503	41855	2072	4228	2234
594	7330.5	2934	157	360	547	6379	592	44063	2554	2441	2542
595	7341.8	3103	142	411	534	7932	494	44332	1723	2183	2459
596	7354.6	3913	117	483	758	7387	667	43404	2399	4379	1835
597	7367.2	3306	145	395	560	6879	573	41360	2264	3174	2545
598	7380.5	5562	142	571	843	6891	584	37270	2784	3836	2692
599	7393.2	4632	146	528	761	8126	605	38277	2559	6054	2105
600	7405.7	3913	189	422	986	6768	650	42071	2208	5550	2075
601	7418.1	4175	182	512	573	7035	626	40605	2602	4292	2358
602	7430.6	8319	127	518	752	5741	757	29944	3335	7253	2576
603	7443.5	6764	146	527	672	6897	857	33680	3492	5951	2449
604	7456.2	10524	157	667	1125	7387	1044	29420	4837	16377	2742
605	7469.6	13415	170	732	1452	9692	1195	28307	5715	16241	3220

606	7481.4	7167	147	528	865	10251	864	34351	3201	6244	2984
607	7493.8	8017	121	692	874	10306	950	35917	4219	8800	2564
608	7506.3	4603	147	396	1211	9623	558	36002	2087	9972	2777
609	7518.5	8458	129	603	1104	7346	1047	33150	4225	14054	2701
610	7531.1	11095	111	760	630	5885	1137	31083	4985	3540	3621
611	7543.3	28292	157	1091	738	10325	2078	24991	10570	2541	5224
612	7554.4	29596	178	1199	729	9016	2112	27959	11294	1890	5864
613	7566.8	28013	117	1165	784	9969	2490	34188	10405	3160	6612
614	7578.2	38162	181	1530	989	7926	3117	35312	11613	25740	7791
615	7591.3	37831	168	1635	1119	8863	2769	33067	11347	23771	7409
616	7602.8	33757	163	1357	1110	9537	2161	30084	10450	27107	6433
617	7614.9	31245	171	1173	1014	9692	1716	28643	9246	26668	5377
618	7627.4	31192	155	1277	1063	11111	2409	34516	11079	19056	6120
619	7640.2	34260	121	1360	928	9973	2452	34131	11679	11859	6674
620	7653.4	29152	159	1282	1047	9418	2421	36211	11210	12719	6276
621	7664.4	25218	160	1185	978	9361	2023	33479	9206	27806	5744
622	7676.6	30993	142	1195	1052	10474	2367	34257	10615	19080	6113
623	7689.3	37574	185	1349	904	10456	2405	33724	11328	3430	6982
624	7701.7	37706	200	1335	937	9837	2375	33241	11371	1921	6270
625	7714.7	24133	141	994	729	6435	1852	34376	7832	2488	4637
626	7726.6	13919	139	724	750	7838	1251	32290	6029	10271	3718
627	7738.9	7172	126	490	650	7057	775	37929	3520	14525	2588
628	7752.5	23662	149	903	1155	9747	1685	29101	7414	21536	4691
629	7765.6	24491	179	837	737	7621	1262	28353	6386	12904	4100
630	7778.6	37522	147	1306	896	8642	2136	26099	10045	20645	5861
631	7790.5	41762	162	1463	954	7306	2435	27349	11463	26407	6785
632	7802.5	38233	159	1303	1211	7636	2364	29783	10420	41368	6797
633	7814.9	33199	167	1271	1027	8653	2402	30336	10400	36757	6055
634	7827.5	13800	145	814	674	4584	1079	38712	5442	20780	3407

635	7839.7	4467	111	466	498	8117	607	41740	2345	18471	1992
636	7852.4	3495	113	360	572	7262	517	43237	2397	17598	1675
637	7864	5330	112	529	644	10535	802	45210	3215	11005	2504
638	7875.8	10301	136	874	637	7702	1061	41544	5545	7421	3703
639	7887.6	18288	133	922	773	5553	1478	36906	7224	6560	4127
640	7899.8	15196	122	710	645	9011	1262	37651	6207	8833	3587
641	7911.8	7653	101	670	595	5338	907	36250	3428	15387	2427
642	7924.8	41600	167	1170	688	8208	2378	28236	11264	6610	6443
643	7936.7	40187	147	1158	628	7316	2387	30151	11239	3669	6604
644	7948.7	38031	159	1148	653	8194	2442	32002	10931	4662	6332
645	7960.9	36967	148	969	707	7844	2377	31504	10900	5009	6163
646	7971.5	21182	141	939	699	8546	1718	34913	8308	8580	4550
647	7983.5	20700	119	937	672	9944	1679	33210	8375	6756	5230
648	7996.1	30515	152	1066	732	8920	1833	29044	9690	7801	5275
649	8007.9	31228	136	1013	672	9600	1741	31986	9073	4593	5612
650	8020.1	35239	162	1033	598	9036	1868	33846	9515	5040	5955
651	8031.7	40510	160	1157	701	7862	2366	32185	11588	7129	6698
652	8044.3	41408	143	1289	907	9100	2655	31047	12640	16692	7177
653	8056.7	40516	126	1188	880	7636	2721	28649	12708	21961	7234
654	8069	46179	176	1265	1065	9010	3130	32651	13878	30063	7390
655	8081.4	30382	117	1125	932	8948	2430	31466	11325	21291	5722
656	8093.4	31332	137	1138	879	8951	2215	31913	10672	24868	6171
657	8105.4	31090	139	1138	994	8718	2005	29493	10102	24162	5674
658	8117.6	30544	108	1051	878	9113	1776	28057	9640	21597	5800
659	8130.2	34799	109	1192	1127	9063	2025	37987	10133	25545	6032
660	8142.2	38564	121	1077	909	8638	1804	29775	9929	24317	5658
661	8153.5	25425	157	997	910	7680	1251	33810	7298	12344	4096
662	8165.6	25694	130	772	813	7554	1145	31624	5861	14670	4090
663	8177.8	6516	127	527	653	5453	731	37444	3205	24365	2011

664	8190.2	7095	97	664	801	2392	574	25253	3934	36680	1938
665	8201.6	8748	104	746	820	4196	877	35864	3773	19388	2326
666	8215.4	8641	106	486	612	6135	779	37536	3112	16669	2547
667	8226.9	7812	120	742	630	5250	826	37253	3466	22714	1998
668	8239.7	17039	89	659	649	4789	1014	29605	4073	23735	2822
669	8251.7	11426	123	661	759	5666	844	35570	3942	22977	2312
670	8263.5	10622	136	734	680	4360	782	33762	3316	23556	2107
671	8276.4	11365	107	686	658	5619	833	35168	4040	21039	2652
672	8288.3	21133	124	917	775	6223	1174	31284	5558	21155	3308
673	8301.4	7674	99	525	638	8603	652	35183	2569	23931	2513
674	8314.7	24525	147	821	771	8333	1217	29697	6173	26057	3866
675	8327.6	33688	175	961	996	7594	1460	26248	7927	28706	4358
676	8339.1	38624	147	1047	1020	6336	1658	24114	9804	33832	5073
677	8350.4	43314	173	1155	999	6771	2028	24874	11048	29911	5411
678	8363	27596	123	754	816	5562	1258	24617	6827	20375	4122
679	8374.9	32233	147	753	923	5367	1326	20183	7786	21658	4254
680	8386.7	35409	138	988	1019	6502	1761	23220	9832	28857	4668
681	8398.3	12820	123	751	751	9005	1019	30696	5269	16962	3397
682	8410.6	9516	137	705	762	13058	916	32315	4290	13143	2884
683	8422.8	13616	116	846	1035	11064	1127	31706	5690	17058	3328
684	8435.3	11199	141	1242	1233	9652	1114	30515	5476	21084	3215
685	8448	8772	143	803	1935	12199	1138	33170	4761	31151	2999
686	8459.5	6447	91	714	858	5420	787	34016	3607	15878	2145
687	8471.6	5534	147	570	834	5524	824	37937	3461	15752	2107
688	8484	7783	134	681	829	5175	1010	37390	4868	14619	2837
689	8497	11132	146	801	820	9880	1037	29347	4978	14427	3030
690	8509.7	8550	109	719	671	11993	875	33324	4007	8938	2521
691	8520.3	11727	78	734	531	5817	873	28619	3783	6617	3314
692	8531.7	6747	89	612	3222	3874	828	31612	3181	51082	1850

693	8543.4	10208	79	797	663	6642	930	26369	4137	13947	2453
694	8555.6	12030	116	749	728	4383	1043	25857	4252	14207	2293
695	8567.4	12293	136	762	1117	6081	1086	31693	4744	19255	2831
696	8578.5	5827	103	527	719	7886	787	36451	3178	12071	1971
697	8590.4	4060	93	551	446	5726	688	38980	3644	8074	2053
698	8602.8	4929	76	551	405	5716	556	32256	3043	5627	1753